# NTNU

Norwegian University of
Science and Technology

# Modelling and System Identification of Pedestrian Bridges - Bårdshaug

## Martin Rønneseth
## Stina Elise Gjøen Simensen

**Department of Structural Engineering**
Faculty of Engineering
**NTNU- Norwegian University of Science and Technology**

# MASTER THESIS 2017

| SUBJECT AREA: | DATE: | NO. OF PAGES: |
|---|---|---|
| Structural Engineering, Dynamics | 09.06.20017 | 146 + 50 pages appendices |

TITLE:

**Modeling and system identification of pedestrian bridges - Bårdshaug**

Modellering og systemidentifikasjon på gangbruer - Bårdshaug

BY:

Martin Rønneseth

Stina Elise Gjøen Simensen

SUMMARY:

The main objective of this thesis has been to evaluate and compare different load models and comfort criteria given in guidelines for pedestrian loading, with respect to accuracy and usability. The guidelines taken into consideration are Eurocode, BS 5400, UK National Annex to Eurocode, Håndbok 185, SÉTRA, ISO 10137, JRC - Design of Footbridges for Human Induced Vibrations and HIVOSS. In addition, a desired outcome has been to obtain an approach to the modelling of a pedestrian bridge in order to achieve accurate dynamic behaviour for the model, and obtain realistic acceleration output when pedestrian loads are applied. A case study was done for Bårdshaug Bridge, a pedestrian bridge located in Orkanger, Norway.

The different guidelines taken into consideration have vast variations in the approach to the simplification of the pedestrian load and how to obtain a comfort criterion; from including only mass and damping, like Eurocode, to also including length, number of pedestrians and natural frequencies, like UK-NA and SÉTRA. The load parameters are weighted differently depending on the guideline, such that a more comprehensive load model does not necessarily yield the most accurate result. The different approaches and simplifications cause large variation in the results, making it challenging to recommend a single guideline for obtaining the most realistic responses. It is shown that a guideline can obtain a good approximation for the acceleration values for one case, but poor approximations for other cases.

It is found that a simplified FE-model is sufficient in order to obtain a good approximation to the dynamic behaviour of a pedestrian bridge under normal use. SÉTRA is found to be the guideline preferable to use when applying pedestrian loading to a structure.

RESPONSIBLE  TEACHER: Nils Erik Anders Rønnquist

SUPERVISOR(S): Gunnstein Thomas Frøseth

CARRIED OUT AT: Department of Structural Engineering, NTNU

# Abstract

The main objective of this thesis has been to evaluate and compare different load models and comfort criteria given in guidelines for pedestrian loading, with respect to accuracy and usability. The guidelines taken into consideration are Eurocode, BS 5400, UK National Annex to Eurocode, Håndbok 185, SÉTRA, ISO 10137, JRC - Design of Footbridges for Human Induced Vibrations and HIVOSS. In addition, a desired outcome has been to obtain an approach to the modelling of a pedestrian bridge in order to achieve accurate dynamic behaviour for the model, and obtain realistic acceleration output when pedestrian loads are applied. A case study was done for Bårdshaug Bridge, a pedestrian bridge located in Orkanger, Norway.

The different guidelines taken into consideration have vast variations in the approach to the simplification of the pedestrian load and how to obtain a comfort criterion; from including only mass and damping, like Eurocode, to also including length, number of pedestrians and natural frequencies, like UK-NA and SÉTRA. The load parameters are weighted differently depending on the guideline, such that a more comprehensive load model does not necessarily yield the most accurate result. The different approaches and simplifications cause large variation in the results, making it challenging to recommend a single guideline for obtaining the most realistic responses. It is shown that a guideline can obtain a good approximation for the acceleration values for one case, but poor approximations for other cases.

It is found that a simplified FE-model is sufficient in order to obtain a good approximation to the dynamic behaviour of a pedestrian bridge under normal use. SÉTRA is found to be the guideline preferable to use when applying pedestrian loading to a structure.

# Sammendrag

Hovedmålet med denne avhandlingen har vært å evaluere og sammenligne ulike lastmodeller og komfortkriterier oppgitt i standarder og regelverk for gangbruer. Fokuset ved sammenligningen har vært på nøyaktighet og brukervennlighet. Regelverkene som er betraktet er Eurokode, Britisk Standard, Britisk Nasjonalt Tillegg til Eurokode, Håndbok 185, SÉTRA, ISO 10137, JRC and HIVOSS. I tillegg har et ønsket resultat vært å skape en fremgangsmåte til en numerisk modell av en gangbru for å oppnå nøyaktig dynamisk respons og realistiske akselerasjonsverdier ved påføring av ganglastmodeller. En case-studie er blitt gjort for Bårdshaug Bro, en gangbru som befinner seg i Orkanger, Norge.

De forskjellige standardene og håndbøkene har store variasjoner i fremgangsmåten for forenklinger av ganglast og hvordan komfortkriteriene oppnås; fra å bare inkludere masse og demping slik som i Eurokode, til å også inkludere spennlengder, antall fotgjengere og egenfrekvenser slik som UK-NA og SÉTRA. De ulike fremgangsmåtene og forenklingene skaper store variasjoner i resultatene, noe som gjør det vanskelig å anbefale én enkelt standard som forutsier mest realistisk respons. Det er ikke nødvendigvis lastmodeller som inkluderer flest lastparametere som gir ønsket resultat, fordi vektleggingen av ulike parametere også har store variasjoner. Det er vist at en standard kan gi realistiske resultater for et lasttilfelle, og urealsitiske resultater ved andre lasttilfeller.

En forenklet numerisk modell er funnet til å gi tilfredsstillende approksimasjoner for dynamisk oppførsel an ganglast ved normal bruk. SÉTRA er hånboken som er funnet til å være foretrukket når en ganglast er påsatt gangbruen.

# Preface

This master thesis is the final submission of the five year study program Master of Science in Civil Engineering. The thesis was conducted between January and June 2017, within the Department of Structural Engineering at the Norwegian University of Science and Technology (NTNU) in cooperation with The Norwegian Public Road Administration.

We would like to express our gratitude to our supervisors at the Department of Structural Engineering NTNU, Professor Anders Rönnquist and Ph.D. Candidate Gunnstein Frøseth, and thank them for always being available with guidance and support throughout the project. We would also like to thank our supervisor at The Norwegian Public Road Administration, Vegard Fossbakken, for help with defining the task, providing necessary documentation and for making it possible to work with this project.

Finally, we would like to thank our fellow students for interesting discussions and great support during the work on this thesis, as well as throughout the last 5 years.

Trondheim, June 9, 2017

_Martin Rønneseth_

Martin Rønneseth

_Stina EGSimensen_

Stina Elise Gjøen Simensen

# Contents

# Acronyms

**BS** British Standards.

**BSI** British Standards Institution.

**CAE** Computer-aided engineering.

**DFT** Discrete Fourier Transform.

**DLF** Dynamic load factor.

**DMF** Dynamic Magnification Factor.

**FE** Finite Element.

**FEM** Finite Element Method.

**FFT** Fast Fourier Transform.

**FRF** Frequency Response Function.

**HIVOSS** Human Induced Vibrations of Steel Structures.

**JRC** Joint Research Centre.

**MAC** Model Assurance Criterion.

**MC** Monte Carlo.

**MDOF** Multiple Degree of Freedom.

**PSD** Power Spectral Density.

**RMS** Root Mean Square.

**SDOF** Single-degree of freedom.

**SLS** Serviceability Limit State.

**SSI** Stochastic Subspace Identification.

**SÉTRA** Service d'Études Techniques des Routes et Autoroutes.

**UK-NA** The United Kingdom National Annex.

# List of Figures

# Chapter 1

# Introduction

## 1.1 Background

The design of pedestrian bridges is becoming more ambitious with new technology and engineering tools. Spectacular structures create landmarks and attractions, and opportunity knocks for prestigious work when a pedestrian bridge is built in a populated area. Pedestrian bridges are becoming increasingly elegant, daring and slender when designed in the Ultimate Limit State, resulting in lightweight bridges with reduced stiffness. The reduced stiffness can lead to trouble for dynamic properties in the Serviceability Limit State, e.g. resonance, if the natural frequencies of the bridge lie within the same frequency domain as the walking frequency of a pedestrian. Resonance occurring from pedestrian induced forces have been known for a long time. In 1831, Broughton Suspension Bridge collapsed due to vertical resonance from marching troops, injuring 20 soldiers. Examples like this have remained a cautionary tale, and troops marching are at several occasions told to break step when crossing a bridge [4].



Figure 1.1: Broughton Suspension Bridge in 1883, rebuilt after the collapse in 1831

In recent time, a similar but unexpected phenomenon garnered massive attention; the infamous opening day of the Millennium Bridge in 2000, where resonance occurred in the lateral direction due to the crowd loading. This exemplifies the complexities and the challenges of predicting dynamic behavior from pedestrian loading. In order to predict the pedestrian loading, simplified methods are included in structural guidelines. The source of the simplifications may vary from guideline to guideline, yielding inconsistent comfort criteria and load models for the same loading scenario.



Figure 1.2: Millennium Bridge

## 1.2 Objective

The thesis investigates seven different design guidelines for pedestrian bridges, focusing on both the given comfort criteria and load models. The objective is to increase the knowledge of modelling pedestrian loads and make the reader aware of strengths and weaknesses regarding the different guidelines. The investigation of the guidelines is done by finding the comfort criteria of the new pedestrian bridge over Orkla near Bårdshaug, and applying the load models to a simplified numerical model for the bridge. The load model results are compared to the comfort criteria, as well as measurement data from the real structure. The guidelines are validated based on the accuracy of results and the degree of user-friendliness in obtaining these results.

The guidelines discussed in this thesis are the Eurocodes, British Standard 5400, UK national annex to the Eurocode, the Norwegian Public Road Administrations guideline - Håndbok 185, Service d' Études Techniques des Routes et Autoroute - SÉTRA, International Organization for Standardizations guideline - ISO 10137, the Guideline for Design of Footbridges for Human Induced Vibrations by Joint Research Centre - JRC and Human induced Vibrations of Steel Structures - HIVOSS.

Figure 1.3: Bårdshaug Bridge

## 1.3 Method

The thesis can be divided into 3 parts; comparing different guidelines for pedestrian loading, modelling Bårdshaug Bridge using the Finite Element Analysis program Abaqus CAE and applying the load models to the Finite Element model. The comfort criteria and load models for the different guidelines are first presented for a general case, before parameters from Bårdshaug Bridge are applied to each load model. All the guideline results are compared against each other and the measured values of vibrations on Bårdshaug Bridge.

The finite element model of Bårdshaug Bridge is a simplified model, calibrated to match the dynamic properties of the real structure. Applying the load models to the Finite Element model is done by creating a Python script. Parameters regarding the dynamic load analysis such as mesh, time steps and loading time are iterated to yield accurate data, while maintaining computational cost effective analysis.

## 1.4 Limitation

- The acceleration measurements done are limited to one bridge only. Having measurements from different bridges would made it easier to validate the results.

- The measurements done on Bårdshaug Bridge were preformed before the work on this thesis started, making it impossible to adjust the loading as desired to test the specific loading scenarios given in the guidelines.

- The simplifications made to the Finite Element model made the model more flexible than the actual bridge, and the response from pedestrian loading are therefore considered conservative.

## 1.5 Thesis Outline

**Chapter 2** describes the theory of random vibrations related to this thesis. The chapter describes how the random vibrations are obtained in a numerical model, and further how numerical data are treated.

**Chapter 3** outlines theory regarding signal processing and modal analyses used in the thesis. The chapter is targeting the readers who are not familiar with signal processing.

**Chapter 4** describes the basics of pedestrian induced forces which are necessary to know in order to understand and be able to consider the quality of the load models presented in the different guidelines. The chapter also presents models for excitation of footbridges and the history of developing the models. The excitation models are the basis for several of the load models given in the guidelines and provides important information in order to understand, utilize and further develop pedestrian load models.

**Chapter 5** revolves around the different design guidelines. The chapter is divided into two parts; the first part describes the critical acceleration allowed on a pedestrian bridge, and the second part describes the method of obtaining the reference acceleration from different load scenarios.

**Chapter 6** regards Bårdshaug Bridge, and consists of a general description of the bridge, system identification of the bridge and details of the numerical model of Bårdshaug Bridge.

**Chapter 7 and 8** presents and discusses the results of the analysis. The result part is comprehensive, including comparison of comfort criteria and load models, comfort criteria and the associated load model, measurement data discussion and resonance influenced loading.

**Chapter 9** contains the conclusion based on the previous chapters, and suggestions for further work on the same topic.

# Chapter 2

# Random Vibrations

This chapter gives an introduction to the basic dynamics which are essential to understand the results of the thesis. Starting with single degree of freedom systems, moving on to multiple degree of freedom systems, Fourier transforms, spectral density, dynamic load factor and the Dirac delta function.

## 2.1 Single Degree of Freedom Systems

A Single-degree of freedom (SDOF) system is the simplest model of a vibrating mechanism. The derivation of the SDOF system introduces important concepts and terminology, it will be used directly for some of the load models presented later and for the description of multiple degree of freedom systems.

A SDOF system is defined by a displacement in only one direction, as illustrated in Figure 2.1. The carriage in Figure 2.1 has a mass $m$, and is connected to the surroundings through a spring with stiffness $k$ and a damper with damping constant $c$. The displacement of the carriage is defined by $u = u(t)$, and an external force $F(t)$, is acting on the carriage. The free body diagram of the system in Figure 2.2 shows how the spring with stiffness $k$ exerts an elastic spring force $f_s$, the damper exerts a damping force $f_d$, and the mass of the carriage exerts an inertia force $f_i$.

$$f_s = ku(t) \tag{2.1}$$

$$f_d = c\dot{u}(t) \tag{2.2}$$

$$f_i = m\ddot{u}(t) \tag{2.3}$$
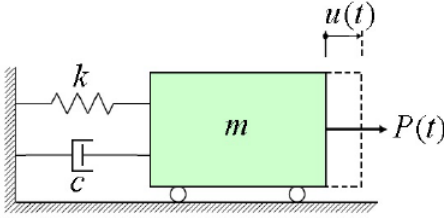
Figure 2.1: Schematic drawing of an SDOF system [1]
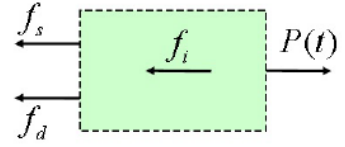
Figure 2.2: Free body diagram for an SDOF system [1]

Equilibrium in the horizontal direction gives the equation of motion for the system in Figure 2.1, which equals the equation of motion for a general SDOF, and is given by the 2nd order differential equation in (2.4).

$$m\ddot{u}(t) + c\dot{u}(t) + ku(t) = F(t) \tag{2.4}$$

The general solution to (2.4) is:

$$u(t) = u_c(t) + u_p(t) \tag{2.5}$$

Where $u_c$ is the complementary solution, and $u_p$ is the particular solution. The complementary solution is found by solving the homogeneous version of Equation (2.4), see Equation (2.6).

$$m\ddot{u}_c(t) + c\dot{u}_c(t) + ku_c(t) = 0 \tag{2.6}$$

The general solution to Equation (2.6) is:

$$u_c(t) = Ae^{\lambda t} \tag{2.7}$$

The non-trivial solution is given by the characteristic equation below:

$$\lambda^2 + \frac{c}{m}\lambda + \frac{k}{m} = 0 \tag{2.8}$$

Which gives:

$$\lambda = -\frac{c}{2m} \pm \sqrt{\left(\frac{c}{2m}\right)^2 - \frac{k}{m}} \tag{2.9}$$

Introducing the definition of the natural frequency $\omega_n$, and the damping ratio $\xi$:

$$\omega_n = \sqrt{\frac{k}{m}} = 2\pi f_n \tag{2.10}$$

$$\xi = \frac{c}{c_{cr}} = \frac{c}{2m\omega_n} \tag{2.11}$$

Where $f_n$ is the natural frequency in Hz, which yields:

$$\lambda = -\xi\omega_n \pm \omega_n\sqrt{\xi^2 - 1} \tag{2.12}$$

(2.12) is inserted in Equation (2.7) to obtain the complementary solution.

When damping is present, the response will decrease exponentially and approach zero. Equation (2.12) gives three characteristic solutions to the equation of motion, depending on the value of the relationship between the damping and the critical damping, $\xi$. Figure 2.3 illustrates the characteristic response for a under damped, over damped and critically damped system.

$\xi > 1 \rightarrow$ The system is over damped
$\xi = 1 \rightarrow$ The system is critically damped
$\xi < 1 \rightarrow$ The system is under damped
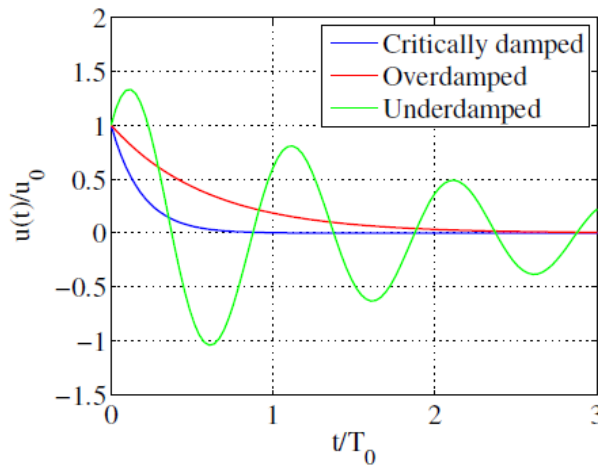


Figure 2.3: Illustration of the different types of damping

Back to the solving of the SDOF system, the equation of motion is given by Equation (2.13) when external force is applied.

$$m\ddot{u}_p(t) + c\dot{u}_p(t) + ku_p(t) = F(t) \tag{2.13}$$

The load used for the further description of SDOF-systems is a simple harmonic load, given in Equation (2.14), and the general form of the particular solution is shown in Equation (2.15).

$$F(t) = F_0 sin(\omega_f t) \tag{2.14}$$

$$u_p(t) = A cos(\omega_f t) + B sin(\omega_f t) \tag{2.15}$$

Introducing the frequency ratio $\beta$ and phase angle $\phi$, the particular solution of the equation of motion is found in Equation (2.16).

$$u_p(t) = \frac{F_0}{k} \frac{1}{\sqrt{(1-\beta^2)^2 + (2\xi\beta)^2}} sin(\omega_f t - \phi) \tag{2.16}$$

Where:

$$\beta = \frac{\omega_f}{\omega_n} \tag{2.17}$$

$$\phi = tan^{-1}\left(\frac{2\xi\beta}{1-\beta^2}\right) \tag{2.18}$$

Observing from Equation (2.16) that if the frequency ratio $\beta$ is unity, i.e. loading frequency $\omega_f$ is equal to the natural frequency $\omega_n$, and the damping ratio $\xi$ is zero the function goes to infinity. In civil engineering structures, the damping ratio is never zero, but great amplifications to the structural response can occur when an external force drives the structure to vibrate at the natural frequency. This phenomenon is known as resonance and civil engineering structures should be designed such that the forced dynamic vibration cause by the force $F_0$ does not resonate with an unacceptable amplitude. The static part of Equation (2.16) which is multiplied with $F_0/k$ is known as the Dynamic Magnification Factor (DMF) describes the phenomenon, such that [5]:

$$DMF = \frac{1}{\sqrt{(1-\beta^2)^2 + (2\xi\beta)^2}} \tag{2.19}$$
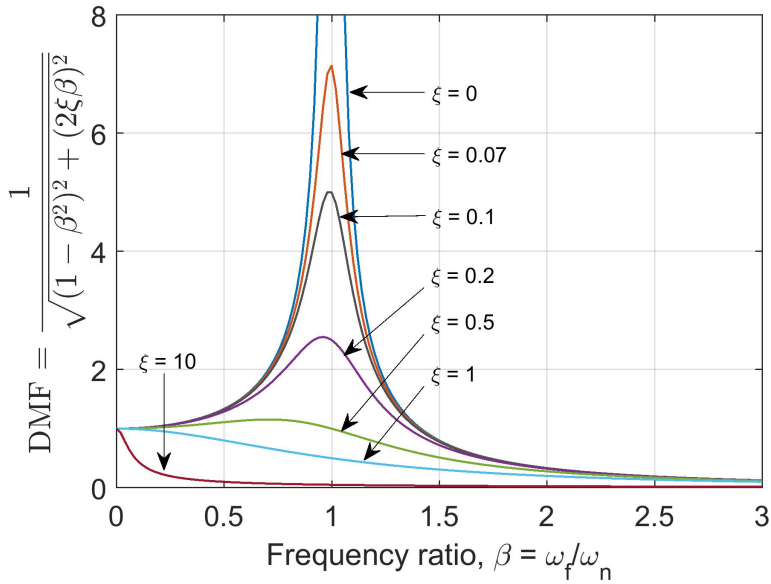
Figure 2.4: DMF as a function of the frequency ratio for different damping ratios $\xi$

## 2.2 Multiple Degree of Freedom Systems

### 2.2.1 Equation of Motion

Most structures can not be simplified enough to be modeled as an SDOF system. Instead the systems are modeled with Multiple Degree of Freedom (MDOF). A system with $n$ degrees of freedom will get $n$ coupled equations of motion, and therefore become more complex than an SDOF system. An MDOF is illustrated in Figure 2.5, and Equation (2.20), (2.21) and (2.22) yield the equations of motion for the spring-, inertial- and damping forces.
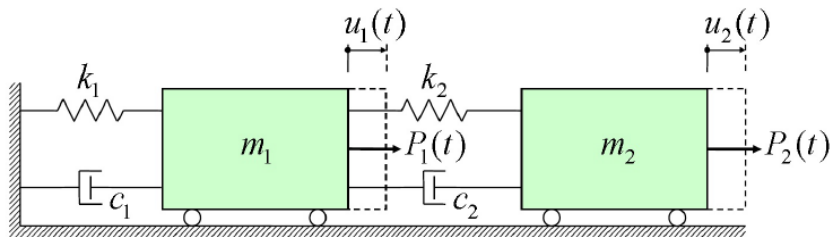


Figure 2.5: Schematic drawing of a two-degree of freedom system [1]

$$Spring\,forces \begin{cases} f_{s1} = k_1 u_1 \\ f_{s2} = k_2(u_2 - u_1) \end{cases} \tag{2.20}$$

$$Internal\,forces \begin{cases} f_{i1} = m_1 \ddot{u}_1 \\ f_{i2} = m_2 \ddot{u}_2 \end{cases} \tag{2.21}$$

$$Damping\,forces \begin{cases} f_{d1} = c_1 \dot{u}_1 \\ f_{d2} = c_2(\dot{u}_2 - \dot{u}_1) \end{cases} \tag{2.22}$$

The equation of motion for the two degrees of freedom system in Figure 2.5, can be written in matrix form as:

$$\begin{bmatrix} m_1 & 0 \\ 0 & m_2 \end{bmatrix} \begin{Bmatrix} \ddot{u}_1 \\ \ddot{u}_2 \end{Bmatrix} + \begin{bmatrix} (c_1 + c_2) & -c_2 \\ -c_2 & c_2 \end{bmatrix} \begin{Bmatrix} \dot{u}_1 \\ \dot{u}_2 \end{Bmatrix} + \begin{bmatrix} (k_1 + k_1) & -k_2 \\ -k_2 & k_2 \end{bmatrix} \begin{Bmatrix} u_1 \\ u_2 \end{Bmatrix} = \begin{Bmatrix} P_1(t) \\ P_2(t) \end{Bmatrix}$$

Which can be generalized as:

$$[\mathbf{M}]\{\ddot{\mathbf{u}}\} + [\mathbf{C}]\{\dot{\mathbf{u}}\} + [\mathbf{K}]\{\mathbf{u}\} = \{\mathbf{P}(t)\} \tag{2.23}$$

Where:

$[M]$     is the mass matrix

$[C]$     is the damping matrix

$[K]$     is the stiffness matrix

$\{P(t)\}$ is the vector of forcing functions

$\{u\}$     is the displacement vector

For civil engineering structures there are an infinite number of degrees of freedom, which can not be hand calculated. A method for solving complex structures is by using the Finite Element Method (FEM). FEM discretizes the structure into a finite number of elements connected by nodes, with a finite number of DOFs at each node. The solution obtained from FEM is an approximation, but can be estimated with great accuracy. To obtain the approximate structural response, the force vector and the mass-, damping- and stiffness matrices are needed. The equation of motion can be derived from the principle of virtual work. For a linear problem that is not time-dependent, the principle of virtual work yields:

$$\int_V \{\delta\boldsymbol{\epsilon}\}^T \{\boldsymbol{\sigma}\} dV = \int_V \{\delta\mathbf{u}\}^T \{\mathbf{F}\} dV + \int_S \{\delta\mathbf{u}\}^T \{\boldsymbol{\Phi}\} dS \tag{2.24}$$

Which yields the elemental stiffness matrix:

$$[\mathbf{k}] = \int_V [\mathbf{B}]^T [\mathbf{E}][\mathbf{B}]dV \tag{2.25}$$

Equation (2.24) gives the the internal work equals the external work, such that the load vectors $r$ are:

$$\{\mathbf{r}^{ext}\} = \int_V [\mathbf{N}]^T \{\mathbf{F}\}dV + \int_S [\mathbf{N}]^T \{\mathbf{\Phi}\}dS \tag{2.26}$$

$$\{\mathbf{r}^{int}\} = [\mathbf{k}]\{\mathbf{d}\} \tag{2.27}$$

Where $\{\mathbf{u}\} = [\mathbf{N}]\{\mathbf{d}\}$ is the displacement vector from the node displacements $\mathbf{d}$ and the interpolation functions between the nodes $\mathbf{N}$, known as shape functions. $\{\boldsymbol{\epsilon}\} = [\mathbf{B}][\mathbf{d}]$ is the strain vector where $[\mathbf{B}] = [\boldsymbol{\partial}][\mathbf{N}]$. $\{\boldsymbol{\sigma}\} = [\mathbf{E}]\{\boldsymbol{\epsilon}\}$ is the internal stress tensor from Hooke's law. $\delta\mathbf{u}$ is the virtual displacement vector and $\delta\boldsymbol{\epsilon}$ is the virtual strain vector. $\mathbf{F}$ and $\mathbf{\Phi}$ are the force vectors working on the structure nodes, and are body forces and surface tractions respectively.

The time-dependent terms are needed in the equation of motion for structural dynamics. The principle of virtual work yields:

$$\int_V \left( \{\delta\mathbf{u}\}^T \rho\{\ddot{\mathbf{u}}\} + \{\delta\mathbf{u}\}^T c\{\dot{\mathbf{u}}\} + \{\delta\boldsymbol{\epsilon}\}^T \{\boldsymbol{\sigma}\} \right) dV \tag{2.28}$$

$$= \int_V \{\delta\mathbf{u}\}^T \{\mathbf{F}\}dV + \int_S \{\delta\mathbf{u}\}^T \{\mathbf{\Phi}\}dS$$

Such that the matrices for mass and damping are obtained:

$$[\mathbf{m}] = \int_V \rho[\mathbf{N}]^T [\mathbf{N}]dV \tag{2.29}$$

$$[\mathbf{c}] = \int_V c[\mathbf{N}]^T [\mathbf{N}]dV \tag{2.30}$$

Where $\rho$ represents the mass density and $c$ is a damping parameter, and yields the equation of motion:

$$[\mathbf{m}]\{\ddot{\mathbf{d}}\} + [\mathbf{c}]\{\dot{\mathbf{d}}\} + \{\mathbf{r}^{int}\} = \{\mathbf{r}^{ext}\} \tag{2.31}$$

When representing the the global system in a Finite Element model, the same equation applies, but all elements are gathered into a singular matrix or vector, represented as capital letters, yielding:

$$[\mathbf{M}]\{\ddot{\mathbf{D}}\} + [\mathbf{C}]\{\dot{\mathbf{D}}\} + [\mathbf{K}]\{\mathbf{D}\} = \{\mathbf{R}^{ext}\} \tag{2.32}$$

## 2.3 Discretization in MDOF

A Finite Element solution performs a numerical analysis, and discretization of the matrices in the equation of motion is necessary.

### 2.3.1 Mass

Two possible solutions for distributing the mass in an FEA is through a consistent mass matrix or lumped mass matrix. The consistent mass matrix utilizes the shape functions $\mathbf{N}$ to distribute the mass along the element, while the lumped mass matrix divides the total element mass to act on the nodes. For a 2-node Euler-Bernouli Cubix beam element element with six DOFs, $\{\mathbf{d}\} = [u_1 \; v_1 \; \theta_1 \; u_2 \; v_2 \; \theta_2]^T$, the consistent mass matrix yields:

$$[\mathbf{m}] = \int_L \rho[\mathbf{N}]^T[\mathbf{N}]A dx$$

$$= \frac{mL}{420} \begin{bmatrix} 140 & 0 & 0 & 70 & 0 & 0 \\ 0 & 156 & 22L & 0 & 54 & -13L \\ 0 & 22L & 4L^2 & 0 & 13L & -3L^2 \\ 70 & 0 & 0 & 140 & 0 & 0 \\ 0 & 54 & 13L & 0 & 156 & -22L \\ 0 & -13L & -3L^2 & 0 & -22L & 4L^2 \end{bmatrix} \tag{2.33}$$

A lumped mass for 3-node Euler-Bernoulli cubic beam element with six DOFs with rotary inertia $\alpha$ yields:

$$[\mathbf{m}] = \frac{mL}{2} \begin{bmatrix} 1 & 0 & 0 & 0 & 0 & 0 \\ 0 & 1 & 0 & 0 & 0 & 0 \\ 0 & 0 & \alpha L^2 & 0 & 0 & 0 \\ 0 & 0 & 0 & 1 & 0 & 0 \\ 0 & 0 & 0 & 0 & 1 & 0 \\ 0 & 0 & 0 & 0 & 0 & \alpha L^2 \end{bmatrix} \tag{2.34}$$

The consistent mass matrix yields more accurate solutions, but the lumped mass matrix is often used as it significantly decreases the computational.

### 2.3.2 Stiffness

The elemental stiffness derived from the principle of virtual work is the general form of the elemental stiffness matrix. There are a wide variety of elements, all with different strain-displacement matrices $\{\mathbf{B}\} = [\partial][\mathbf{N}]$. An example of the basic 2-node beam elemental stiffness with six DOFs is shown i Equation (2.35).

$$[\mathbf{k}] = \int_V [\mathbf{B}]^T [\mathbf{E}][\mathbf{B}] dV = \begin{bmatrix} a & 0 & 0 & -a & 0 & 0 \\ 0 & 12b & -6bL & 0 & -12b & -6bL \\ 0 & -6bL & 4bL^2 & 0 & 6bL & 2bL^2 \\ -a & 0 & 0 & a & 0 & 0 \\ 0 & -12b & 6bL & 0 & 12b & 6bL \\ 0 & -6bL & 2bL^2 & 0 & 6bL & 4bL^2 \end{bmatrix} \tag{2.35}$$

Where $a = EA/L$ and $b = EI/L^3$. Just like for the mass, the accuracy and the computational cost is dependent on the choice of the element type. In a global system where the local element is rotated relative to the global axis, the local element matrix may be oriented through a transformation matrix when the global stiffness **K** is obtained.

### 2.3.3 Damping

As shown in Section 2.1, the damping dissipates energy of the structure when vibration occurs. Structural damping can be divided into two categories, viscous and non-viscous damping. Viscous damping dissipates the energy per cycle in vibration, such that the damping is proportional to the amplitude squared and frequency. Non-viscous damping can be categorized into three; hysteresis damping, coulomb damping and radiation damping. Hysteresis damping is internal damping that dissipates energy within the material, e.g. plastic deformation in the material. Coulomb damping is internal damping associated with dry friction, such as the structure slipping in joints. Radiation damping is external damping through energy loss to surrounding mediums, such as soil supporting the structure [6]. The damping in civil engineering structures is often considered small, and viscous damping is enough to sufficiently describe structural damping. The viscous damping is often represented by proportional damping and modal damping. Modal damping is where a mode is assigned its own value of the damping ratio. The viscous damping can easily be represented in a dynamic equation, and the formulation of the viscous damping was developed by Rayleigh, commonly known as Rayleigh damping.

**Rayleigh damping**

Rayleigh damping is a viscous damping proportional to a linear combination of mass and stiffness, shown in Equation (2.36) [7].

$$[\mathbf{C}] = \alpha[\mathbf{M}] + \beta[\mathbf{K}] \tag{2.36}$$

Where:

$\alpha$   is a the mass proportional Rayleigh damping coefficient, proportional to $\omega$

$\beta$   is the stiffness proportional Rayleigh damping coefficient, proportional to $\omega^{-1}$

The Rayleigh damping is widely used in structural analysis to model internal structural damping. If the damping ratios of two modes are known, the two damping coefficients $\alpha$ and $\beta$ can be obtained and implemented in the model from:

$$\xi_{i,n} = \frac{\alpha}{2\omega_i} + \frac{\beta\omega_n}{2} \tag{2.37}$$

Such that:

$$\alpha = \frac{2\xi_i\omega_i\omega_n^2 - 2\xi_n\omega_n\omega_i^2}{\omega_n^2 - \omega_i^2} \tag{2.38}$$

$$\beta = \frac{2\xi_n\omega_n - 2\xi_i\omega_i}{\omega_n^2 - \omega_i^2} \tag{2.39}$$
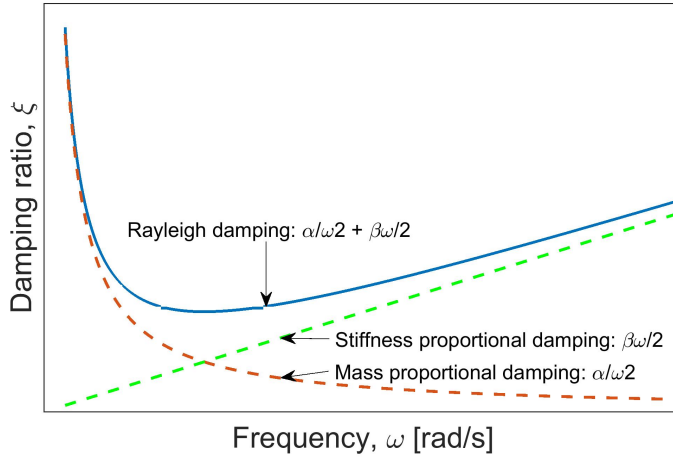


Figure 2.6: Rayleigh damping

The Rayleigh damping is dependent on the frequency where the higher frequencies are damped proportional to the stiffness damping, and must be operated carefully to avoid over-damping.

## 2.3.4 Free Vibration of MDOF Systems

When the damping $\mathbf{C}$ and external forces $\mathbf{R}^{ext}$ of a structure are zero and the nodal displacement associated with vibration are $\{\mathbf{D}\} = \{\overline{\mathbf{D}}\}sin(\omega t)$, where $\{\overline{\mathbf{D}}\}$ are the nodal amplitudes known as eigen vectors, the equation of motion yields the eigenvalue problem:

$$\left([\mathbf{K}] - \omega^2[\mathbf{M}]\right)\{\overline{\mathbf{D}}\} = 0 \tag{2.40}$$

Equation (2.40) is known as the dynamic stiffness matrix, where $\omega^2$ is the eigenvalue and $\omega$ is the natural frequency of the structure. Solving the eigenvalue problem yields a

vector with equal number of eigenvalues as there are degrees of freedom in the system. The Rayleigh quotient obtains the eigenvalues for any mode $i$ from multiplying the dynamic stiffness matrix Equation (2.40) with the nodal amplitudes $\{\overline{\mathbf{D}}\}$:

$$\omega_i^2 = \frac{\{\overline{\mathbf{D}}\}_i[\mathbf{K}]\{\overline{\mathbf{D}}\}_i}{\{\overline{\mathbf{D}}\}_i[\mathbf{M}]\{\overline{\mathbf{D}}\}_i} \tag{2.41}$$

## 2.4 Direct Integration Methods

Integration is needed when performing a dynamic analysis, and direct integration is used to calculate the response of history using step-by-step integration over time. If the nodal displacements $\mathbf{D}$ and velocities $\dot{\mathbf{D}}$ are known at time $t = 0$, the response at time $t = T$ can be estimated by direct integration. This requires discretization in time, where the time interval are equally dividing the whole time series into $n$ number of steps, such that $\Delta t = T/n$. A finite difference approximation is used on the derivatives of $\mathbf{D}$, such that the acceleration is integrated to find the velocities and displacement of the next step, as accelerations are assumed to vary over the time interval. The method of direct integration calculates the equation of motion at time step $n+1$, and depending on the assumption used to integrate the accelerations, different algorithms are developed to estimate the velocities and displacement at the end step. The algorithms can be classified as explicit or implicit. In explicit methods, the displacement $\mathbf{D}_{n+1}$ are obtained directly from the equilibrium at one or more preceding time steps. While in implicit methods, the displacements $\mathbf{D}_{n+1}$ are obtain indirectly from the equilibrium at the next time step $\mathbf{t}_{n+1}$. The following sections will discuss both methods and their appropriate applications.

### 2.4.1 Explicit Direct Integration

Explicit methods are conditionally stable, and requires that the time step $\Delta t$ to be less than a critical time step $\Delta t_{cr}$, so that the numerical process does not become unstable and "blows up". The number of time intervals can be rather large, but each time step can be executed quickly. If the mass is considered lumped, like shown in Equation (2.34), the calculation can be executed even faster [8].

The explicit dynamic algorithm is based on the Taylor series expansion of the displacement $u$ at time step $n + 1$ and $n - 1$ for a SDOF system:

$$u_{n+1} = u_n + \Delta t \dot{u}_n + \frac{\Delta t^2}{2}\ddot{u}_n + \frac{\Delta t^3}{6}\dddot{u}_n + \cdots \tag{2.42}$$

$$u_{n-1} = u_n - \Delta t \dot{u}_n + \frac{\Delta t^2}{2}\ddot{u}_n - \frac{\Delta t^3}{6}\dddot{u}_n + \cdots \tag{2.43}$$

From adding and subtracting the two equations above and disregarding higher order terms, the conventional central difference equations are obtained, which are approximations

of the velocity and acceleration:

$$\dot{u}_n = \frac{u_{n+1} - u_{n-1}}{2\Delta t} \tag{2.44}$$

$$\ddot{u}_n = \frac{u_{n+1} - 2u_n + u_{n-1}}{\Delta t^2} \tag{2.45}$$

Substituting into the equation of motion and sorting the terms yields:

$$\left(\frac{m}{\Delta t^2} + \frac{c}{2\Delta t}\right)u_{n+1} = P_n - \left(\frac{m}{\Delta t^2} - \frac{c}{2\Delta t}\right)u_{n-1} - \left(k - \frac{2m}{\Delta t^2}\right)u_n \tag{2.46}$$

The equation above is also valid for an MDOF system, and can be neatly rewritten to obtain the displacement at time $n + 1$, such that:

$$\{\mathbf{D}\}_{n+1} = [\mathbf{K}^{eff}]^{-1}\{\mathbf{R}^{eff}\}_n \tag{2.47}$$

Where:

$$[\mathbf{K}]^{eff} = \frac{1}{\Delta t^2}[\mathbf{M}] + \frac{1}{2\Delta t}[\mathbf{C}] \tag{2.48}$$

And

$$\{\mathbf{R}^{eff}\}_n = \{\mathbf{R}^{ext}\} - \left(\frac{1}{\Delta t^2}[\mathbf{M}] - \frac{1}{2\Delta t}[\mathbf{C}]\right)\{\mathbf{D}\}_{n-1} - \left([\mathbf{K}] - \frac{2}{\Delta t^2}[\mathbf{M}]\right)\{\mathbf{D}\}_n \tag{2.49}$$

If the mass and and damping matrices $\mathbf{M}$ and $\mathbf{C}$ are not diagonal, the effective stiffness $\mathbf{K}^{eff}$ must be calculated and factorized to obtain the displacement $\mathbf{D}_{n+1}$, which greatly increases the computational cost per time step. The explicit methods are good for analysis over a short time span, like contact, fracture or impact problems, because of the cost efficient calculation for each time step. This requires that the damping is present for high frequencies, such that the stiffness proportional damping $\mathbf{C} = \beta\mathbf{K}$ is included. In order to compute the displacements $\mathbf{D}_{n+1}$ without sacrificing the cost effectiveness, computation of the stiffness for each time step can be bypassed by introducing the preferred form of the central difference method, known as half-step central differences. The half-step central differences lags the velocity half a time step, such that:

$$\dot{u}_{n+\frac{1}{2}} = \frac{1}{\Delta t}(u_{n+1} - u_n) \tag{2.50}$$

$$\dot{u}_{n-\frac{1}{2}} = \frac{1}{\Delta t}(u_n - u_{n-1}) \tag{2.51}$$

Following the same procedure as before, finding acceleration at time step $n$, intergrating and inserting into the equation of motion, the equation of motion for an MDOF system can be written as:

$$\frac{1}{\Delta t^2}[\mathbf{M}]\{\mathbf{D}\}_{n+1} = \{\mathbf{R}^{ext}\}_n - \{\mathbf{R}^{int}\}_n + \frac{1}{\Delta t^2}[\mathbf{M}]\left(\{\mathbf{D}\}_n + \Delta t\{\dot{\mathbf{D}}\}_{n-\frac{1}{2}}\right) - [\mathbf{C}]\{\dot{\mathbf{D}}\}_{n-\frac{1}{2}}$$
(2.52)

Where $\{\mathbf{R}^{int}\}_n = [\mathbf{K}]\{\mathbf{D}_n\}$ if linear conditions applies.

As mentioned earlier in this section, due to the quick calculation of each time step and the generally small time steps due to the conditionally stable criteria $\Delta t \leq \Delta t_{cr}$, the explicit methods are ideal for high speed dynamic simulations. It is worth noting that with time step $\Delta t$ only slightly smaller than $\Delta t_{cr}$ yields the most accurate results in the explicit method, and that the cost efficiency per time step is increased by enforcing diagonal mass and damping matrices.

## 2.4.2 Implicit Direct Integration

The most common implicit methods in use are unconditionally stable, such that the numerical process is stable for all sizes of the time step interval $\Delta t$. The implicit methods are calculating the equilibrium at the next time step, an the equation solving per time step is therefore more cost expensive than the explicit methods [9].

Starting with an SDOF system, and letting $\tau$ be a time within the time interval $\Delta t$ such that $0 \leq \tau \leq \Delta t$.
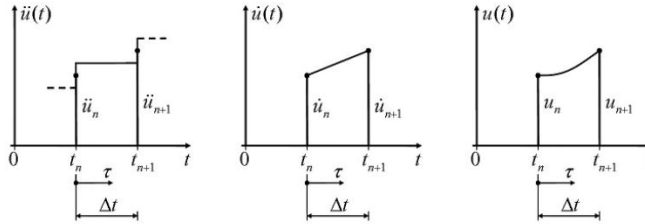


(a) Constant Acceleration.
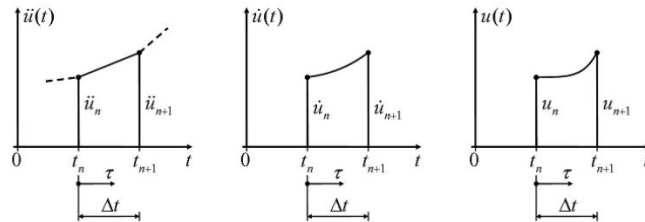
(b) Linear Acceleration.

Figure 2.7: Time steps with constant and linear accelerations and their integrals

17

Consider a constant average acceleration over the time step $\Delta t$:

$$\ddot{u}(\tau) = \frac{1}{2}(\ddot{u}_{n+1} + \ddot{u}_n) \tag{2.53}$$

Obtain the velocity and displacement through integration where the boundary conditions are $\dot{u}(\tau = 0) = \dot{u}_n$ and $u(\tau = 0) = u_n$

$$\dot{u}(\tau) = \dot{u}_n + \frac{\tau}{2}(\ddot{u}_{n+1} + \ddot{u}_n) \tag{2.54}$$

$$u(\tau) = \tau \, \dot{u}_n + \frac{\tau^2}{4}(\ddot{u}_{n+1} + \ddot{u}_n) \tag{2.55}$$

Obtain the velocities and displacement at time step $n + 1$ is done by setting $\tau$ to the end of the time interval, $\tau = \Delta t$, such that:

$$\dot{u}_{n+1} = \dot{u}_n + \frac{\Delta t}{2}(\ddot{u}_{n+1} + \ddot{u}_n) \tag{2.56}$$

$$u_{n+1} = u_n + \frac{\Delta t}{2}(\dot{u}_{n+1} + \dot{u}_n) \tag{2.57}$$

Then, consider a linear acceleration with the same boundary conditions as before:

$$\ddot{u}(\tau) = \ddot{u}_n + \frac{\tau}{\Delta t}(\ddot{u}_{n+1} - \ddot{u}_n) \tag{2.58}$$

$$\dot{u}(\tau) = \dot{u}_n + \tau \, \ddot{u}_n + \frac{\tau^2}{2\Delta t}(\ddot{u}_{n+1} - \ddot{u}_n) \tag{2.59}$$

$$u(\tau) = u_n + \tau \, \dot{u}_n + \frac{\tau^2}{2}\ddot{u}_n + \frac{\tau^3}{6\Delta t}(\ddot{u}_{n+1} - \ddot{u}_n) \tag{2.60}$$

Velocities and displacement at time step $n + 1$ are obtained by substituting $\tau = \Delta t$:

$$\dot{u}_{n+1} = \dot{u}_n + \frac{1}{2}\Delta t\big(\ddot{u}_{n+1} + \ddot{u}_n\big) \tag{2.61}$$

$$u_{n+1} = u_n + \Delta t \, \dot{u}_n + \Delta t^2 \Big(\frac{1}{6}\ddot{u}_{n+1} + \frac{1}{3}\ddot{u}_n\Big) \tag{2.62}$$

The use of the difference equations in Equation (2.61) and (2.62) from linear acceleration is preferable to constant average acceleration because of greater accuracy and continuity of the acceleration. However, the difference equations from linear acceleration are conditionally stable, while the difference equations from constant average acceleration are unconditionally stable. The two methods for obtaining difference equations can be generalized into a single set of equations for velocity and displacement at time step $n + 1$ with the Newmark Method. Introducing the parameters $\gamma$ and $\beta$ such that the difference

equations from linear and constant average acceleration over the time step can be described as [10]:

$$\dot{u}_{n+1} = \dot{u} + \Delta t\big(\gamma\ddot{u}_{n+1} + (1-\gamma)\ddot{u}_n\big) \tag{2.63}$$

$$u_{n+1} = u_n + \Delta t\, \dot{u}_n + \frac{\Delta t^2}{2}\big(2\beta\ddot{u}_{n+1} + (1-2\beta)\ddot{u}_n\big) \tag{2.64}$$

Such that:

$\gamma = \frac{1}{2}$, $\beta = \frac{1}{4}$ gives constant average acceleration method

$\gamma = \frac{1}{2}$, $\beta = \frac{1}{6}$ gives linear acceleration method

From the Newmark method the accelerations and velocities are obtained:

$$\ddot{u}_{n+1} = \frac{1}{\beta\Delta t^2}\big(u_{n+1} - u_n - \Delta t\, \dot{u}_n\big) - \Big(\frac{1}{2\beta} - 1\Big)\ddot{u}_n \tag{2.65}$$

$$\dot{u}_{n+1} = \frac{\gamma}{\beta\Delta t}\big(u_{n+1} - u_n\big) - \Big(\frac{\gamma}{\beta} - 1\Big)\dot{u}_n - \Delta t\Big(\frac{\gamma}{2\beta} - 1\Big)\ddot{u}_n \tag{2.66}$$

The displacements and its derivatives can be obtained the same way for an MDOF system by substituting $u_n$ with $\mathbf{D}_n$, $\dot{u}_n$ with $\dot{\mathbf{D}}_n$, etc:

$$\{\ddot{\mathbf{D}}\}_{n+1} = \frac{1}{\beta\Delta t^2} + \Big(\{\mathbf{D}\}_{n+1} - \{\mathbf{D}\}_n - \Delta t\{\dot{\mathbf{D}}\}_{n+1}\Big) - \Big(\frac{1}{2\beta} - 1\Big)\{\ddot{\mathbf{D}}\}_n \tag{2.67}$$

$$\{\dot{\mathbf{D}}\}_{n+1} = \frac{\gamma}{\beta\Delta t} + \Big(\{\mathbf{D}\}_{n+1} - \{\mathbf{D}\}_n\Big) - \Big(\frac{\gamma}{\beta} - 1\Big)\{\dot{\mathbf{D}}\}_n - \Delta t\Big(\frac{1}{2\beta} - 1\Big)\{\ddot{\mathbf{D}}\}_n \tag{2.68}$$

Finally substituting the difference equations from the Newmark method into the MDOF equation of motion (2.32) to obtain:

$$\{\mathbf{D}\}_{n+1} = [\mathbf{K}^{eff}]^{-1}\{\mathbf{R}^{eff}\}_{n+1} \tag{2.69}$$

Where

$$[\mathbf{K}^{eff}] = \frac{1}{\beta\Delta t^2}[\mathbf{M}] + \frac{\gamma}{\beta\Delta t}[\mathbf{C}] + [\mathbf{K}] \tag{2.70}$$

$$\begin{aligned}
\{\mathbf{R}^{eff}\} = \{\mathbf{R}^{ext}\}_{n+1} \\
+ [\mathbf{M}]\Big(\frac{1}{\beta\Delta t^2}\{\mathbf{D}\}_n + \frac{1}{\beta\Delta t}\{\dot{\mathbf{D}}\}_n + \Big(\frac{1}{2\beta} - 1\Big)\{\ddot{\mathbf{D}}\}_n\Big) \\
+ [\mathbf{C}]\Big(\frac{\gamma}{\beta\Delta t}\{\mathbf{D}\}_n + \Big(\frac{\gamma}{\beta} - 1\Big)\{\dot{\mathbf{D}}\}_n + \Delta t\Big(\frac{\gamma}{2\beta} - 1\Big)\{\ddot{\mathbf{D}}\}_n\Big)
\end{aligned} \tag{2.71}$$

From Equation (2.70) it is observed that the effective stiffness $\mathbf{K}^{eff}$ is never diagonal due to the stiffness $\mathbf{K}$ term. Meaning that the implementation of diagonal mass and/or damping matrices does little to improve the cost effectiveness, and that if nonlinearities

happen in the time step the effective stiffness $\mathbf{K}^{eff}$ must be calculated for each time step. The implicit methods are ideal for analysis where the response period $T$ of interest are long, because of the unconditionally stable linear average acceleration, e.g. plasticity problems where nonlinearities are smooth, or for a pedestrian walking across a footbridge. The accuracy of the implicit methods are also improved compared to the explicit, as the effective stiffness matrix $\mathbf{K}^{eff}$ may be updated for every time step.

The integration method is conditionally stable for time step $\Delta t < \Delta t_{cr}$. The critical time step $\Delta t_{cr}$ is calculated from the Newmark parameters $\gamma$ and $\beta$, such that:

$$\Delta t_{cr} \leq \frac{\Omega_{crit}}{\omega_{max}} \tag{2.72}$$

Where:

$$\Omega_{crit} = \frac{\xi\left(\gamma - \frac{1}{2}\right) + \sqrt{\frac{\gamma}{2} - \beta + \xi^2\left(\gamma - \frac{1}{2}\right)^2}}{\frac{\gamma}{2} - \beta} \tag{2.73}$$

$\omega_{max}$ is the highest natural frequency from the eigenvalue problem

$\xi$      is the damping ratio.

A generalization of the Newmark methods, known as the HHT $\alpha$-method, is recommended to account for damping at high frequencies without sacrificing accuracy. Numerical damping in the Newmark methods only assures a first degree accuracy, while the HHT $\alpha$-method assures a second order accuracy for algorithmic damping [11]. The HHT $\alpha$-method yields an alternative Newmark method of the equation of motion with the introduction of the parameter $\alpha_H$:

$$\begin{aligned}
\{\mathbf{R}_\alpha^{ext}\} = {}& [\mathbf{M}]\{\ddot{\mathbf{D}}\}_{n+1} \\
& + (1 + \alpha_H)[\mathbf{C}]\{\dot{\mathbf{D}}\}_{n+1} - \alpha_H[\mathbf{M}]\{\ddot{\mathbf{D}}\}_n \\
& + (1 + \alpha_H)[\mathbf{K}]\{\mathbf{D}\}_{n+1} - \alpha_H[\mathbf{K}]\{\mathbf{D}\}_n
\end{aligned} \tag{2.74}$$

Where $\mathbf{R}_\alpha^{ext}$ is $\mathbf{R}^{ext}$ at time $(1+\alpha_H)t_{n+1} - \alpha_H t_n = t_{n+1} + \alpha_H\Delta t$. The HHT $\alpha$-method is unconditionally stable when:

$$-\frac{1}{3} \leq \alpha_H \leq 0, \ \gamma = \frac{1}{2}(1 - 2\alpha_H) \ and \ \beta = \frac{1}{4}(1 - \alpha_H)^2$$

## 2.5 Fourier Transforms

This section is based on earlier work done for NTNU, by the authors of the thesis.

### 2.5.1 Classical Fourier Transform

The Fourier transform is a generalization of the complex Fourier series, an expansion of a periodic function $f(t)$ in terms of an infinite sum of sines and cosines as the length approaches infinity [12].

The Fourier transform turns a function the time domain into a function in the frequency domain [13]. The classical theory of the Fourier transform and its transverse is defined in Equation (2.75) and (2.76):

$$F(\omega) = \frac{1}{2\pi} \int\limits_{-\infty}^{\infty} f(t)e^{-i\omega t} d\omega \tag{2.75}$$

$$f(t) = \int\limits_{-\infty}^{\infty} F(\omega)e^{i\omega t} dt \tag{2.76}$$

For the classical Fourier theory to be true, several conditions has to be satisfied. For engineering applications, the condition with the biggest impact is:

$$\int\limits_{-\infty}^{\infty} |f(t)| dt < \infty \tag{2.77}$$

Such that the classical theory only applies to functions which goes to zero when time goes to infinity, such that Equation (2.77) is satisfied.

### 2.5.2 Discrete Fourier Transform

Gathered stochastic response data from structures lies in the time domain, and in order to do a modal response analysis it is necessary to change it into the frequency domain. If the data series are not continuous, the classical Fourier theory Equation (2.75) cannot be used. For cases like this, the Discrete Fourier Transform (DFT) is introduced, shown in Equation (2.78). The DFT makes it possible to do a modal response analysis of sampled values. The DFT is defined for discrete time series where $x(t)$ is sampled over a time period, $T$, with constant sampling intervals, $\Delta$.

$$X_k = \frac{1}{N} \sum_{k=0}^{N-1} x_r e^{-i2\pi \frac{kr}{N}} \tag{2.78}$$

$$x_r = \sum_{k=0}^{N-1} X_k e^{i2\pi \frac{kr}{N}} \tag{2.79}$$

Where:

$X_r$  is the discrete value of $x(t)$ at time $t = r\Delta$

$N$  is the total number of samples measured over the time period $T = \Delta N$

$r$  is the number of the sample $r = 0, 1, 2, ..., N - 1$

$k$  is the frequency component $k = 0, 1, 2, ..., N - 1$

$\Delta$  is the constant interval between each sample

### 2.5.3  Fast Fourier Transform

When $X_r$ is worked out directly using the DFT, $N^2$ operations are performed. In order to decrease the number of operations, the Fast Fourier Transform (FFT) is introduced. FFT is an algorithm used to calculate the DFT's which reduces the number of operations considerably, in addition to increase the accuracy [13]. By applying the FFT the accuracy increases as a result of less round-off errors, and $X_k$ is obtained after $N log_2 N$ operations.

## 2.6  Spectral Density

This section is based on earlier work done for NTNU, by the authors of the thesis.

The spectral density describes the signals energy distribution over the frequency, and is found from the Fourier transform of the auto-correlation function $R_{ii}$. A Fourier transform of the auto-correlation gives the auto-spectral density, and a Fourier transform of the cross correlation $R_{ij}$ gives the cross spectral density, as shown in Equation (2.80) and (2.81).

$$S_{xx}(\omega) = \frac{1}{2\pi} \int\limits_{-\infty}^{\infty} R_{xx}(\tau) e^{-i\omega t} d\tau \tag{2.80}$$

$$S_{xy}(\omega) = \frac{1}{2\pi} \int\limits_{-\infty}^{\infty} R_{xy}(\tau) e^{-i\omega t} d\tau \tag{2.81}$$

The auto-spectral density, $S_{xx}(\omega)$, gives a representation of the density of the variance of a stochastic signal [13]. Because the Fourier transform is an integration from $-\infty$ to $\infty$ and $R_{xx}$ is an even function, the auto spectrum will only consist of real values. While the cross spectrum will include imaginary values, as the cross correlation, $R_{xy}$, is a odd function [14].

The response spectrum transitions the broad band characteristics of the spectral density into a narrow banded response spectrum, the peaks of the graph represent the natural frequencies of the system. The response spectrum is connected with the spectral density by Equation (2.82) and (2.83).

$$S_{yy}(\omega) = H(\omega)^H S_{xx}(\omega) H(\omega) \tag{2.82}$$

$$S_{\ddot{y}\ddot{y}} = \omega^4 H(\omega)^H S_{xx}(\omega) H(\omega) \tag{2.83}$$

Where $S_{xx}$ is the load spectrum and $H(\omega)$ is the complex Frequency Response Function (FRF). The FRF described the relation between an input signal $X(\omega)$ and an output signal $Y(\omega)$ in the frequency domain [13]:

$$H(\omega) = \frac{Y(\omega)}{X(\omega)} \tag{2.84}$$

For discrete times series, the input $X(\omega)$ and an output signal $Y(\omega)$ can be calculated using the DFT. The spectral density $S_{xx}(\omega)$ from a discrete time series $x(t)$ can be obtained from:

$$S_{xx}(\omega) = \frac{1}{N} \left| \sum_{n=0}^{N-1} x(n) e^{-\frac{2\pi i \omega n}{N}} \right|^2 \tag{2.85}$$

Where N is the number of discrete values in the signal.

## 2.7 Dynamic Load Factor

The Dynamic load factor (DLF) is a factor used to illustrate a dynamic load by using a static load. The static load is multiplied with the DLF, and the multiplication is assumed to account for variance in the load due to dynamic events such as vibration. The DLF can be defined as:

$$Dynamic\ load\ =\ Static\ load\ x\ Dynamic\ load\ factor$$

## 2.8 Dirac Delta Function

The Dirac Delta function is a distribution which express a real number line which has the value zero everywhere except at zero. The function is used in some of the load models which will be presented in later chapters, and given in Equation (2.86), and illustrated in figure 2.8 [15].

$$\delta(z - z_p(t)) \tag{2.86}$$

The function is defined by:

$$\delta(t) = \begin{cases} 0 & t \neq 0 \\ \infty & t = 0 \end{cases}$$
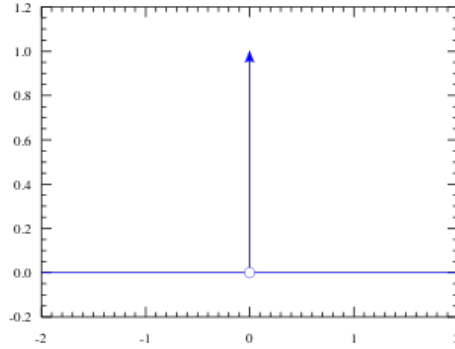
Figure 2.8: Delta Dirac Function

With:

$$\int_{t_1}^{t_2} dt \delta(t) = 1 \tag{2.87}$$

If $O \in [t_1, t_2]$ it has an infinitely high peak at the origin, $t = 0$, and the function can be seen as a Gaussian limit (2.88), or Lorentzian limit (2.8):

$$\delta(t) = \lim_{\sigma \to 0} \frac{1}{\sqrt{2\pi}\sigma} e^{-t^2/2\sigma^2} \tag{2.88}$$

$$\delta(t) = \lim_{\sigma \to 0} \frac{1}{\pi} \frac{\epsilon}{t^2 + \epsilon^2} \tag{2.89}$$

The graph is infinitely high with an infinitely thin spike at the origin, and an area of unity under the spike, and the Dirac delta function is a hypothetical function. When used in load models, the Dirac delta function represents the density of an idealized point mass. The most important property of the Dirac delta function is to express that $\delta(t)$ vanishes for all values except $t = 0$, and from this follows:

$$\int dt f(t) \delta(t) = f(0) \tag{2.90}$$

$$f(t)\delta(t) = f(0)\delta(t) \tag{2.91}$$

$f(0)$ is independent of the time, and can therefore be found outside the integral as:

$$\int dt f(t) \delta(t - t_0) = f(t_0) \tag{2.92}$$

## 2.9 Monte Carlo Simulations

Monte Carlo (MC) simulations are a way of modelling the probability of a the different outcomes of a process which has a large amount of random variables and therefore are too complicated to solve analytically [2]. MC takes the average of repeated random samplings,

in order to obtain numerical results to solve problems which are deterministic in principle. MC simulations makes it possible to simulate a process with many complex factors, in 4 steps [16].

1. Establish a mathematical model for the process.

2. Define the mean and standard deviation (a probability distribution) for each factor in the model.

3. Create random data of the factors, using the parameters found in (2)

4. Simulate and analyze the output of the process

The results are calculated several times, each time using a different set of random values from the probability functions. MC simulations are ideal for simulation of pedestrian loads and prediction of footbridge response given that the probability distribution of the parameters are know. Parameters like walking frequency, pedestrian weight, force and speed amplitude will then be found from an appropriate probability distribution [17]. The simulation of the load can be generated with respect to the distribution of each parameter characterizing the load. When the simulation of the stochastic load is generated, the response of a bridge with can be found by solving the equation of motion [18].

# Chapter 3

# Signal Processing and Modal Analysis

Performing measurements on a structure requires precision and patience. The recording equipment has to be installed correctly according to location and relative axis-system. It is important to avoid disturbing the equipment while performing a recording, e.g. disconnection or movements, such that a continuous data series is obtained. Recording data continuously for a couple of hours several times is often required to obtain sufficient data to perform a modal analysis. A modal analysis is performed to identify the structures response to vibration, such as the resonating frequencies, modal shapes and damping. The methodology of how to obtain these modal properties are discussed throughout this chapter.

## 3.1   Welch Method

This section is based on earlier work done for NTNU, by the authors of the thesis.

The power spectral density for stochastic processes, will often contain a lot of of noise. In order to decrease the noise, the Welch method can be used. The Welch method decreases the noise of the power spectral density by preforming the power spectral estimate combining spectral windowing and the FFT. The method is based on overlapped segments and averaging of modified periodograms [19].

When applying the Welch method, the data series are first divided into $n$ overlapping segments of length $l$, and for each segment the response spectrum is calculated individually. The outer parts of the response spectra are dependent of the close by spectra and will therefore increase the noise. In order to avoid this, a modified periodogram window is

applied to each spectrum, e.g. the Hann window in Figure 3.1, and the periodograms are averaged.

Using Welch method reduces the variance associated with the periodogram estimate and power spectrum. When independent quantities are averaged the variance is cut by one over the average quantity. The disadvantage with using Welch method is that when the signals, to which the FFT is applied, are shortened and averaged, the spectra are low-passed and thus the peaks appear less narrow [20]. The length of the segments will influence the estimate reliability and frequency resolution [21]. Short segments produce the most averages, which results in less noise and a smooth spectrum with good variance properties. Long segments on the other hand produce the best frequency resolution, but the worst variance properties [22, 20].
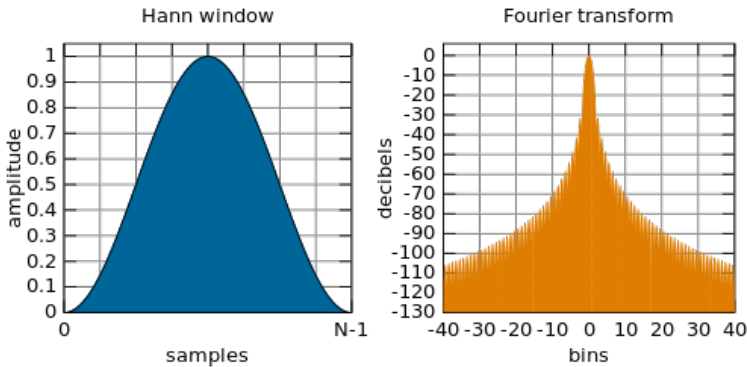


Figure 3.1: Hann function and its frequency response

## 3.2 Peak Piking Method

A peak-picking method is used to identify the natural frequencies of a structure. The peak-picking method is applied to the response spectrum from measurement data, where the natural frequencies are identified at peaks in the response spectrum plot [23]. Measurement data are commonly found with accelerometers to record vibrations. The vertical and horizontal natural frequencies are obtained from the measurement data through a FFT. While the torsional natural frequencies are obtained from FFT after combining vertical data into angular data. The natural frequencies obtained from the peak-picking method is further used in the modal analysis to obtain modal shapes and damping.

Figure 3.2 and 3.3 illustrates peak picking method applied to the response spectrum of the measurement data from Bårdshaug Bridge, in the vertical direction. Bårdshaug Bridge will be further discussed in Chapter 6.
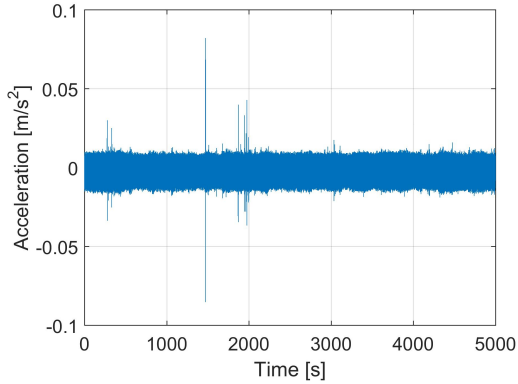
Figure 3.2: Acceleration from measurement data
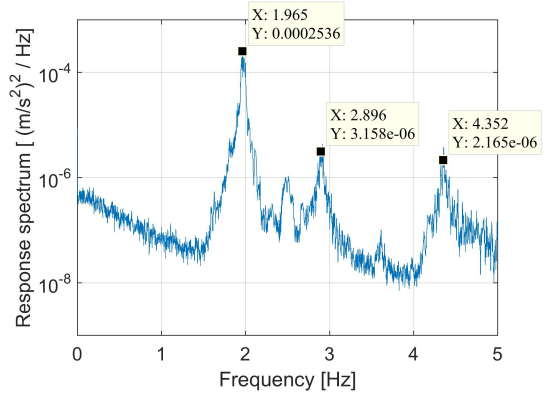
Figure 3.3: Response spectrum of the measurement data

## 3.3 Identifying Modes

To identify the mode shapes from the natural frequencies the measurement data the auto- and cross response spectrum are used. The auto response spectrum value for a specific natural frequency is picked from each sensor across the bridge's length before it is normalized. The auto response spectrum does not contain any negative values, so the sign of the values must be found to obtain the modal shape. It is not possible to correctly tell if two separate points are moving in the same or opposite direction for a modal shape, i.e. in phase or in anti-phase in the response spectrum. To determine if different measuring points are in phase or in anti-phase the cross spectrum is used. The cross spectrum contains a complex quantity where the angle between the real and complex values are used to determine if two nodes are in phase or 180 degrees out of phase. For values at approximately 0 or 180 degrees at the natural frequency the sign is obtained [24]. The modal shape is dependent on the the number of sensors on the bridge, as well as the location of these sensors. Figure 3.4 illustrates an example of the phase-spectrum.
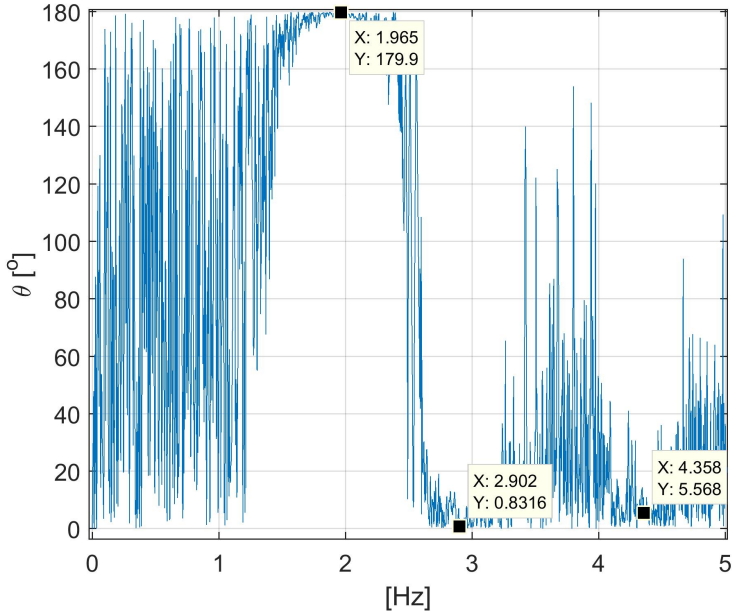
Figure 3.4: Phase-spectrum from measurement data of Bårdshaug Bridge

Finding the relative motion and normalizing the auto response spectrum density for all measurement points on the bridge, the modal shape is finally obtained. Examples of mode shapes from Bårdshaug Bridge are shown in Figure 3.5 and 3.6.
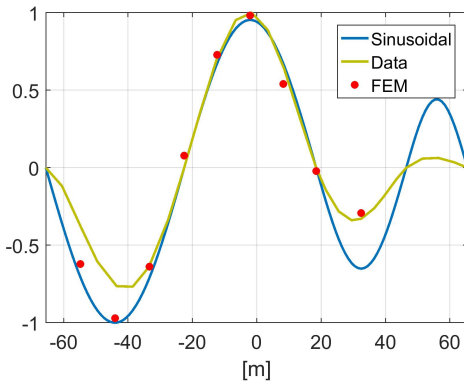


Figure 3.5: Vertical mode shape for natural frequency 1.97 Hz of Bårdshaug Bridge
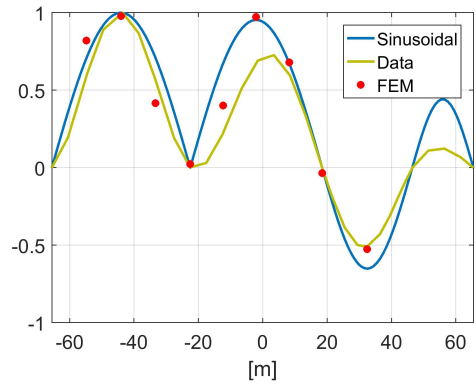


Figure 3.6: Vertical mode shape for natural frequency 2.92 Hz of Bårdshaug Bridge

## 3.4 Damping

The damping is a major part of the structural design and describes how the energy is dissipated through friction in joints and supports and the material itself. Damping is a desired dynamic property for civil engineering structures to reduce the response of structures when excited. The damping ratio for concrete and steel pedestrian bridges is expected to be at a level below 1 % [25].

**Logarithmic decrement**

Finding the damping of a civil engineering structure can be done by exciting the structure at the natural frequency of the structure and record the acceleration while it is falling to rest, as illustrated in Figure 3.7. The damping ratio is represented as linear viscous damping form the decaying acceleration in a logarithmic plot, see Figure 3.8. The acceleration damping is assumed exponential:

$$Y = ae^{-nt} \tag{3.1}$$

$$y = ln(a) - nt \tag{3.2}$$

and the damption ratio is found:

$$\xi = \frac{n}{\omega_n} \tag{3.3}$$
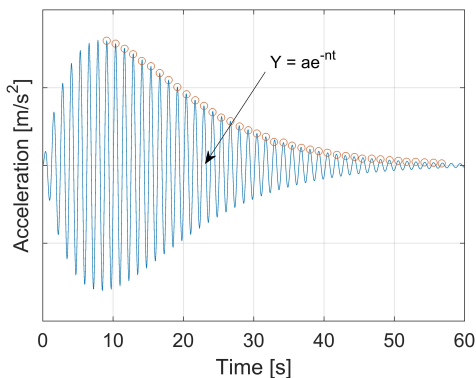


Figure 3.7: Example of acceleration including peak values
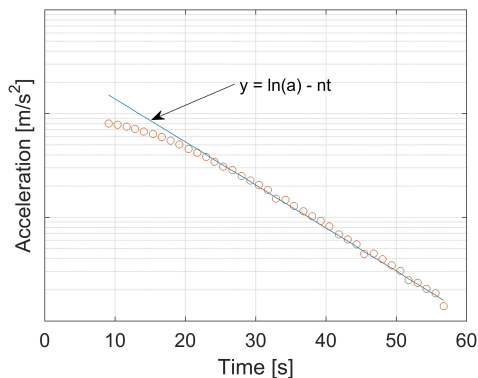
Figure 3.8: Logarithmic linearization of peak values from Figure 3.7

**Half power bandwidth method**

For a mathematical model of a structure the damping ratio is easily estimated by applying a dynamic load with the natural frequency of the structure and making it fall to rest.

However, it is difficult to manually excite a real structure such that the acceleration decays of free motion. Estimation of the damping ratio from measurement data can instead be found from using the half power bandwidth method. This is beneficial because the applied loads does not have to occur at a natural frequency of the structure. The half power bandwidth uses the frequency response spectrum or the response auto-spectrum around a narrow-banded peak to determine the damping. Letting $\omega_1$ and $\omega_2$ be two frequencies on each side of the natural frequency $\omega_n$ such that [26]:

$$\frac{1}{2}|H(\omega_n)|^2 = |H(\omega_1)|^2 = |H(\omega_2)|^2 \tag{3.4}$$

The dynamic response factor at $\omega_1$ and $\omega_2$ shall be $\frac{1}{\sqrt{2}}$ times the amplitude at the resonating frequency $\omega_n$.
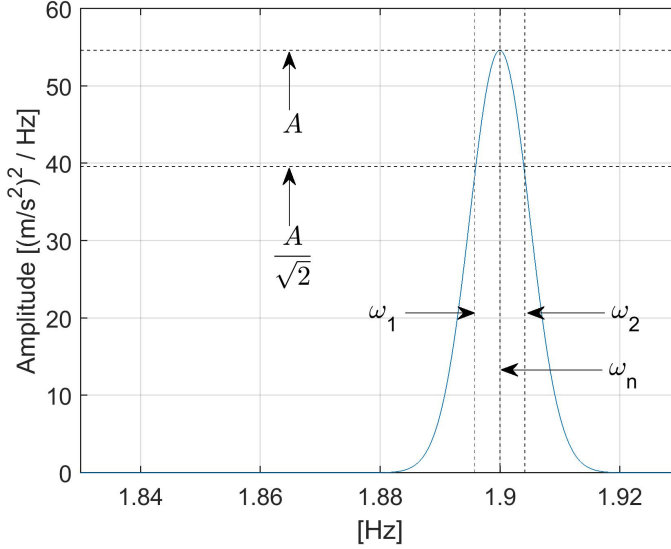


Figure 3.9: Half power bandwidth

The expression from Equation 3.4 becomes:

$$\frac{1}{\sqrt{[1 - (\frac{\omega}{\omega_n})^2]^2 + [2\xi\frac{\omega}{\omega_n}]^2}} = \frac{1}{\sqrt{2}}\frac{1}{2\xi\sqrt{1 - \xi^2}} \tag{3.5}$$

With the assumption of small damping ratio, Equation (3.5) can be rewritten as

$$\xi = \frac{\omega_2 - \omega_1}{2\omega_n} \tag{3.6}$$

Where:

$\xi$     is the damping ratio [-]

$\omega_n$    is the natural frequency

$\omega_{1,2}$ is the frequency on both sides of the resonating frequency where the dynamic response factor is $\frac{1}{\sqrt{2}}$ times the amplitude at the resonating frequency

The half power bandwidth has to be performed with caution due to the uncertainties of the measurement data, making the width of the frequency response function or the auto-spectrum inaccurate. Determining the damping ratio from decaying acceleration is therefore a preferred method. Despite the inaccurate nature of the half power bandwidth method, it is commonly used to obtain the damping ratio of higher order modes as these are difficult to manually excite such that the structure reliably falls to rest.

## 3.5 Model Assurance Criterion

The Model Assurance Criterion (MAC) is a statistical indicator to compare mode shapes, and a helpful tool when performing a modal analysis [27]. The method is often used when comparing a mathematical model with data obtained from experiments. The MAC compares consistency between modal shapes. It is obtained a value between 0 and 1, 1 yields perfect correspondence between the modal shapes, and 0 yields no correspondence. The MAC is calculated by normalizing the scalar product of two sets of modal shape vectors and yields the MAC matrix, which can be illustrated in a 3D-plot, see Figure 3.10 [28]:

$$MAC_{ij} = \frac{|\sum\limits_{q=1}^{N_0} \psi_{Ai}\psi_{Xj}^*|^2}{\sum\limits_{q=1}^{N_0} \psi_{Ai}\psi_{Ai}^* \sum\limits_{q=1}^{N_0} \psi_{Xj}\psi_{Xj}^*} \tag{3.7}$$

or:

$$MAC_{ij} = \frac{(\{\psi_A\}_i^T\{\psi_X\}_j^*)^2}{\{\psi_A\}_i^T\{\psi_A\}_i^*\{\psi_X\}_j^T\{\psi_X\}_j^*} \tag{3.8}$$

Where:

$\psi_{A_i}$ is the mode shape vector $i$ from source A

$\psi_{X_j}$ is the mode shape vector $j$ from source X

$\psi^*$ is the complex conjugate

Every mode shape found from the two sources are compared with each other. A MAC of a value greater than 0.9 indicate consistent correspondence.
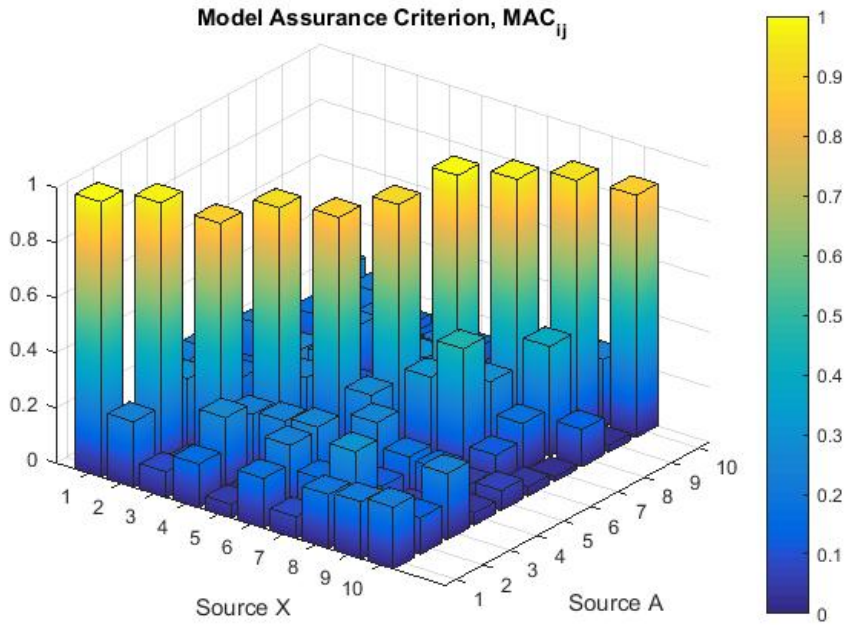
Figure 3.10: Visualization of $\text{MAC}_{ij}$ matrix for ten modes, where source A and X have consistent correspondence for the modal shapes when i = j

# Chapter 4

# Pedestrian Induced Forces

Pedestrian induced loads are complex and dependent on several variables, where the most important factors are weight, step length and walking frequency [2]. The exact movement of a human is hard to predict, especially for a structure in resonance. In order to calculate the dynamic behaviour of a pedestrian bridge, a good load model has to be be applied to the finite element model, and in order to choose the right load model, the walking-induced dynamic loading has to be understood. Pedestrian induces forces occur in all directions, but forces in lateral and longitudinal direction are small compared to the vertical direction. The vertical forces have therefore through history been considered by structural engineers as the greatest concern for pedestrian bridges [29]. On the opening day of the Millennium Bridge in 2000 an unexpected phenomenon occurred as the footbridge obtained great lateral excitation due to crowd loading. This sparked interest for the study of horizontal vibration due to pedestrian induced forces, and horizontal vibrations has been considered with caution since. In this chapter both lateral and vertical pedestrian induced force will be discussed, and in addition the phenomena of synchronization will be explained briefly.

## 4.1 Vertical Forces

In 1982 Wheeler published research on single pedestrian loading in vertical direction, dividing the movement into six stages from slow walking to running. Figure 4.1 shows Wheeler's presentation of the vertical dynamic pedestrian induced load. The graphs represent vertical ground reaction forces due to walking and running for one foot, where first peak is the heel hitting the ground and the second peak the front of the foot pushing off the ground [2]. Later research has shown that this approach to the single step load distribution is satisfactory. Wheelers approach to the dynamic pedestrian induced load from two feet, is illustrated in Figure 4.2.
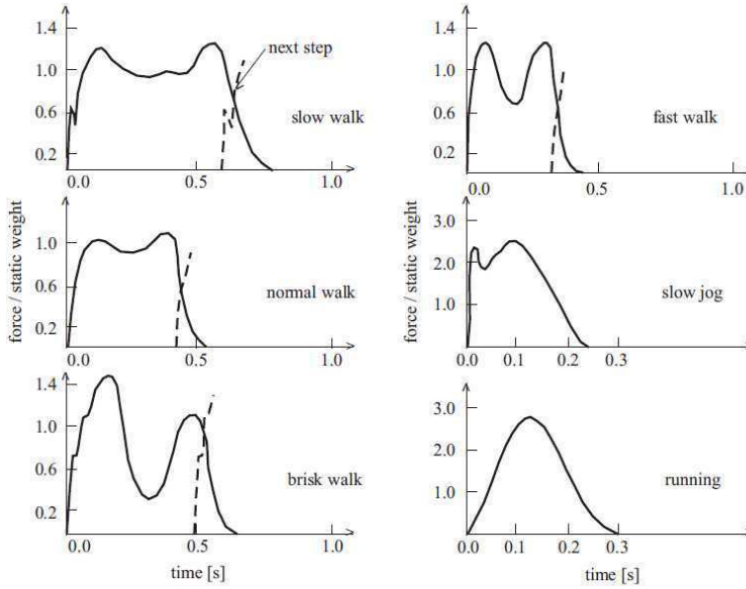
Figure 4.1: Vertical dynamic pedestrian induced load, Wheeler 1982
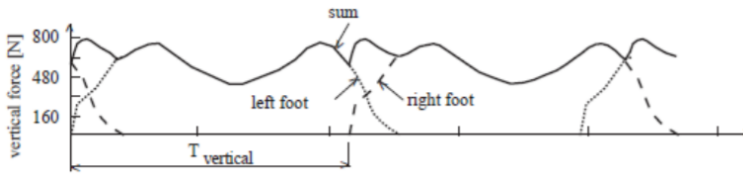


Figure 4.2: Vertical dynamic pedestrian induced load two feet [2]

A great amount of research has been published regarding average stepping frequency for a pedestrian. The average walking frequency is defined to between 1.8-2 Hz, a definition underpinned by several researches as shown in Table 4.1 collected by Ingólfsson et al (2007). N is the number of individuals used for the testing.

Table 4.1: Stepping frequency from various research

| Author | N | $\mu_{fp}$ [Hz] |
|---|---|---|
| Matsumoto et al 1972 | 505 | 1.99 |
| Kerr and Bishop 2001 | 40 | 1.9 |
| Zivanovic et al. 2005 | 1976 | 1.87 |
| Pachi and Ji 2005 | 200 | 1.86 |
| Ingólfsson 2006 | 19 | 1.83 |
| Pachi and Ji 2005 | 200 | 1.80 |

## 4.2 Lateral Forces

The lateral forces induces by pedestrian has a lower amplitude than the vertical, but the lateral forces are still important when constructing pedestrian bridges. Pedestrians are more sensitive to vibrations in the lateral direction than in the vertical direction and as a result of this the criteria for lateral vibrations are stricter. The characteristics of the lateral forces differs from the vertical, e.g. while the vertical induced forces increase with the speed, the lateral forces are bigger for walking than for running [2]. In addition the frequency of the lateral components from pedestrian induced forces are half the vertical walking step frequency. This follows from that the period is defined between two following left or right footsteps, while the vertical is defined between one left and one right, illustrated in Figure 4.3 [2].
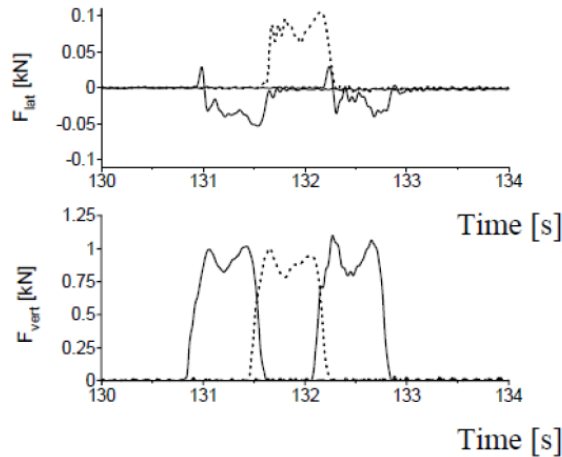


Figure 4.3: Lateral and vertical ground reaction [2]

## 4.3 Synchronization

Synchronization, or lock-in effect, are the names of the phenomena which occurs when pedestrians adapt to the natural frequency and phase of a structure. Synchronization is likely to occur if the natural frequency lies near the walking frequency, and causes big excitation of the structure due to relatively low forces [30]. In the vertical direction the synchronization has its origin in the natural adapting mechanism in order to reduce forces in the human body. By adapting the frequency of the vibrations into the step the pedestrian reduces the forces acting on its legs [31]. In horizontal direction small movements in the structure make the pedestrians feel unstable, and as a result they widen their steps and synchronize with the horizontal mode of the structure. This leads to an

increased acceleration in the horizontal direction, which again makes the pedestrians widen their step further. Synchronization in the horizontal direction is especially a problem for slender pedestrian bridges with horizontal natural frequencies around 1 Hz.

## 4.4 Models of Pedestrian Induced Forces

In order to predict the dynamic behaviour of a pedestrian bridge, it is necessary to define a load model of the pedestrian dynamic forces to apply to a structural model. Over the last years several load models for excitation of footbridges has been developed, and the following section will present some of the existing load models. The section will show the development of both vertical and lateral load models, and link the models up to the load models presented in different guidelines in Chapter 5.

### 4.4.1 Models for Vertical Excitation of Footbridges

**Blanchard's Model**

One of the earliest deterministic load models for vertical pedestrian load was developed by Blanchard et al in 1977 [18]. This load model has been used as a base for several codes as for example the UK National Annex to Eurocode, which will be presented in Chapter 5. The load model is based on a simplification of the pedestrian step, containing identical and perfectly repeatable footfalls, with a time period T. The vertical force $F_P(t)$ is defined as a Fourier series, given in Equation (4.1) [18].

$$F_p(x,t) = G\alpha * sin(2\pi f_p t)\delta(x - 0.9f_p t) \qquad [N] \quad (4.1)$$

Where:

| | |
|---|---|
| $G$ | is the weight of one pedestrian [N] |
| $\alpha$ | is the dynamic load factor (DLF) |
| $f_p$ | is the pedestrian pacing rate [Hz] |
| $\delta(x - 0.9f_p t)$ | is the Dirac Delta function centred at $x = 0.9f_p t$, following the assumption of a constant pedestrian speed of $v_p = 0.9f_p t$. |

The model is developed by measurements of vertical forces on fixed force plates, and does not take to account the interaction between the pedestrians and the bridge [32]. The load model is based on resonance due to only the first harmonic with DLF equal to 0.275 [18], and is therefore a simple model to apply, but the usability can be followed by a decrease of accuracy.

**Bachmann & Ammann's Model**

In 1987 Bachmann and Ammann further developed Blanchards load model, and presented a new model which reports the relationship between the pedestrians pacing rate and the dynamic force [32]. Bachmann and Ammann developed the basic sinusoidal time histories proposed by Blanchard et al in terms of defining Fourier coefficients of the first three harmonics, as shown in Equation (4.2) [32]. Unlike Blanchards model, this load model exhibits an overlap between the individual contact times for each foot [30]. The model is used as a basis for the load models in guidelines as e.g. ISO 10137 and the french bridge design standard SÉTRA.

$$F_p(t) = G + \Delta G_1 sin(2\pi f_s t) + \Delta G_2 sin(4\pi f_s t - \phi_2) + \Delta G_3 sin(6\pi f_s t - \phi_3) \ \ [N] \quad (4.2)$$

Where:

$G$ 　 is the weight of one person (often assumed to be 700 N) [N]

$\Delta G_1$ is the load component (amplitude) of 1st harmonic [N]

$\Delta G_2$ is the load component (amplitude) of 2nd harmonic [N]

$\Delta G_3$ is the load component (amplitude) of 3rd harmonic [N]

$f_s$ 　 is the pacing rate [Hz]

$\phi_2$ 　 is the phase angle of the 2nd harmonic relative to the 1st harmonic [rad]

$\phi_3$ 　 is the phase angle of the 3rd harmonic relative to the 1st harmonic [rad]

The Fourier amplitude coefficient of the 1st harmonic is found in literature, e.g. Bachmann and Ammanns own results, to be [30]:

$\Delta G_1 = 0.4G$ for $f_s = 2.0$ Hz

$\Delta G_1 = 0.5G$ for $f_s = 2.4$ Hz

with linear interpolation between

$\Delta G_2 \cong \Delta G_3 \cong 0.1G$ 　 for $f_s \cong 2Hz$

The phase angles are hard to predict and create a large uncertainty to the equation. The values can be approximated to $\Delta G_2 = \Delta G_3 = \pi/2$, but if it is desired to find the most unfavourable combination of the harmonics, the exact phase angles needs to found. This is not the case for situations where a forced vibration induced by walking is described by one harmonic, as the phase angles will be immaterial.

**Brownjohn's Model**

In 2004 Brownjohn et al's presented a load model which differs form the previous presented load models by being defined in the frequency domain, instead of the time domain [33]. The models defined in the time domain assumes that a load from multiple people can be calculated by taking the effect of a single person walking at a single natural frequency and multiplying it by an appropriate factor [33]. Models defined in the frequency domain differs from this by using Gaussian distribution of pacing rates and input parameters when calculating the effect of the load from multiple pedestrians.

Brownjohn's model presents the Power Spectral Density (PSD) of the acceleration response $S_a(f)$ to the relevant harmonic of the walking force. This is obtained from the PSD of the force induced by N pedestrians, $S_{Pn}$, (4.4), multiplied with the acceleration frequency response function of the bridge, $H(F)$, as shown in Equation (4.3) [13][33].

$$S_a(f) = |H(f)|^2 S_{P,n} \tag{4.3}$$

.

$$S_{P,n} = \frac{N}{2n}W^2\phi(f_p)G_n^2(f_p) \tag{4.4}$$

Where:

$n$      is the number of forcing harmonics considered [-]

$W$      is the average pedestrian weight [N]

$\phi(f_p)$    is the probability distribution of pacing rate [-]

$G_n(f_p)$ is the DLF, dependent on pacing frequecy for the first harmonics, and constant for higher harmonics. $G_1(f_p) = 0.37f_p - -0.42$, $G_2 = 0.053$, $G_3 = 0.043$, $G_4 = 0.041$, $G_5 = 0.027$, $G_6 = 0.018$ [-]

Further development of the formula accounts of the effects of mode shape and the synchronization between pedestrians. A new formula, based on the resemblance with the turbulent buffeting wind loading, is presented in Equation (4.5). The model now accounts for the synchronization by a coherence function. The disadvantage is that the coherence function taking in the synchronization is only defined for either full or no synchronization, it is still a challenge to predict when the synchronization will happen, and how many of the pedestrians will synchronize at the same time.

$$S_{a,synch}(f) = \psi_Z^2|H(f)|\int_0^L\int_0^L\psi_{z1}\psi_{z2}coh(f,z_1,z_2)dz_1dz_2 \tag{4.5}$$

$\psi_z, \psi_{z1}, \psi_{z2}$ is the weighting of the mode shapes at the response point, $z$, and at the two points $z_1$ and $z_2$ [-]

**Butz's Model**

Butz's load model is the base of several of the guidelines considered in Chapter 5; JRC, HIVOSS and partly of SÉTRA. This model further develop Brownjohns load model, and while Brownjohn et al only accounts for the probability distribution of the step frequency, Butz also accounts for the probability distribution for the pedestrian mass, looking at amplitude and pedestrian arrival times in a stream of pedestrians [33].

In order to derive PSD function for vibration response, Butz use MC simulations. Butz found an empirical peak factor dependent on the crowd density $k_p$, which multiplied with the Root Mean Square (RMS) acceleration value $\sigma_a$ represents the 95th percentile of the peak acceleration, see Equation (4.6). $k_p$ accounts for the correlation and dependence between parameters such as step frequency, walking speed and stream density, and is given in Table 4.2, and the function for $\sigma_a$ is given in Equation (4.7) [33].

$$a_{peak,95\%} = k_p \sigma_a \qquad [\text{m/s}^2] \quad (4.6)$$

Table 4.2: Values of $k_p$ for different crowd densities

| Crowd density [pedestrians/m$^2$] | $k_p$ [-] |
|---|---|
| $0 \leq 0.5$ | 3.92 |
| $0.5 \leq 1$ | 3.80 |
| $1 \leq 1.5$ | 3.74 |

The RMS is given as:

$$\sigma_a = \sqrt{\frac{C k_F N}{M_i^2} k_1(f_i) \zeta^{k2(fi)}} \qquad [\text{m/s}^2] \quad (4.7)$$

$M_i$        is the modal mass of mode $i$ [kg]

$\zeta_i$        is the modal damping of mode $i$ [Ns/m]

$f_i$        is the modal frequency of mode $i$ [Hz]

$N$        is the number of pedestrians on the bridge [-]

$C$ and $k_f$ are the empirical factors depending on the crowd density [-]

## 4.4.2    Models for Lateral Excitation of Footbridges

Until year 2000, most research in connection with load models for pedestrian loads were focused on vertical excitation. A big step forward in the research of lateral pedestrian induced vibration in bridges came after the Millennium bridge in London was closed due to large lateral vibrations in June 2000. As a result of this and other similar scenarios, the focus in the later years has been largely aimed at the lateral excitation.

**Dallard's Model**

After the closing of the Millennium Bridge, Dallard et al did a full scale crowd experiments on the bridge. The results showed that the lateral velocity of the bridge was proportional to the dynamic force induced by the pedestrians [34]. They concluded that the pedestrian induced loading can be modelled as negative line dampers, with constant velocity proportional to load coefficient $c_p = 300$ Ns/m.

Dallard et al suggest a random vibration prediction approach; a model of for lateral excitation of footbridges based on a SDOF equation. The model assumes that the dynamic force for each pedestrian, $\tilde{f}(t)$, is linearly proportional with the local velocity of the bridge, $\dot{z}_{local}$, by [34, 35]:

$$\tilde{f}(t) = k\dot{z}_{local} \qquad\qquad \text{[N]} \quad (4.8)$$

Where:

$k$ \qquad is the pedestrian damping constant (set to 300 Ns/m) [Ns/m]

$\dot{z}_{local}$ is the local velocity, which is related to the modal [m/s] velocity by: $\dot{z}_{local} = \phi\dot{z}$

$\phi$ \qquad is the mode shape [-]

The pedestrians' contribution to the modal force is therfore given by:

$$f(t)_{pedr} = \phi\tilde{f}(t) = \phi k\dot{z}_{local} = \phi^2 k\dot{z} \qquad\qquad \text{[N]} \quad (4.9)$$

Dallard et al found that until a certain number of pedestrians, the bridge did not get any lateral response. When the number of pedestrians reached a critical point, a small increase in the number of pedestrian loads would make the lateral response diverge quickly. From this Dallard et al developed Arup's stability criterion, which expresses the maximum number of pedestrians to prevent instability, when uniformly disturbed pedestrian load is applied to the bridge [36].

$$N_{cr} = \frac{4\pi f M \zeta}{c_p \frac{1}{L} \int_0^L [\phi(x)]^2 dx} \qquad\qquad \text{[-]} \quad (4.10)$$

$M$ \quad is the modal mass [kg]

$\zeta$ \quad is the modal damping [Ns/m]

$f$ \quad is the modal frequency [Hz]

$\phi(x)$ is the mode shape [-]

$L$ \quad is the bridge length [m]

An alternate version of Equation 4.10 is presented in the guidelines Hånbok 185 and JRC described in Chapter 5 as part of the control for lateral vibrations.

**Nakamura's Model**

Nakamura's model for lateral excitation of footbridges is a dynamic model based on synchronous walking, published in 2002. Nakamura states that synchronous walking is a problem until the vibrations reach a certain level. After this level of acceleration is reached the synchronous walking will end, and the girder will stop alternating because the pedestrians will moderate their movements [35].

Nakamuras model, given in Equation (4.12), is based on observations and research done on the Toda park bridge (the T-bridge) in Japan which got strongly excited as a result of pedestrian loading at its opening i day in 1989 [37]. The model is a modification of Dallards model, and takes into account how girder mass, damping ratio and density of pedestrian affect the lateral vibration and the dynamic force induced by pedestrians synchronization [35, 34].

Nakamura's model is based on that if the modes of vibration are well separated, the lateral pedestrian induced excitation can be modeled as a SDOF dynamic model using the modal analysis of first lateral mode. The derivation of he model starts with the equation on motion given in Equation (4.11), and the load $F_P(t)$ is given in Equation (4.12). $F_P$ is the modal lateral dynamic force induced by the pedestrians on the bridge deck.

$$M_B x''_B(t) + C_B x'_B(t) = F_P(t) \qquad \text{[N]} \quad (4.11)$$

Where

$M_B$, $C_B$ and $K_B$   is the modal mass [kg], damping [Ns/m] and stiffness coefficient [N/m]

$x_B$, $x'_B$ and $x''_B$   is the modal displacement [m], velocity [m/s] and acceleration [m/s²] of the girder

$F_P$          is the modal lateral dynamic force induced by all pedestrians on the bridge deck found using Equation (4.12) [N]

$$F_P(t) = k_1 k_2 H[x'_B(t)] G(f_b) M_P g \qquad \text{[N]} \quad (4.12)$$

Where

$k_1$          is the ratio of the lateral force to the pedestrian's weight. Assumed to be 0.04 based on the reference by Bachmann and Ammann (1987) [-]

$k_2$          is the percentage of pedestrians who synchronized the girder vibration, set to 0.2 [-]

$H(x'_B)$      is the function to describe the pedestrians' synchronization nature, found from Equation (4.13) [-]

$G(f_b)$ is the function to describe how pedestrians synchronize with the bridge's natural frequency, set to 1.0 because no data is available so far, and future studies are required to clarify this [-]

$M_P$ is the modal mass for the first lateral mode [kg]

Where:

$$H[x'_B(t)] = \frac{x'_B(t)}{k_3 + |x'_B(t)|} \qquad\qquad \text{[-]} \quad (4.13)$$

# Chapter 5

# Design Guidelines

The common way to design a pedestrian bridge with respect to vibrations is in the Serviceability Limit State (SLS), with an upper acceleration limit to be perceived by the pedestrians, known as a comfort criteria. These comfort criteria are compared to the appropriate acceleration response from a dynamic load model to ensure that the structure does not obtain large accelerations. As described in Section 4.4 there are different methods to estimate the response from pedestrian induced forces, and subsequently the guidelines regarding footbridges have different methods for obtaining comfort criteria and load models. In this chapter the comfort criteria and load models from guidelines with different origins will be presented, and later related to the finite element model of Bårdshaug Bridge in Chapter 6 and 7. The guidelines presented in this chapter are:

**5.1** Eurocodes

**5.2** British Standard 5400, BS 5400

**5.3** UK National Annex to Eurocode, UK-NA

**5.4** Statens Vegvesen Håndbok N400 and 185

**5.5** Service d'Études Techniques des Routes et Autoroutes, SÉTRA

**5.6** ISO 10137, by the International Organization for Standardization 10137

**5.7** Design of Lightweight Footbridges for Human Induced Vibrations, by Joint Research Centre

**5.8** Human Induced Vibrations of Steel Structures, HIVOSS

## 5.1 Eurocode

Eurocodes are the European standards for designing structures. Developed by the European Committee for Standardisation, the Eurocodes are broken into ten main parts. In this chapter, the parts relevant for footbridges will be considered, these are:

- Eurocode 0 - NS-EN 1990 - Basis for Structural Design

- Eurocode 1 - NS-EN 1991 - Actions on Structures

- Eurocode 2 - NS-EN 1992 - Design of Concrete Structures

- Eurocode 3 - NS-EN 1993 - Design of Steel Structures

- Eurocode 4 - NS-EN 1994 - Design of Composite Steel and Concrete structures

- Eurocode 5 - NS-EN 1995 - Design of Timber Structures

Supplementing the Eurocodes are amendments, corrigendum and national annexes. These are continuously changing to iterate the latest edition of the Eurocodes. Amendments and corrigendums are adding, replacing and correcting information in the Eurocode, while the national annexes adds information to take into account the regional differences if required. The UK national annex is presented in Section 5.3.

### 5.1.1 Comfort criteria

Eurocode 0, Annex A2, defines a comfort criteria which gives the maximum acceleration in any part of the bridge deck [38]. National Annex values should be used for cases where this is relevant. The comfort criteria given in Eurocode are shown in Table 5.1.

Table 5.1: Reccomended maximum accelerations in Eurocode 0

| Load case | Acceleration limit [m/s$^2$] |
|---|---|
| Vertical vibration | 0.7 |
| Lateral vibration | 0.2 |
| Exceptional crowd conditions | 0.4 |

Eurocode 0 states that a verification of the comfort criteria should be found if the fundamental natural frequency is less than 5 Hz for vertical vibrations, and less than 2.5 Hz for lateral and torsional vibrations. It is noted under the comfort criteria in Eurocode 0 that the data used in calculations and the results are subject to very high uncertainties. The analyst may have to account for the installation of dampers after completion of the structure if the comfort criteria is not satisfied by a significant margin.

For guidance on vibration response on a bridge under SLS, Eurocode 4 refers to:

- Eurocode 0 - Annex 2.4, which describes the comfort criteria (see Table 5.1)

- Eurocode 1 part 2 - Chapter 5.7 and 6.4, which describes a method of obtaining the natural frequencies of the bridge [39] [40] (see Annex A)

- Eurocode 3 part 2 - Chapter 7.7 to 7.10, which e.g. informs that steel structures may be designed such that the first natural frequency is in the appropriate domain and/or by adding suitable damping devices to increase comfort [41].

## 5.1.2 Load model

The Eurocodes do not provide load models for pedestrian induced forces on steel or concrete footbridges, except the load models provided in the National Annexes, which for the United Kingdom will be discussed in Section 5.3. However, Eurocode 5-2 Annex B does provide a load model for timber bridges. The annex applies to timber bridges, with simply supported beams or truss systems, excited by pedestrians. For one person crossing the bridge, the predicted vertical and horizontal acceleration $a_{vert,lat}$ in m/s$^2$ is given as:

$$a_{vert,1} = \frac{200}{M\xi} \qquad \text{for} \quad f_{ver} \leq 2.5Hz \qquad (5.1)$$

$$a_{vert,1} = \frac{100}{M\xi} \qquad \text{for} \quad 2.5 < f_{ver} \leq 5.0Hz \qquad (5.2)$$

$$a_{vert,jog} = \frac{600}{M\xi} \qquad \text{for} \quad 2.5 \leq f_{lat} \leq 3.5Hz \qquad (5.3)$$

$$a_{hor,1} = \frac{50}{M\xi} \qquad \text{for} \quad 0.5 \leq f_{lat} \leq 2.5Hz \qquad (5.4)$$

Where:

$M$     is the total mass of the brdige, given by $M = ml$ [kg]

$l$     is the span of the bridge [m]

$m$     is the mass per unit length (self-weight) of the bridge [kg/m]

$\xi$     is the damping ratio, given in Table 5.2 [-]

$f_{vert}$     is the fundamental natural frequency in vertical direction [Hz]

$f_{hor}$     is the fundamental natural frequency in horizontal direction [Hz]

Table 5.2: Damping ratios for timber bridges from Eurocode 5

| Type of timber structure | Damping ratio [%] |
|---|---|
| Strucures without Mechanical Joints | 1.0 |
| Structures with Mechanical Joints | 1.5 |

For $n$ pedestrians crossing the bridge the acceleration is predicted as:

$$a_{vert,n} = 0.23 a_{vert,1} n k_{vert} \qquad [\text{m/s}^2] \quad (5.5)$$

$$a_{hor,n} = 0.18 a_{hor,1} n k_{hor} \qquad [\text{m/s}^2] \quad (5.6)$$

Where:

$n$     is the number of pedestrians, given in Table 5.3 [-]

$a_{vert,1}$ is the vertical acceleration from a single pedestrian from Equation (5.1) or (5.2) $[\text{m/s}^2]$

$a_{hor,1}$ is the horizontal acceleration from a single pedestrian from Equation (5.4) $[\text{m/s}^2]$

$k_{vert}$ is a coefficient dependent on $f_{vert}$, found in Figure 5.1 [-]

$k_{hor}$ is a coefficient dependent on $f_{hor}$, found in Figure 5.2 [-]

Table 5.3: Number of pedestrians on the bridge deck

| Pedestrians | [n] |
|---|---|
| Group | 13 |
| Continuous stream | 0.6 $A$ |

Where $A$ is the total bridge deck area in m$^2$.
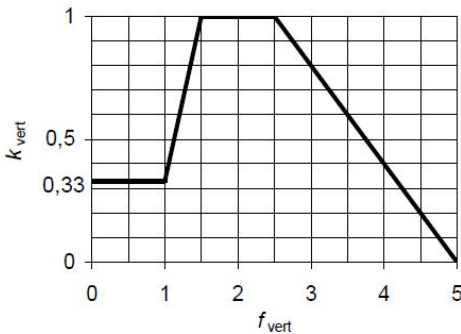


Figure 5.1: Coefficient for vertical acceleration from several pedestrians
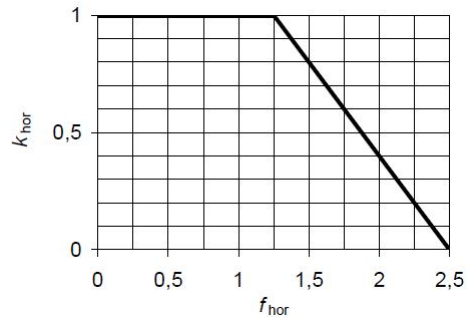


Figure 5.2: Coefficient for horizontal acceleration from several pedestrians

## 5.2 BS 5400

The British Standards Institution (BSI) produces guidelines in the United Kingdom. Each guideline is named by British Standards (BS) and a code, and BS 5400 is the guideline regarding steel, concrete and composite bridges. Pedestrian loading in BS 5400 is based on Blanchard's early research of vertical pedestrian induced fores on a fixed surface and does not account for interaction between the pedestrian and the bridge. Alongside BS 5400 is the revision of the guideline, BD 37/01, and both the guideline and the revision are considered in the following section.

### 5.2.1 Comfort criteria

**Vertical**

For structures where the fundamental natural frequency, $f_0$, exceeds 5 Hz the serviceability of vibration is considered to be satisfactory [42]. For structures where the $f_0$ is less than or equal to 5 Hz, the maximum vertical acceleration of any part of the structure shall satisfy:

$$a \leq 0.5 f_0^{0.5} \qquad \text{[m/s}^2\text{]} \quad (5.7)$$

The maximum vertical acceleration $a$ can be derived using a simplified or a general method.

### 5.2.2 Load model

**Simplified method**

The vertical acceleration can be found using a simplified method. This method is only valid for single, two or three-span continuous and symmetric structures where the cross section is constant and supported on bearings that can be idealized as simply supported. The maximum vertical acceleration for the simplified method is given in Equation (5.8):

$$a = 4\pi^2 f_0^2 y_s K \psi \qquad \text{[m/s}^2\text{]} \quad (5.8)$$

Where:

$f_0$ is the the bridge's first natural frequency in the vertical plane [Hz]

$y_s$ is the static deformation for a pointload (700 N) at the middle span [m]

$K$ is the configuration factor dependent on the number of spans and the ratio of the length of the span, see Figure 5.3 [-]

$\psi$ is the dynamic load factor dependent of the length of the span and the damping ratio $\xi$, see Figure 5.4 [-]
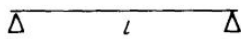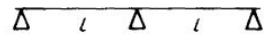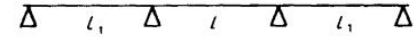
| Bridge configuration | | | $K$ |
|---|---|---|---|
| | | — | 1.0 |
| | | — | 0.7 |
| | **Ratio $l_1/l$** | | |
| | 1.0 | | 0.6 |
| | 0.8 | | 0.8 |
| | 0.6 or less | | 0.9 |

Figure 5.3: Configuration factor $K$ from ratio of span length $l_1/l$
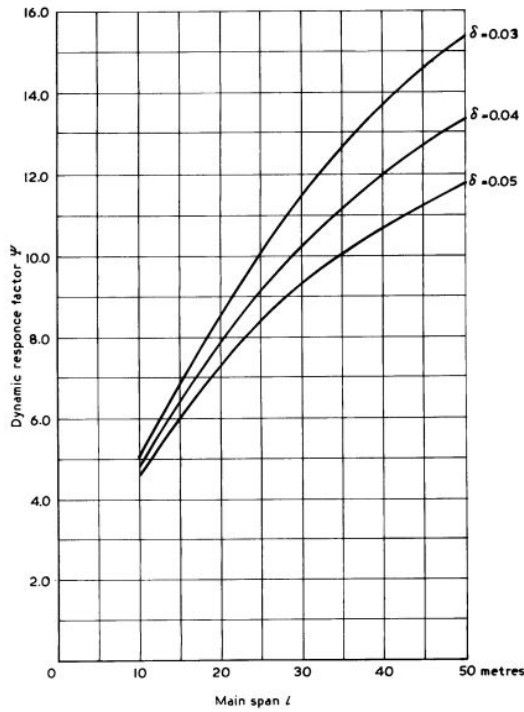


Figure 5.4: Dynamic load factor $\psi$

For natural frequencies over 4 Hz, the acceleration shall be reduced linearly from zero to 70 % at 5 Hz. The reduction factor $r$ is multiplied to the Equation 5.8, where:

$$r = \begin{cases} 1.0 & f \leq 4 \\ 3.8 - 0.7f & 4 < f \leq 5 \\ 0.0 & f > 5 \end{cases} \tag{5.9}$$

The bridge's first natural frequency, excluding the pedestrian loads is evaluated from BD 37/01, and in Equation (5.10).

$$f_0 = \frac{C^2}{2\pi l^2} \sqrt{\frac{EIg}{M}} \qquad \text{[Hz]} \quad (5.10)$$

$C$  is the configuration factor, see Figure 5.5 [-]

$l$   is the length of the main span [m]

$E$  is the modulus of elasticity. The short-term modulus of elasticity shall be used for concrete [kN/m$^2$]

$I$   is the second moment of area of the cross section at the mid span [m$^4$]

$g$  is the acceleration due to gravity [m/s$^2$]

$M$  is weight per unit length of the full cross-section at mid span [kN/m]
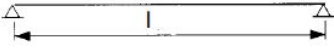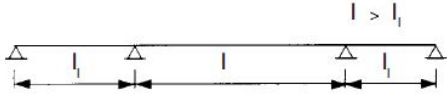


Figure 5.5: Configuration factor C

In the absence of more precise information, the logarithmic decrements of the decay of vibration due to structural damping $\delta$ is given in Table 5.4

Table 5.4: Logarithmic decrement of decay of vibration $\delta$

| Bridge superstructure | $\delta$ |
|---|---|
| Steel with asphalt or epoxy surfaceing | 0.03 |
| Composite steel/concrete | 0.04 |
| Prestressed and reinforced concrete | 0.05 |

**General method**

For structures which do not satisfy the requirements in the simplified method, the general method is used. In the general method the acceleration is calculated assuming a single pedestrian walking over the bridge, applying a dynamic load represented by a pulsating point load $F$, moving across the main span of the structure at a constant speed $v_t$. Where $F$ is given by:

$$F = 180 \sin(2\pi f_0 T) \qquad \text{[N]} \quad (5.11)$$

where $T$ is time in seconds, and

$$v_t = 0.9 f_0 \qquad \text{[m/s]} \quad (5.12)$$

A reduction in acceleration is reduced linearly from zero to 70 % from 4 Hz to 5 Hz after the formulas in Equation (5.9).

**Horizontal**

There are no method for deriving the acceleration in the lateral direction in BS 5400. The revision to BS 5400, BD 37/01, do however state that lateral acceleration should be controlled if the horizontal natural frequency is less than 1.5 Hz. A method for deriving the maximum horizontal acceleration shall be chosen from literature by the analyst.

## 5.3 UK National Annex to Eurocode

The United Kingdom National Annex (UK-NA) to Eurocode 1 part 2 (EN-1991-2) gives further guidelines on how to obtain the comfort criteria and load models for pedestrian induced forces.

### 5.3.1 Comfort criteria

UK-NA gives a maximum vertical acceleration in order to fulfill the SLS criteria. The maximum vertical acceleration calculated from the load models provided in UK-NA should not exceed the design acceleration limit given by [43]:

$$a_{limit} = 1.0 k_1 k_2 k_3 k_4 \qquad \text{[m/s}^2\text{]} \quad (5.13)$$

and

$$0.5 \leq a_{limit} \leq 2.0 \qquad \text{[m/s}^2\text{]} \quad (5.14)$$

Where $k_1$, $k_2$ and $k_3$ are the response modifiers:

$k_1$ is site usage factor, see Table 5.5 [-]

$k_2$ is route redundancy factor, see Table 5.6 [-]

$k_3$ is height of structure factor, see Table 5.7 [-]

$k_4$ is an exposure factor that reflect the quality of walking surface, parapet design and other comfort-enhancing features. Can be set between 0.8 and 1.2, and the value should be determined for the individual project. If the exposure factor is not determined for the project, the value 1.0 is used.

Table 5.5: Recommended values for the site usage factor $k_1$

| Bridge function | $k_1$ |
|---|---|
| Primary route for hospitals or other high sensitivity routes | 0.6 |
| Primary route for school | 0.8 |
| Primary route for sport stadiums or other high usage routes | 0.8 |
| Major urban centres | 1.0 |
| Suburban crossings | 1.3 |
| Rural environments | 1.6 |

Table 5.6: Recommended values for the route redundancy ractor $k_2$

| Route redundancy | $k_2$ |
|---|---|
| Sole means of access | 0.7 |
| Primary route | 1.0 |
| Alternative routes readily available | 1.3 |

Table 5.7: Recommended values for the structure height factor $k_3$

| Bridge height | $k_3$ |
|---|---|
| Greater than 8 m | 0.7 |
| 4 m to 8 m | 1.0 |
| Less than 4 m | 1.1 |

If there are no significant lateral modes with frequencies below 1.5 Hz it may be assumed that unstable lateral responses will not occur, otherwise the comfort criteria from Eurocode 0 shall be used, see Table 5.1.

## 5.3.2 Load model

UK-NA presents two load models based on the bridge categories shown in Table 5.9. The first load model simulates the vertical load from a single pedestrian or a group, and the second load model simulates the vertical load from a crowd. The single pedestrian load is modeled as a concentrated load moving across the longest bridge span, while the crowd load is modeled as an uniformly distributed load applied over the whole bridge deck adapted to the considered mode shape [2].

**Single pedestrians and groups**

The concentrated load is recommend to be a pulsating force moving across the bridge over the main span at a constant speed. The load model is given by:

$$F(N) = F_0 k(f_v)\sqrt{1 + \gamma(N-1)}sin(2\pi f_v t) \qquad \text{[N]} \quad (5.15)$$

Where:

$F_0$     is the reference amplitude, see Table 5.8 [N]

$N$     is the number of pedestrians, see Table 5.9 [-]

$f_v$     is the natural frequency of the considered vertical mode [Hz]

$k(f_v)$ is the factor given in Figure 5.6, considering harmonic response, realistic pedestrian population and pedestrian sensitivity to vibration [-]

$t$     is the elapsed time [s]

$\gamma$     is the reduction factor to accomplish for unsynchronization of pedestrians, given in Figure 5.7, as a function of structural damping $\delta$, given in Equation (5.16) and Table 5.10 [-]

$$\delta = 2\pi\xi \qquad \text{[-]} \quad (5.16)$$

Where:

$\xi$ is the structural damping ratio, see Table 5.10 [-]

Table 5.8: Reference load and crossing speed given in UK-NA

| Load parameters | Walking | Jogging |
|---|---|---|
| Reference load. $F_0$ [N] | 280 | 910 |
| Pedestrian crossing speed, $v_t$ [m/s] | 1.7 | 3 |

Table 5.9: Bridge classes with corresponding group sizes $N$ and crowd densities $d$

| Bridge class | Bridge usage | Group size (walk) | Group size (jog) | Crowd density, $d$ (walk) |
|---|---|---|---|---|
| A | Rural locations seldom used and in sparsely populated areas. | $N = 2$ | $N = 0$ | 0 |
| B | Suburban locations likely to experience slight variations in pedestrian loading intensity on an occasional basis. | $N = 4$ | $N = 1$ | 0.4 |
| C | Urban routes subject to significant variation in daily usage (e.g. structures serving access to offices and schools). | $N = 8$ | $N = 2$ | 0.8 |
| D | Primary access to major public assembly facilities such as sport stadiums or major public transportation facilities. | $N=16$ | $N = 4$ | 1.5 |
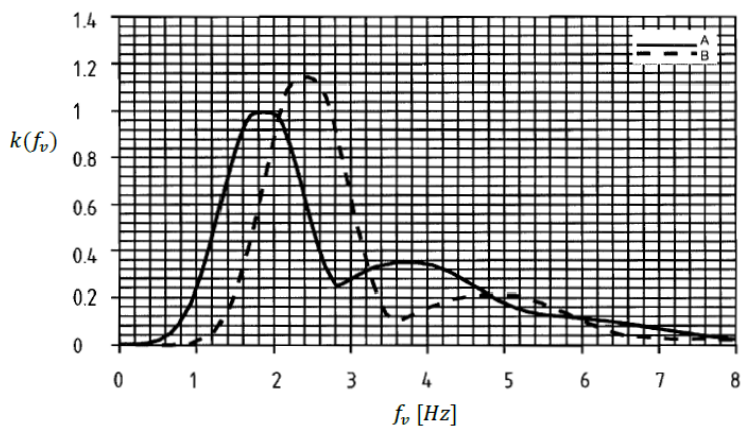


Figure 5.6: Relationship between $k(f_v)$ and mode frequencies $f_v$ for walking (curve A) and jogging (curve B) pedestrians
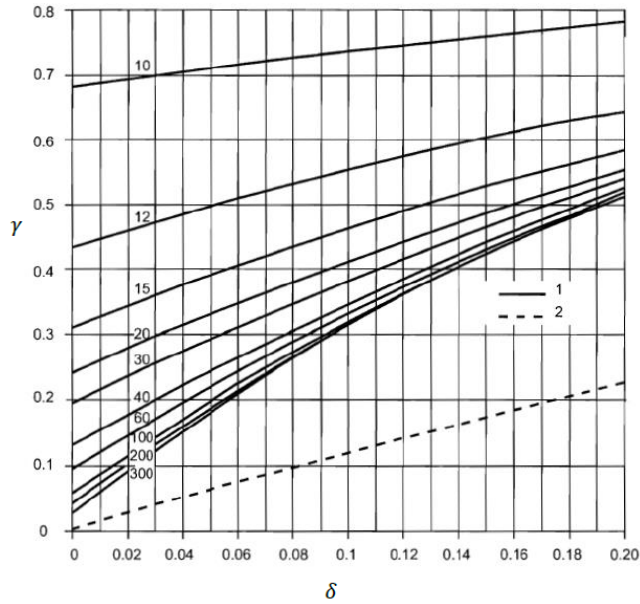
Figure 5.7: Reduction factor $\gamma$ as a function of damping $\delta$. Accounts for desynchronized pedestrians in groups of various size (curve 1), and crowds (curve 2)

Table 5.10: Damping ratios $\xi$ reccomended in UK-NA

| Bridge type | $\xi$ lower limit of percentage of critical damping [%] | |
| --- | --- | --- |
| | Span L < 20 m | Span L ≥ 20 m |
| Steel and composite | 05 + 0.125 (20 - L) | 0.5 |
| Pre-stressed concrete | 1.0 + 0.07 (20 - L) | 1.0 |
| Filler beam and reinforced concrete | 1.5 + 0.07 (20 - L) | 1.5 |
| Timber structures without mechanical joints | 1.0 | |
| Timber structures with mechanical joints | 1.5 | |

**Crowds**

The uniformly distributed load model simulates pedestrian streams crossing the bridge. The load is adapted to the considered mode shape and applied over the entire bridge deck.

$$w(N,t) = 1.8\frac{F_0}{A}k(f_v)\sqrt{\gamma\frac{N}{\lambda}}sin(2\pi f_v t) \qquad [\text{N/m}^2] \quad (5.17)$$

Where:

$F_0$, $k(f_v)$, $\gamma$ and $f_v$    are found the same way as single pedestrians and groups, see Equation (5.15) [-]

$N$        is the number of pedestrians, found from Equation (5.18) [-]

$A$        is the bridge deck area [m$^2$]

$\lambda$        is the reduction factor for for the effective number of pedestrians when loading from only some parts of the spans contributes to the considered mode, given in Equation (5.19) [-]

$$N = \rho A = \rho S b \qquad \text{[-]} \quad (5.18)$$

Where:

$\rho$   is the crowd density according to bridge class, see Table 5.9 [ped/m$^2$]

$S$   is the span length [m]

$b$   is the width of bridge deck exposed to pedestrian loading [m]

$$\lambda = 0.634 \frac{S_{eff}}{S} \qquad \text{[-]} \quad (5.19)$$

$$S_{eff} = \frac{Area_1 + Area_2}{0.634 \gamma_{max}} \qquad \text{[m]} \quad (5.20)$$

Where

$Area_1$ and $Area_2$   are defined in Figure 5.8 [m$^2$]

$S_{eff}$    is the effective span length, see Figure 5.8. In all cases it is conservative to use $S_{eff} = S$ [m]

$b$      is the width of bridge deck exposed to pedestrian loading [m]

The distributed load model results in a load in N/m$^2$, in order to be consistent among the models, this load should be given in N/m. This is done by multiplying the load amplitude with the bridge width, $b$.
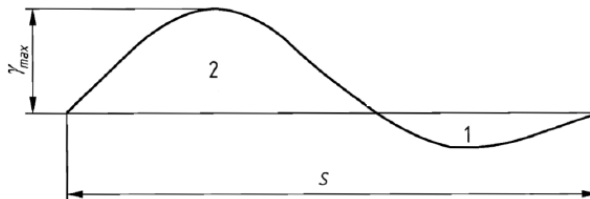


Figure 5.8: Illustration of effective span length of $area_1$ and $area_2$.

## 5.4 Statens Vegvesen Håndbok

The Norwegian Public Roads Administration, Statens Vegvesen, presents regulations for designs of all public roads in Norway, called "Håndbøker". Håndbok N400 was published in April 2015, and is the Norwegian Public Road Administrations latest published guideline. Håndbok N400 states that all footbridges should be considered in regards to the pedestrian's comfort, with focus on dynamic loads from wind and traffic in lateral and vertical direction [44]. Håndbok N400 advices the reader to use exactly the same comfort criteria as Eurocode 0 - Basis of Structural Design (Section 5.1.1), and will therefore not be utilized further in this chapter. An older version of the guideline, Håndbok 185, which is still in use, presents comfort criteria and a load model for pedestrian bridges and will be further discussed in this section.

### 5.4.1 Comfort criteria

Håndbok 185 states that footbridges prone to excitation shall be designed such that the reference acceleration, $a_r$, in the vertical direction satisfies the following criterion [45]:

$$a_r \leq 0.25 f^{0.7782} \qquad \text{[m/s}^2\text{]} \quad (5.21)$$

where $f$ is the first natural frequency in the vertical direction in Hz.

### 5.4.2 Load model

The load model in Håndbok 185 yields estimation of the acceleration through hand calculation from the following equation, similar to the simplified method from BS 5400:

$$a_r = 4\pi^2 f^2 W_s K \psi r \qquad \text{[m/s}^2\text{]} \quad (5.22)$$

Where:

$W_s$   is the static deformation for a point load (700 N) [m]

$K$   is the configuration factor dependent on the number of spans and the ratio of the length of the span, see Figure 5.9 and Table 5.11 [-]

$\psi$   is the dynamic load factor dependent on the length of the span and the damping ratio $\xi$, see Figure 5.10

$\xi$   is the damping ratio of the construction [-]

$r$   is the correction factor for the reference acceleration, $a_r$, function of the first natural $f$ [-]

$$r = \begin{cases} 1.0 & f \leq 4 \\ 3.0 - f/2 & 4 < f < 6 \\ 0.0 & f \geq 6 \end{cases}$$

Footbridges with the first natural frequency in the vertical direction greater than 6 Hz is not considered prone to dynamic excitation.
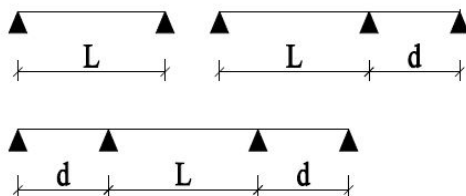


Figure 5.9: Definition of the span width ratio $d/L$ to determine $K$

Table 5.11: Configuration factor $K$

| $d/l$ | $K$ | |
|---|---|---|
| see figure 5.9 | 2 spans | 3 spans |
| 1.00 | 0.70 | 0.60 |
| 0.8 | 0.92 | 0.82 |
| 0.6 | 0.96 | 0.92 |
| 0.4 | 0.96 | 0.92 |
| 0.2 | 0.95 | 0.92 |

**Horizontal direction**

A control of the bridge shall be performed if horizontal natural frequencies lay in the domain $0.5 < f < 1.3$ Hz. The criteria is for a critical number of pedestrians causing horizontal vibration on the bridge:

$$N_L = \frac{8\pi\xi f M}{k} \qquad [\text{-}] \quad (5.23)$$

Where:

$N_L$   is the number of pedestrians evenly distributed across the bridge giving unacceptable horizontal vibrations [-]

$\xi$   is the damping ratio [-]
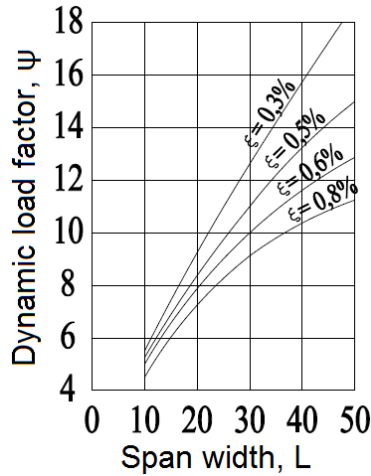
Figure 5.10: Vertical dynamic pedestrian induced load, Wheeler 1982

$f$    is the horizontal frequency [Hz]

$M$    is the modal mass of the bridge [kg]

$k$    is the ratio of induced force and velocity (= 300 Ns/m) [Ns/m]

## 5.5   SÉTRA

Service d'Études Techniques des Routes et Autoroutes (SÉTRA) is the french standard for roads and highways, and was made in order to summarize previously obtained knowledge about dynamical behavior of pedestrian bridges. The methodology in the report is based on tests and measurements performed on the Solferino Pedestrian Bridge in Paris, as well as laboratory tests and previous research.

### 5.5.1   Comfort criteria

The comfort criteria for in SÉTRA is dependent on the level of comfort chosen for the individual project, the definitions of the three comfort levels are given in table 5.12. The comfort criterion is automatically considered as met if the risk of resonance is considered negligible after evaluation of the natural frequencies. Table 5.13 shows the acceleration ranges associated with the comfort levels, in vertical and horizontal direction [46].

Table 5.12: Definition of comfort level for footbridges, SÉTRA

| Comfort level | Definition |
|---|---|
| Maximum | Acceleration undergone by the structure are practically imperceptible to the users |
| Average | Accelerations undergone by the structure are merely perceptible to the users |
| Minimum | Under rare loading configurations, accelerations undergone by the structure are perceived by the users, but do not become intolerable |

Table 5.13: Acceleration ranges for vertical and horizontal vibrations

| Comfort level | Acceleration range [m/s$^2$] | |
|---|---|---|
| | Vertical | Horizontal |
| Maximum | < 0.50 | < 0.15 |
| Average | 0.50 - 1.00 | 0.15 - 0.30 |
| Minimum | 1.00 - 2.50 | 0.30 - 0.80 |
| Critical | > 2.50 | > 0.80 |

For maximum, average and minimum comfort level, the natural frequencies are determined for 2 mass assumptions; empty footbridge and footbridge loaded with 700 N per square meter. The horizontal acceleration is limited in any case to 0.10 m/s$^2$ to avoid lock-in effect.

There are four frequency ranges corresponding to a risk of resonance. Table 5.14 and 5.15 defines the frequency range for vertical and longitudinal, and horizontal vibrations respectively.

Table 5.14: Frequency range risk of the vertical and longitudinal vibrations

| Risk | Frequency [Hz] | | | | | |
|---|---|---|---|---|---|---|
| | 0 | 1 | 1.7 | 2.1 | 2.6 | 5 |
| Maximum | | | | | | |
| Average | | | | | | |
| Minimum | | | | | | |
| Negligible | | | | | | |

Table 5.15: Frequency range risk of the horizontal vibrations

| Risk | Frequency [Hz] | | | | | |
|------|---|---|---|---|---|---|
| | 0 | 0.3 | 0.5 | 1.1 | 1.6 | 2.5 |
| Maximum | | | 🟥 | | | |
| Average | | 🟦 | | 🟦 | | |
| Minimum | | | | | 🟨 | |
| Negligable | 🟩 | | | | | 🟩 |

For a simply supported bridges with constant inertia, SÉTRA suggests that the maximum acceleration can be found from theoretical calculations:

$$a_{max} = \frac{1}{2\xi} \frac{4F}{\pi \rho S} \qquad [\text{m/s}^2] \quad (5.24)$$

Where:

$\xi$    is the damping ratio of the structure, see table 5.16 [-]

$F$    is the linear load on the bridge [N/m]

$\rho S$   is the total linear density [kg/m]

Table 5.16: Damping ratios for different materials, $\xi_m$, from SÉTRA

| Type | Critical damping ratio |
|------|------------------------|
| Reinforced concrete | 1.3 % |
| Pre-stressed concrete | 1 % |
| Mixed | 0.6 % |
| Steel | 0.4 % |
| Timber | 1 % |

### 5.5.2   Load model

Similarly to UK-NA, SÉTRA distinguish between using concentrated load, for simulated single pedestrians and groups, and distributed load, for simulating pedestrian crowds. SÉTRA gives models for vertical, lateral and longitudinal oriented concentrated loads and vertical distributed loads. The load models are based on Fourier series and has its background in Bachmann and Ammann's model (see Section 4.4.1). Following from Bachmann and Ammanns's model it is not taken to consideration overlapping between steps or synchronization, which makes SÉTRA's model easy to interpret. It is important to keep in mind that the load models for multiple pedestrians does not include the static

load of the pedestrians, and if it is desired to obtain the deflection, this load has to be added to the total mass of the footbridge.

**Concentrated load model**

The concentrated load proposed in SÉTRA is modeled as a moving force along the span. The load is constructed by a Fourier series up to 4th order in the vertical direction and 1st order in the lateral direction. However, it is suggested in the guideline to limit both loads to 1st order to decrease computational costs.

For single pedestrians and groups SÉTRA gives the following concentrated load model:

$$P(x,t) = F(t)\delta(x - v_t) \qquad \text{[N]} \quad (5.25)$$

Where:

$F(t)$      is the load of a human walking or running [N]

$\delta(x - v_t)$   is the space component, described by a Dirac Delta Function (see Section 2.8), where $x$ is the pedestrian's relation to the center line of the walkway [-]

$v_s$      is the walking speed [m/s]

The periodic function $F(t)$ is given as a Fourier series:

$$F(t) = G_0 + G_1 sin(s\pi f_m t) + \sum_{i=2}^{n} G_i sin(2\pi i f_m t - \phi_i) \qquad \text{[N]} \quad (5.26)$$

Where:

$G_0$   is the static force in vertical direction ( $\approx 700$ N) [N]

$G_1$   is the first harmonic amplitude, see Table 5.17 [N]

$G_i$   is the i-th harmonic amplitude, see Table 5.17 [N]

$f_m$   is the walking frequency, see Table 5.18 for values given in SÉTRA [Hz]

$\phi_i$   is the phase angle of the i-th harmonic, see Table 5.17 [-]

$n$    is the number of harmonics used [-]

$G1$, $G2$ and $G3$ are the Fourier coefficients, and are calculated from a mean frequency of 2 Hz and implemented to the harmonic amplitudes shown in Table 5.17. Coefficients for harmonics over 3 are not included as they will have values lower than 0.1, and does not contribute significantly.

As mentioned, it is recommended in SÉTRA only include the Fourier sum to the first harmonic. Following, the load models given in Equation (5.27), (5.28) and (5.29) can be adapted considering respectively vertical, lateral and longitudinal action.

Table 5.17: Harmonic amplitude and phase angles given in SÉTRA

| Number of harmonic, i | Harmonic amplitude [N] | Phase angle [rad] |
|---|---|---|
| 1 | $G_1 = 0.4G_0$ | - |
| 2 | $G_2 = 0.1G_0$ | $\phi_2 = \pi/2$ |
| 3 | $G_3 = 0.1G_0$ | $\phi_3 = \pi/2$ |

Table 5.18: Step frequency ranges for walking and jogging given in SÉTRA

| Activity | Step frequency range, [Hz] |
|---|---|
| Walking | $1.6 \leq f_s \leq 2.4$ |
| Jogging | $2.0 \leq f_s \leq 3.5$ |

$$F_{ver}(t) = G_0 + 0.4G_0 sin(2\pi f_m t) \qquad \text{[N]} \quad (5.27)$$

$$F_{lat}(t) = 0.05G_0 sin(2\pi(\frac{f_m}{2})t) \qquad \text{[N]} \quad (5.28)$$

$$F_{long}(t) = 0.02G_0 sin(2\pi f_m t) \qquad \text{[N]} \quad (5.29)$$

**Distributed load model**

For crowd loading SÉTRA presents a load model of distributed loads, given in Equation (5.30). The loads shall be applied until steady-state conditions are reached.

$$F_v(t) = dP cos(2\pi f_v t)N_{eq}\psi \qquad \text{[N/m}^2\text{]} \quad (5.30)$$

Where:

$d$    is the density of pedestrians, found from Table 5.20 [ped/m$^2$]

$P$    is the lateral load amplitude, depended on the direction of the loading, found in Table 5.19 [N]

$f_v$    is the natural frequency of the considered vertical mode [Hz]

$N_{eq}$ is the equivalent number of pedestrians, found in Table 5.21 [-]

$\psi$    is the modification factor, found from Figure 5.11 [-]

Table 5.19: Static load P for varying loading directions

| Loading direction | Vertical | Longitudinal | Lateral |
|---|---|---|---|
| Static force, P [N] | 280 | 140 | 35 |

Table 5.20: The density $d$ of the pedestrian crowd for pedestrian bridge, from SÉTRA

| Class | Description | Density, $d$, of the crowd |
|---|---|---|
| I | Very dense crowd | 1 pedestrians/m$^2$ |
| II | Dense crowd | 0.8 pedestrians/m$^2$ |
| III | Sparse crowd | 0.5 pedestrians/m$^2$ |

Table 5.21: Equivalent number of pedestrians, from SÉTRA

| Density class | Equivalent number of pedestrians, $N_{eq}$ |
|---|---|
| I | $N_{eq} = 1.85\sqrt{1/n}$ |
| II | $N_{eq} = 10.8\sqrt{\xi/n}$ |
| III | $N_{eq} = 10.8\sqrt{\xi/n}$ |

Where:

$\xi$ is the critical damping ratio, from Equation (5.31), (5.32) and Table 5.16 on page 62 [-]

$n$ is the the number of pedestrians on the bridge [-]
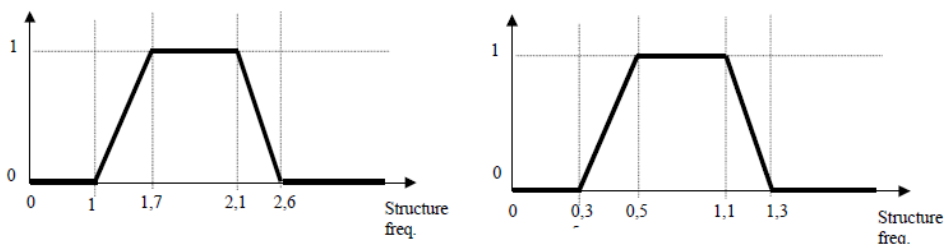


Figure 5.11: Factor $\psi$ in the case of walking, for vertical and longitudinal vibrations on the left, and lateral vibrations on the right, first harmonic.

For bridges made of different materials it is recommended to use is the average damping ratio of the different materials, weighted by their contribution to the overall rigidity.

$$\xi_{mode\ i} = \frac{\sum_{material\ m} \xi_m k_{m,i}}{\sum_{material\ m} k_{m,i}} \qquad \text{[-]} \quad (5.31)$$

Where $k_{m,i}$ is the contribution of material $m$ to the overall rigidity in mode $i$. $k_{m,i}$ can be difficult to determine, and the guideline therefore presents a general formula which can be used for footbridges with approximately constant section, see Equation (5.32).

$$\xi_{mode\ i} = \frac{\sum_{material\ m} \xi_m EI_m}{\sum_{material\ m} EI_m} \qquad \text{[-]} \quad (5.32)$$

Where $EI$ is the contribution of the material $m$ to the overall rigidity.

# 5.6 ISO 10137

The International Organization of Standardization is an independent and non-governmental organization which has produced over 21 000 International Standards and related documents covering almost every industry. Each standard is named ISO, followed by a number, and ISO 10137 forms the basis for design of structures-, serviceability of buildings, and walkways, against vibrations.

## 5.6.1 Comfort criteria

The comfort criteria for pedestrian bridges is described in Annex C in ISO 10137. The acceptable acceleration for a pedestrian bridge is dependent on the natural frequencies of the structure, and is factored based on a critical frequency domain. The vertical vibration of an empty footbridge shall not exceed 60 times the acceleration found from the base curve for vertical direction, see Figure 5.12 [47]. If a person is standing still on the bridge while there is pedestrian traffic, the acceptable acceleration can not exceed 30 times the acceleration from the same base curve. For horizontal vibration the acceleration can not exceed 60 times the acceleration found in the base curve for horizontal direction, see Figure 5.13 and Table 5.22.
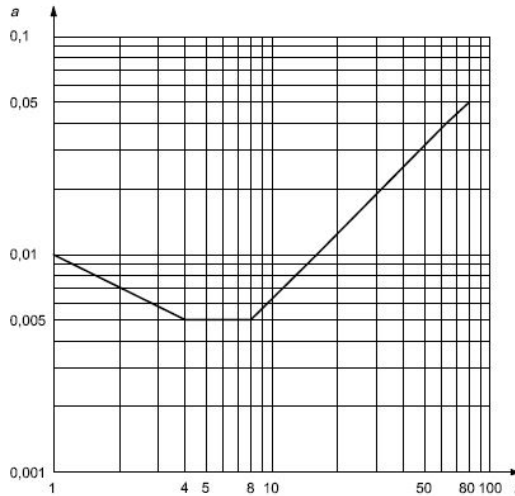


Figure 5.12: Base curve for acceleration in vertical direction, $a$ is in m/s$^2$ and $f$ is in Hz
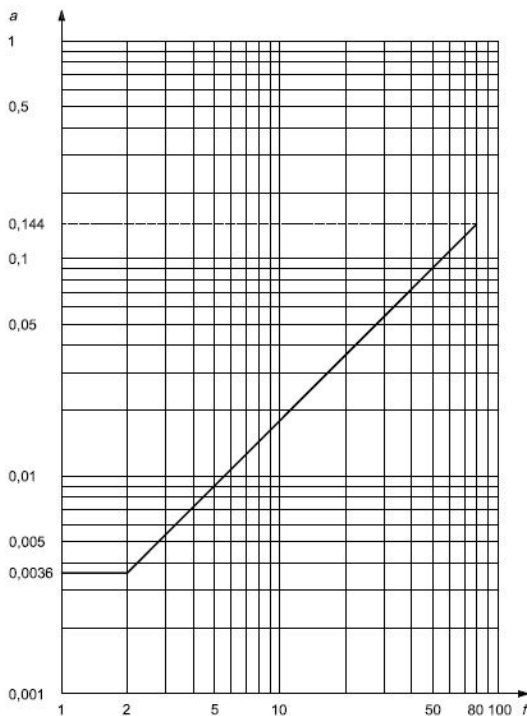
Figure 5.13: Base curve for acceleration in horizontal direction, $a$ is in m/s$^2$ and $f$ is in Hz

Table 5.22: Acceleration from base curves in critical domains

| Direction | Mutliplier | Frequency [Hz] | Acceleration criterion [m/s$^2$] |
|---|---|---|---|
| Vertical | 30 | 1 | 0.30 |
| | 60 | | 0.60 |
| | 30 | 2 | 0.21 |
| | 60 | | 0.42 |
| | 30 | 3 | 0.22 |
| | 60 | | 0.34 |
| | 30 | 4 - 8 | 0.15 |
| | 60 | | 0.30 |
| Horizontal | 60 | 1 - 2 | 0.22 |

The base curve for vertical direction, Figure 5.12 and Table 5.22, shows that the critical frequency domain between is between 4 and 8 Hz. However, the relevant acceleration criterion is in the domain 1 to 4 Hz, as this is the range of the walking frequency. The critical domain in the horizontal acceleration base curve is between 1 and 2 Hz.

### 5.6.2 Load model

The load models in ISO 10137 are based on Bachmann and Ammann's model (Section 4.4). In ISO 10137 both vertical and lateral pedestrian induced force are described as Fourier series, and the load models are given in Equation (5.33) and (5.34).

$$F_{ver}(t) = Q(1 + \sum_{n=1}^{k} \alpha_{n,ver} sin(2\pi ft + \phi_{n,ver})) \qquad \text{[N]} \quad (5.33)$$

$$F_{lat}(t) = Q(1 + \sum_{n=1}^{k} \alpha_{n,lat} sin(2\pi ft + \phi_{n,lat})) \qquad \text{[N]} \quad (5.34)$$

Where:

$Q$      is the static load of the participating person [N]

$\alpha_n$      is the Fourier coefficient corresponding to the nth harmonic, given in Table 5.23 [-]

$f$      is the step frequency. For lateral vibrations, $f$ is half the vertical frequency [Hz]

$\phi_n$      is the phase angle of the nth harmonic in vertical/lateral direction, chosen to $\pi/2$ for a conservative approach [rad]

$n$      is the number of harmonics considered (1 is used after advise from guideline) [-]

$k$      is the number of harmonics which characterize the forcing function in the frequency range of interest. The number of harmonics $k$ that is needed for an accurate model is dependent on the complexity of the load and its time history [-]

Table 5.23: Numerical coefficients for pedestrian load models, ISO 10137

| Activity | Harmonic number | Common range of forcing frequency $nf$ [Hz] | Numerical coefficient for vertical direction $\alpha_{n,v}$ | Numerical coefficient for lateral direction $\alpha_{n,l}$ |
|---|---|---|---|---|
| Walking | 1 | 1.2 to 2.4 | 0.37(f-1.0) | |
| | 2 | 2.4 to 4.8 | 0.1 | |
| | 3 | 3.6 to 7.2 | 0.06 | 0.1 |
| | 4* | 4.8 to 9.6 | 0.06 | |
| | 5* | 6.0 to 12.0 | 0.06 | |
| Running | 1 | 2 to 4 | 1.4 | |
| | 2 | 4 to 8 | 0.4 | 0.2 |
| | 3 | 6 to 12 | 0.1 | |

*These harmonics are not relevant for pedestrian perception and can be neglected.

The lateral/horizontal numerical coefficient, $\alpha_{n,l}$, is used for structures with horizontal natural frequencies of a value around half of the walking and running frequency ($\approx 1$ Hz). $\alpha_{n,l}$ does not take to account for the synchronization between the user and the structure observed for example at the Millennium Bridge in London [35] [29].

However, previous research (i.e. [2]) has concluded that the load model can be simplified to regard only one Fourier coefficient, leaving the load model to be:

$$F_{ver}(t) = Q(1 + \alpha_{1,ver}sin(2\pi fnt))N_{eq} \qquad [N] \quad (5.35)$$

And as the amplitude is not effected by the static load, this can be written as:

$$F_{ver}(t) = Q\alpha_{1,ver}sin(2\pi fnt)N_{eq} \qquad [N] \quad (5.36)$$

The load model presented in ISO 10137 has some simplifications which can lead to inaccurate acceleration values:

- The load models are simplifications of the pedestrian load histories presented in the same guideline, shown in Figure 5.14 and 5.15. Figures shows how the load varies throughout the step, however the model is an simple sinus curve.

- Neither a walking speed or an area where the load should be applied is specified. The guideline outlines that the load should be applied to achieve the worst case scenario.
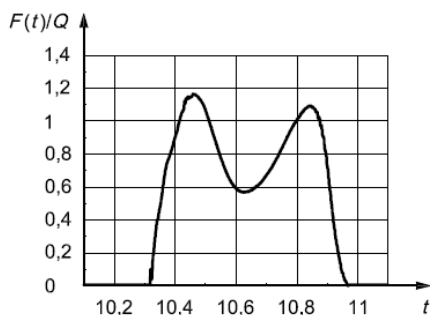


Figure 5.14: Vertical force for a single pedestrians walking, from ISO 10137
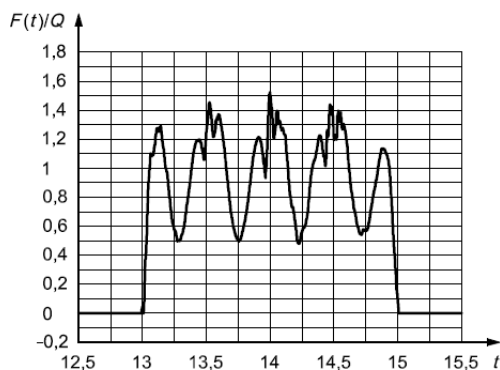


Figure 5.15: The force of a single pedestrian walking across a 3m long instrumented platform

Where:

$t$ \qquad is the time [$s$]

$F(t)/Q$ is the normalized amplitude [-]

ISO 10137 takes to account for the imperfect coordination of a group of people, by multiplying a coordination factor $C(N)$ to the the loads, Equation (5.33) or (5.34). Such that the loads become:

$$F(t)_N = F(t)C(N) \qquad \text{[N]} \quad (5.37)$$

Where:

$$C(N) = \frac{\sqrt{N}}{N} \qquad \text{[-]} \quad (5.38)$$

And N is the number of pedestrians in the group.

## 5.7 JRC - Design of Footbridges for Human Induced Vibrations

Joint Research Centre (JRC) is the European Comission's scientific and knowledge service that provide independent scientific advice and support to EU policies. In 2009 JRC published a guideline for design of lightweight footbridges for human induced vibrations with both a comfort criteria and load model. The guideline is named Design of Footbridges for Human Induced Vibrations, but will for the rest of the thesis be written as *JRC*.

### 5.7.1 Comfort criteria

Similar to SÉTRA, JRC defines ranges of acceleration for different comfort classes, see Table 5.24 [48]. JRC also defines the critical range of natural frequencies of footbridges with pedestrian excitation, see Table 5.25.

Table 5.24: Acceleration criteria for vertical and horizontal vibrations

| Comfort level | Acceleration range [m/s$^2$] | |
|---|---|---|
| | Vertical | Horizontal |
| Maximum | < 0.50 | < 0.10 |
| Average | 0.50 - 1.00 | 0.10 - 0.30 |
| Minimum | 1.00 - 2.50 | 0.30 - 0.80 |
| Critical | a > 2.50 | a > 0.80 |

Table 5.25: Critical ranges of natural frequencies in different directions JRC

| Direction | Frequency range [Hz] |
|---|---|
| Vertical | $1.25 \leq f_i \leq 2.3$ |
| Longitudinal | $1.25 \leq f_i \leq 2.3$ |
| Lateral | $0.5 \leq f_i \leq 1.2$ |

If the 2nd harmonic of the natural frequency in the vertical or longitudinal direction is not in the domain 2.5 to 4.6 Hz, the critical frequency range expands to $1.25 \text{ Hz} \leq f_i \leq 4.6 \text{ Hz}$. Lateral vibrations are not affected by 2nd harmonic pedestrian loads.

The 1st harmonic motion in lateral direction has to be checked for lock-in effect. This is done by calculation the number of pedestrians $N_L$ that could lead to a removal of the damping of the structure, causing a sudden amplified response. The equation is similar to Equation 5.23 from Håndbok 185 in Section 5.4.1, and is an alternate version of the critical number of pedestrians from Dallard et al's equation:

$$N_L = \frac{8\pi\xi f m^*}{k} \qquad [\text{-}] \quad (5.39)$$

Where:

$N_L$ is the number of pedestrians evenly distributed across the bridge giving unacceptable horizontal vibrations [-]

$\xi$ is the damping ratio [-]

$f$ is the natural frequency [Hz]

$m^*$ is the modal mass of the bridge [kg]

$k$ is the ratio of induced force and velocity (= 300 Ns/m) [Ns/m]

An alternative approach is to define a trigger acceleration that would initiate the lock-in phenomenon:

$$0.10 < a_{lock-in} < 0.15 \qquad [\text{m/s}^2] \quad (5.40)$$

### 5.7.2 Load model

JRC presents a load model with uniformly distributed harmonic load adapted to the considered mode shape. The uniformly distributed harmonic load model is given in Equation (5.41) and can be used to simulate both load from walking and jogging pedestrians.

$$p(t) = P cos(2\pi f_s t) n' \psi \qquad [\text{N/m}^2] \quad (5.41)$$

Where:

$P$ is the static load from a single pedestrian, depended on considered direction, see Table 5.27 [N]

$f_s$ is the step frequency [Hz]

$n'$ is the equivalent number of pedestrian, dependent on traffic class, see Table 5.28 [-]

$S$ is the bridge deck area [m²]

$\psi$ is the reduction factor considering the probability that the step frequency and the natural frequency will coincide, see Figure 5.16, 5.17, and 5.18 [-]

Table 5.26: Traffic classes to estimate the pedestrian density, JRC

| Traffic Class | Density $d$ [Ped/m²] | Description |
|---|---|---|
| TC 1 | Group of 15 ped | Very weak traffic |
| TC 2 | 0.2 | Weak traffic |
| TC 3 | 0.5 | Dense traffic |
| TC 4 | 1.0 | Very dense traffic |
| TC 5 | 1.5 | Exceptional dense traffic |

When a stream becomes dense, the correlation between pedestrians increases, but the dynamic load tends to decrease. If the density of pedestrians exceeds the upper limit value of 1.5 ped/m² walking will be close to impossible, and the dynamic effects will significantly reduce.

Table 5.27: Force amplitude relative to the diretion of analysis, from JRC

| Traffic class | P [N] | | |
|---|---|---|---|
| | Vertical | Longitudinal | Lateral |
| TC 1 - TC 5 | 260 | 140 | 35 |

Table 5.28: Equivalent number of pedestrians relative to traffic class, from JRC

| Traffic class | Equivalent number of pedestrians, $n'$ |
|---|---|
| TC 1 - TC 3 | $n' = \frac{10.8\sqrt{\zeta n}}{S}$ |
| TC 4 - TC 5 | $n' = \frac{1.85\sqrt{n}}{S}$ |

Where:

$\zeta$ is the structural damping, see Table 5.29 [-]

$S$ is the bridge deck area [m²]

$n$ is the number of pedestrians, found from Equation (5.42) [-]

Number of pedestrians on the bridge deck is calculated according to traffic class by:

$$n = S\rho \qquad [\text{-}] \qquad (5.42)$$

Where:

$\rho$     is the pedestrian density $[\text{ped/m}^2]$

Table 5.29: Damping ratios for service limit state design, from JRC

| Construction type | Minimum $\xi$ | Average $\xi$ |
|---|---|---|
| Reinforced concrete | 0.8 % | 1.3 % |
| Prestressed concrete | 0.5 % | 1.0 % |
| Composite steel-concrete | 0.3 % | 0.6 % |
| Steel | 0.2 % | 0.4 % |
| Timber | 1.0 % | 1.5 % |
| Stress-ribbon | 0.7 % | 1.0 % |
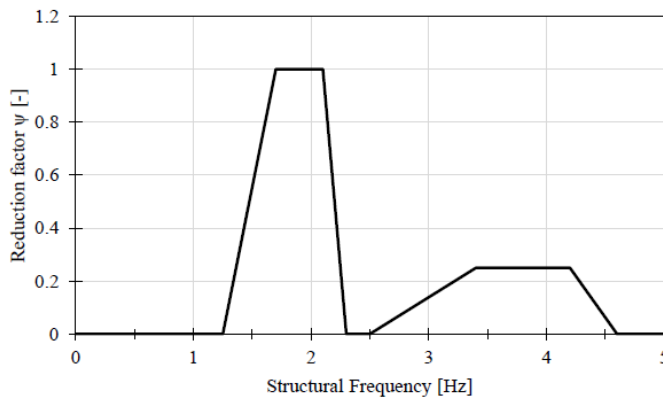


Figure 5.16: Reduction factor, $\psi$, for walking in vertical direction, from JRC
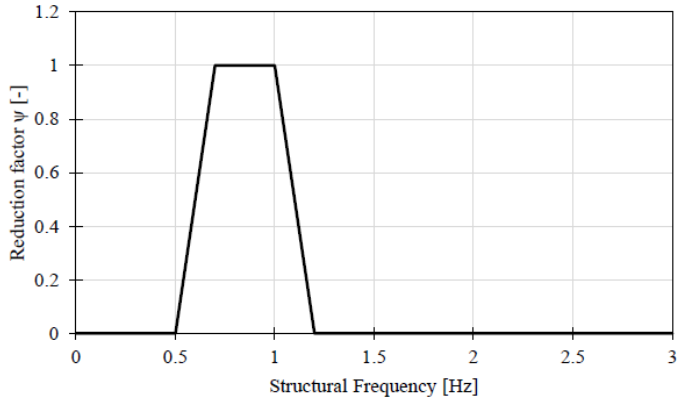
Figure 5.17: Reduction factor, $\psi$, for walking in lateral direction, from JRC
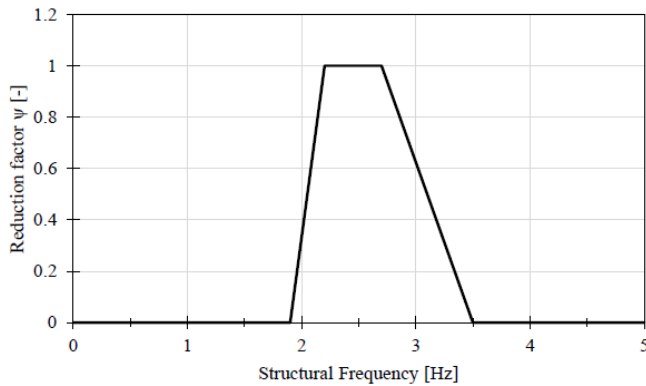


Figure 5.18: Reduction factor, $\psi$, for jogging in vertical direction, from JRC

## 5.8   HIVOSS

Human Induced Vibrations of Steel Structures (HIVOSS) is based on results from a research project determining an advanced load models for synchronous pedestrian excitation and optimized design guidelines for steel foot bridges - SYNPEX. The aim of SYNPEX is to develop advanced load models for synchronous pedestrian excitation and use the research to optimize the design guidelines for steel footbridges [49]. The pedestrian comfort criteria and load model presented in HIVOSS is exatly the same as presented in JRC from Section 5.7.2 [50], and will not be repeated.

## 5.9  Summary of Guidelines

The following section summarizes the comfort criteria and load models presented in this chapter. Comments and examples of usage are shown by solving the comfort criteria and load models for Bårdshaug Bridge in Section 7.1 and 7.2.

### 5.9.1  Comfort criteria

Table 5.30: Summary of comfort criteria

| Guideline | Comfort criteria [m/s$^2$] | |
|---|---|---|
| | Vertical | Horizontal |
| Eurocode, Table 5.1 | $a_c = 0.7$ | $a_c = 0.2$ |
| BS 5400, Equation (5.7) | $0.50 < a_c < 1.12$ | $a_c = 0.2^*$ |
| UK NA:EC, Equation (5.14) | $0.50 < a_c < 2.00$ | $a_c = 0.2^*$ |
| SVV Håndbok, Equation (5.21) * | $0.25 < a_c < 0.87$ | $a_c = 0.2^*$ |
| SÉTRA, Table 5.13 | $0.50 < a_c < 2.50$ | $a_c = 0.1$ |
| ISO 10137, Table 5.22 | $0.15 < a_c < 0.60$ | $a_c = 0.22$ |
| JRC/HIVOSS, Table 5.24 | $0.50 < a_c < 2.50$ | $0.10 < a_c < 0.15$ |

* Not specified in the guideline, Eurocode is applied.

Noting from the table above that the critical acceleration in the vertical direction ranges from 0.15 to 2.50 m/s$^2$, while the critical acceleration in the horizontal direction ranges from 0.1 to 0.22 m/s$^2$.

## 5.9.2 Load models

Table 5.31: Summary of the load models for the concentrated loads

| Guideline | Load model - concentrated loads |
|-----------|--------------------------------|
| Eurocode | $a_{vert,1} = \frac{200}{M\xi}$ |
| | $a_{hor,1} = \frac{50}{M\xi}$ |
| BS 5400 | $F = 180\sin(2\pi f_0 T)$ |
| UK-NA | $F_{vert}(T) = 180 sin(2\pi f_0 T)$ |
| SÉTRA | $F_{vert}(t) = G_0 + 0.4G_0 sin(2\pi f_m t)$ |
| | $F_{lat}(t) = 0.05G_o sin(2\pi(\frac{f_m}{2})t)$ |
| Håndbok 185 | $a_r = 4\pi^2 f^2 W_s K \psi r$ |
| ISO 10137 | $F_{ver}(t) = Q(1 + \sum_{n=1}^{k} \alpha_{n,ver} sin(2\pi f t + \phi_{n,ver}))$ |
| | $F_{lat}(t) = Q(1 + \sum_{n=1}^{k} \alpha_{n,lat} sin(2\pi f t + \phi_{n,lat}))$ |
| JRC/HIVOSS | - |

Table 5.32: Summary of the load models for the distributed loads

| Guideline | Load model - distributed loads [N/$m^2$] |
|-----------|------------------------------------------|
| Eurocode | $a_{vert,n} = 0.23 a_{vert,1} n k_{vert}$ |
| | $a_{hor,n} = 0.18 a_{hor,1} n k_{hor}$ |
| BS 5400 | - |
| UK-NA | - |
| SÉTRA | $F_{vert}(t) = dP cos(2\pi f_v t) N_{eq} \psi$ |
| Håndbok 185 | - |
| ISO 10137 | - |
| JRC/HIVOSS | $p_{vert}(t) = P cos(2\pi f_s t) n' \phi$ |

# Chapter 6

# Bårdshaug Bridge

## 6.1   Description of Bårdshaug Bridge

Bårdshaug Bridge is a pedestrian bridge located in Orkanger in Norway, constructed and designed by The Norwegian Public Roads Administration (Statens Vegvesen). The bridge was opened in October 2016, and is a composite bridge, built without interaction between the parts. The bridge is 134 meters long and 4 meters wide, it is supported by three concrete columns, dividing the bridge into 5 spans, see Figure 6.1 and 6.3.



Figure 6.1: Picture of Bårdshaug Bridge [3]

The cross section of the girder consists of two I-beams of varying size with a concrete slab resting on top. The concrete slab is poured in situ, and the concrete is not anchored to the steel beams, so that the concrete slab and steel beams are interacting mostly through friction. Small concrete consoles are poured around the top flange of the steel beams to ensure interaction and prevent slipping in lateral direction.
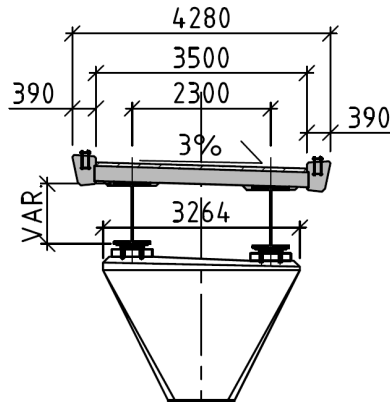
Figure 6.2: Cross section of concrete deck and steel beams on arbirtary column, Bårdshaug Bridge, dimensions in mm. From internal documents at Statens Vegvesen.
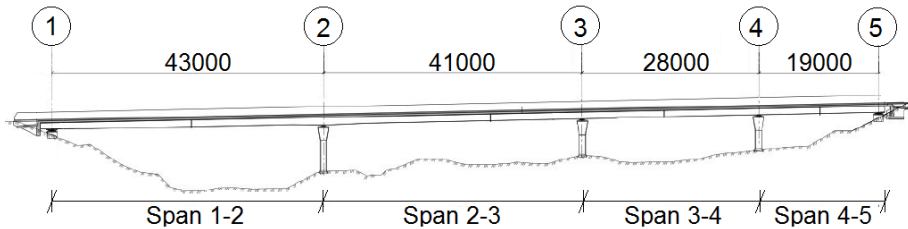


Figure 6.3: Numbering of columns and dimensions and labeling of the bridge spans of Bårdshaug Bridge, seen from the side, dimensions in mm. From internal documents at Statens Vegvesen.

The steel beams are stiffened by steel trusses every six meters. The steel trusses are only connected to the steel beams, and does not increase the interaction between the steel beams and the concrete slab. The steel trusses are excluded from the Finite Element (FE)-model of the bridge and the properties are therefore discussed closer in Section 6.3.

## 6.2  System Identification

Before the work on this thesis began, the acceleration response of Bårdshaug Bridge was measured by placing 19 triaxial sensors throughout the bridge. The location of the 18 first accelerometers are illustrated in Figure 6.4. Accelerometers are paired, creating nine sensor pairs on the girder, while the last accelerometer is placed on column number 3, see Figure 6.4. Acceleration values found from a 1.5 hour long time series is presented in Table 6.1 and 8.5.

Table 6.1: Accelerations in vertical direction from measurement data

| Acceleration [m/s$^2$] | | |
|---|---|---|
| Max | 95th-percentile | RMS |
| 0.3982 | 0.0248 | 0.0165 |

Table 6.2: Accelerations in horizontal direction from measurement data

| Acceleration [m/s$^2$] | | |
|---|---|---|
| Max | 95th-percentile | RMS |
| 0.1947 | 0.0153 | 0.0122 |
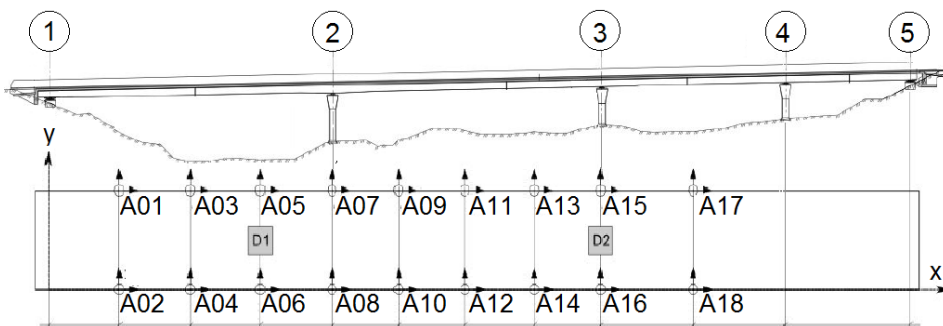


Figure 6.4: Placements of accelerometers on bridge deck of Bårdshaug Bridge. x in longitudinal direction, y in horizontal direction and z in vertical direction (out of plane) [3]

A report identifying the natural frequencies, modal shapes and structural damping of Bårdshaug Bridge was made by Ph.D. candidates Øyvind Wiig Pettersen and Gunnstein Thomas Frøseth. The results from the report are used as a base for the system identification done in this thesis. A new modal analysis of the measurement data is performed, and new modes are identified. The results of the latest modal analysis is given in Table 6.3.

Table 6.3: Natural frequencies and mode shapes from measurement data

| Mode | Mode shape | Frequency [Hz] |
|------|-----------|---------------|
| V1 | Span 1-2 and 2-3 antiphase | 1.97 |
| V2 | Span 2-3 dominant | 2.47 |
| V3 | Span 1-2 dominant, 2-3 in phase | 2.54 |
| V4 | Span 1-2 and 2-3 in phase | 2.90 |
| V5 | Span 3-4 dominant, all spans in phase | 4.36 |
| H1 | Column 2 and 3 in phase | 1.85 |
| H2 | Column 2 and 3 in antiphase | 2.72 |
| T1 | Span 1-2 and 2-3 in antiphase | 3.81 |
| T2 | Span 1-2 and 2-3 in antiphase | 4.45 |
| T3 | Span 1-2 and 2-3 in phase | 4.58 |

In the report Stochastic Subspace Identification (SSI) was used to find the natural frequencies [3]. SSI was chosen to identify the modes because a pedestrian bridge like Bårdshaug Bridge, with ambient loads, has a low excitation level of the acceleration and therefore less prominent peaks in a response spectrum. A peak picking method can difficult to use for measurement data with a lot of noise, when acceleration response of the structure and noise become hard to distinguish.

From the SSI it is also possible to establish the mode shapes. The accuracy of the modal shapes are not as good as the accuracy of the natural frequencies, but it gives a good idea of what the modes will look like.

Figure 6.5, 6.6 and 6.7 shows the response spectra of the acceleration for Bårdshaug Bridge. The spectra are made using Welch method with 20 hanning windows, and are used to obtain the natural frequencies using the peak picking method. The peaks which does not have an associated mode occur because of noise, and noise is also the reason that some modes appear on the side of the peak. Following the response spectra are Figures 6.8-6.17, illustrating of the mode shapes described in Table 6.3. The modes presented in this section are the ones that will be used to verify the accuracy of the FE-model in Section 6.3.
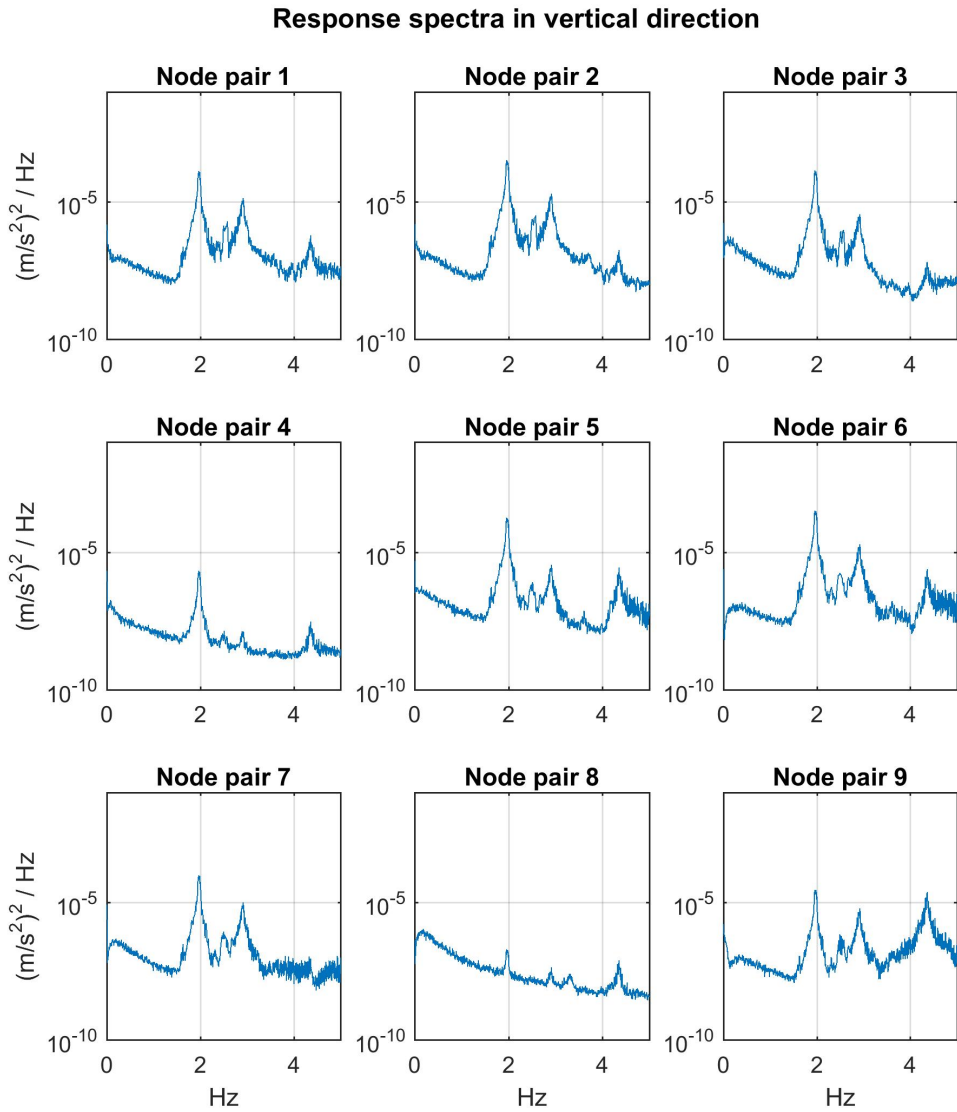
Figure 6.5: Response spectra in vertical direction

**Response spectra in horizontal direction**
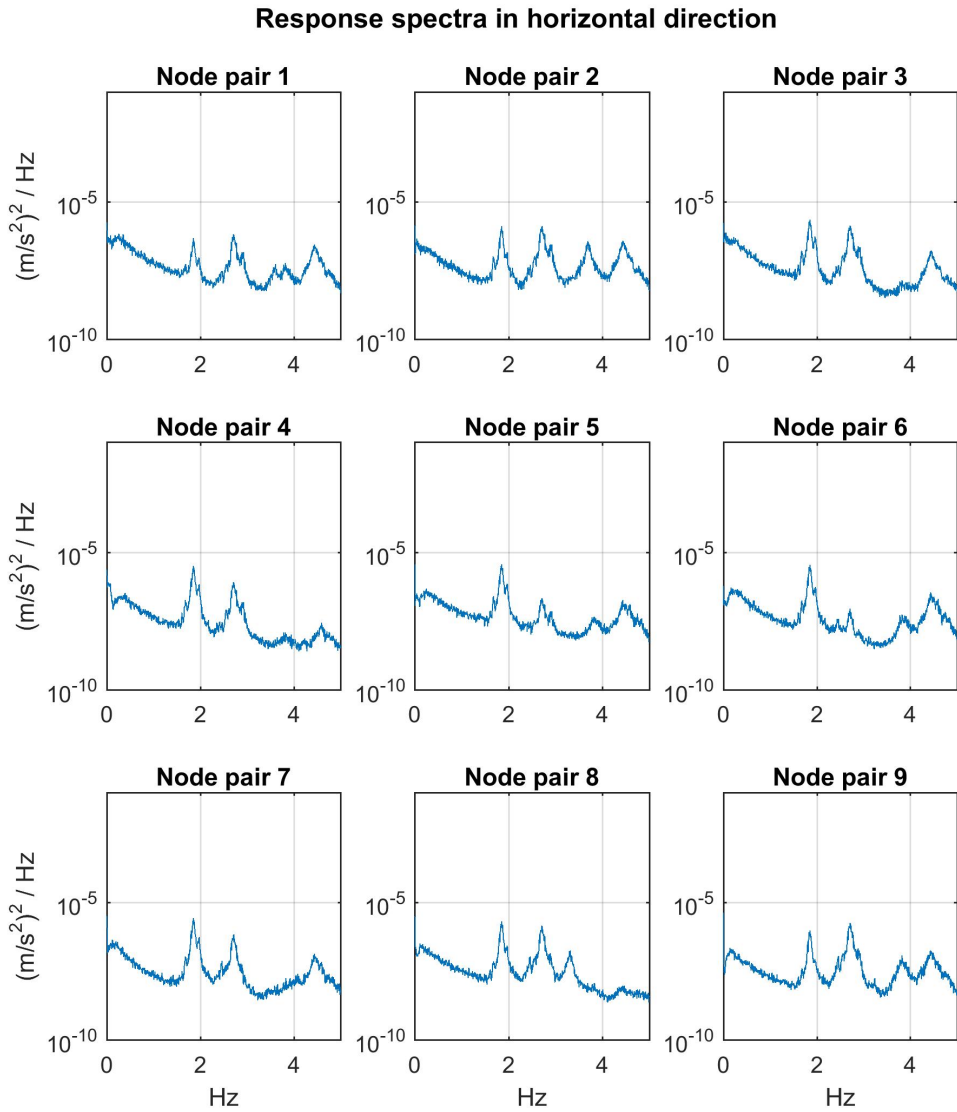


Figure 6.6: Response spectra in horizontal direction
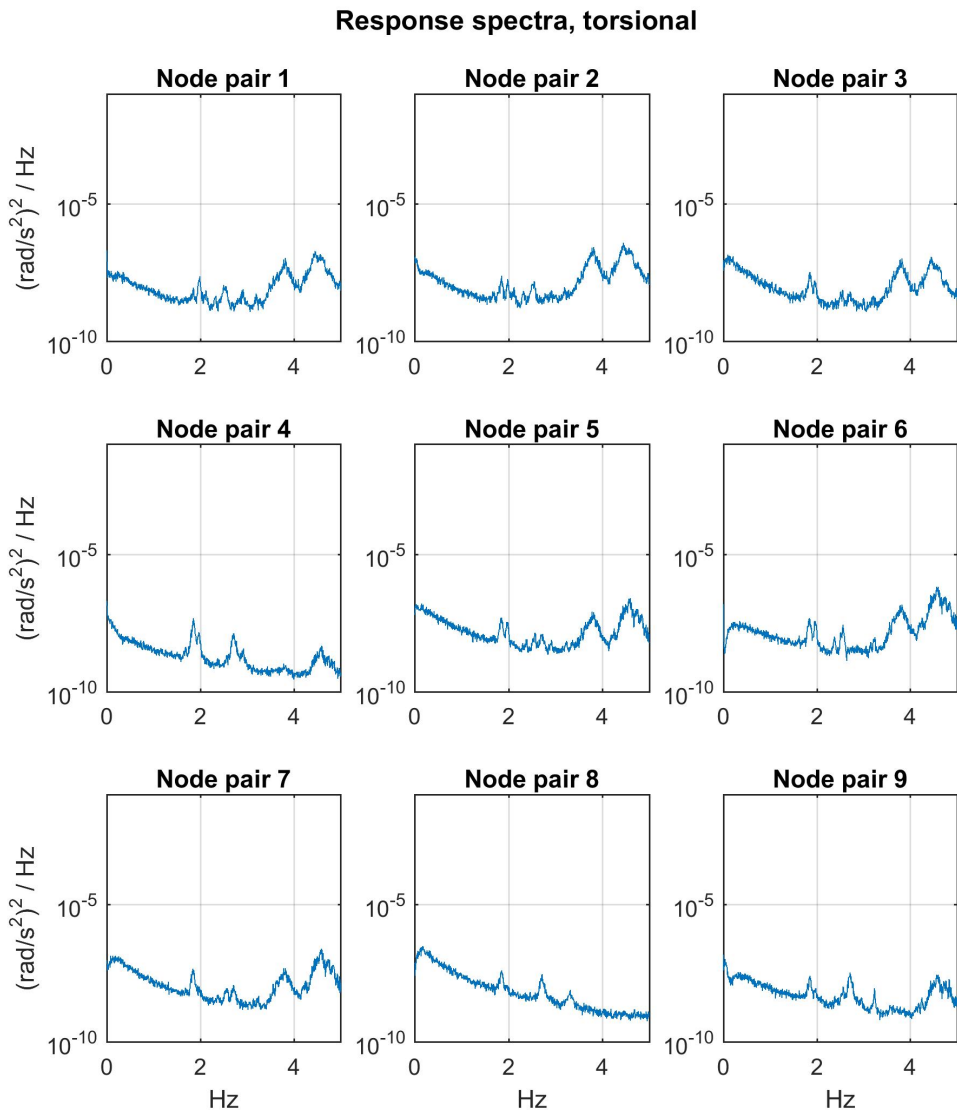
Figure 6.7: Response spectra of the rotational angle about the longitudinal axis, torsion
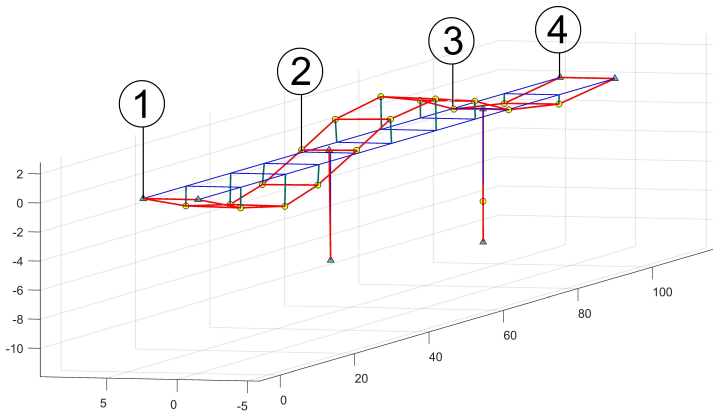
Figure 6.8: V1 (1.97 Hz)
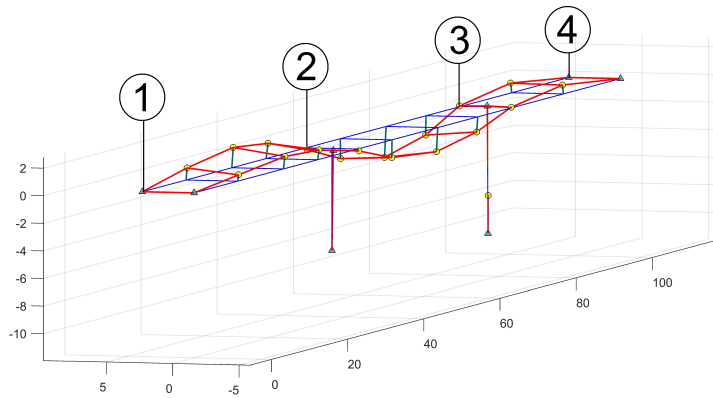


Figure 6.9: V2 (2.47 Hz)
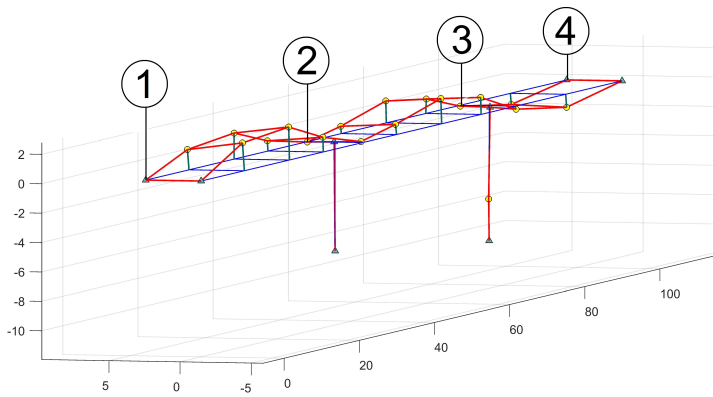


Figure 6.10: V3 (2.54 Hz)
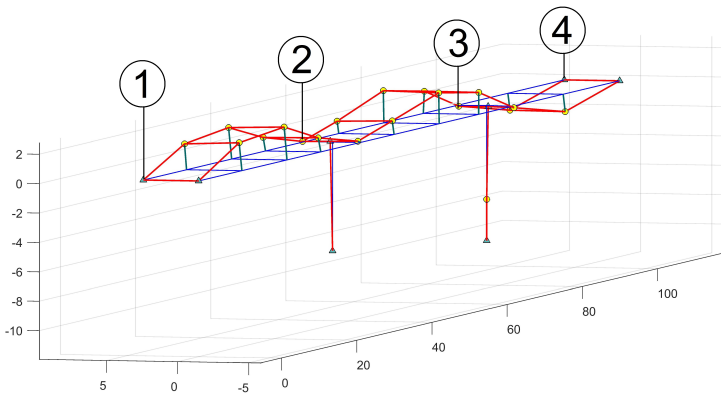
Figure 6.11: V4 (2.90 Hz)
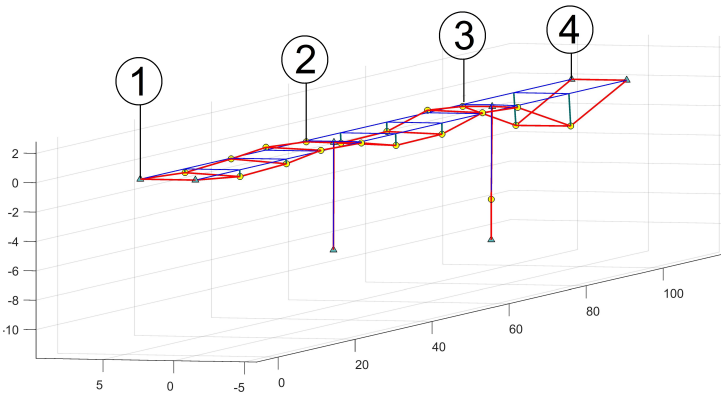


Figure 6.12: V5 (4.36 Hz)
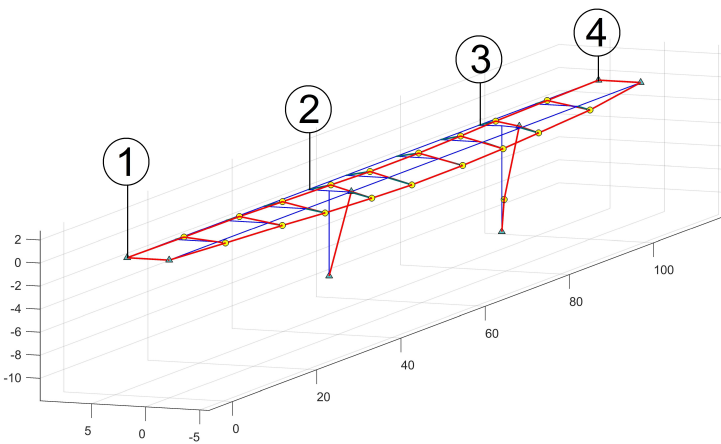


Figure 6.13: H1 (1.85 Hz)
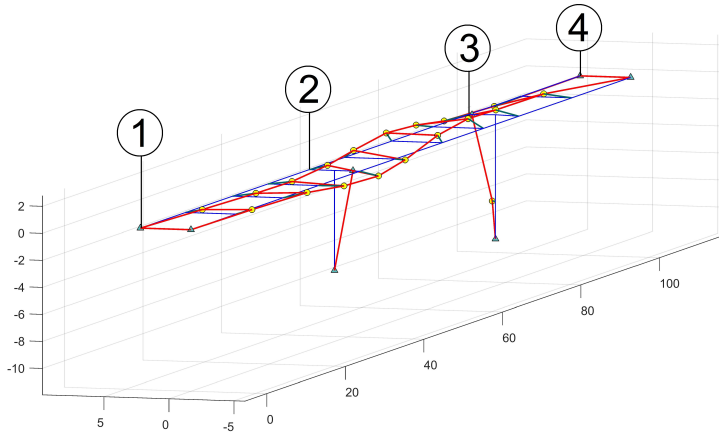
Figure 6.14: H2 (2.72 Hz)
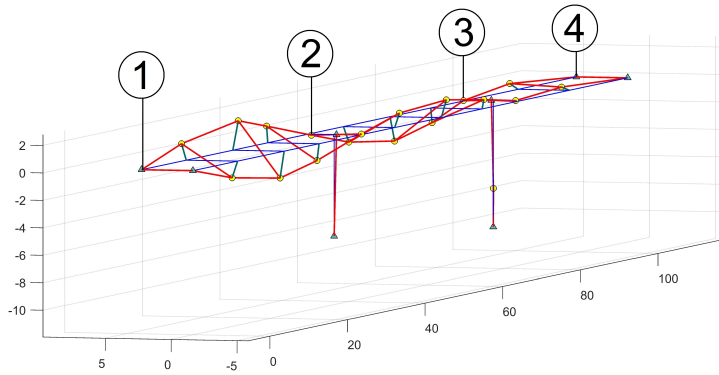


Figure 6.15: T1 (3.81 Hz)
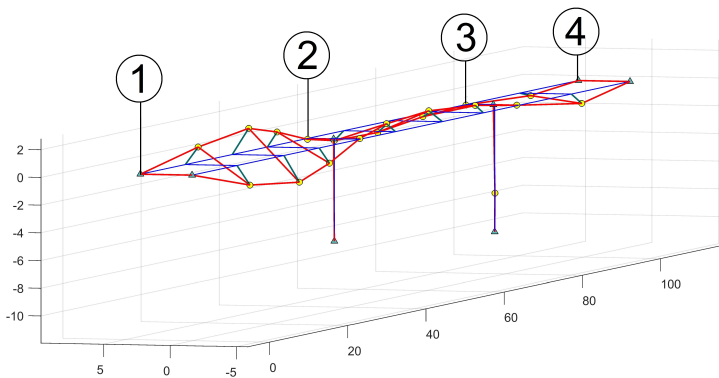


Figure 6.16: T2 (4.45 Hz)
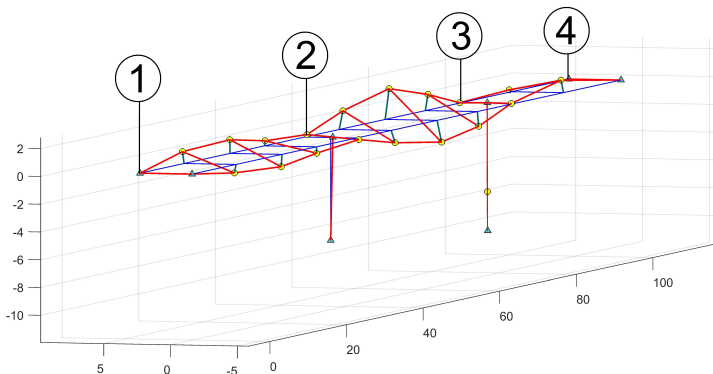
Figure 6.17: T3 (4.58 Hz)

## 6.3   Finite Element Analysis of Bårdshaug Bridge

Before the inception of this thesis, a finite element model of Bårdshaug Bridge was made by Statens Vegvesen in the design process of the structure. The model was created using the software RM Bridge to perform global static and modal analysis. The modal analysis from RM Bridge yields natural frequencies which does not coincide with the natural frequencies found in the system identification for Bårdshaug Bridge (Secction 6.2). Using the information provided from the system identification and structural data provided by Statens Vegvesen, a new finite element model is created for this thesis using the Computer-aided engineering (CAE) software Abaqus. The two main goals of the new model is to improve the model such that modal analysis can be better understood and applied to similar projects in the future, and be further used in this thesis to estimate the response from pedestrian induced forces.

Abaqus is chosen for modelling the bridge because the software is good at handling dynamic analysis, design can be done directly in 3D and because the software is available through NTNU licensing. For the dynamic analysis performed in Abaqus, an implicit direct integration method is chosen. As described in Section 2.4, the implicit methods are preferred for analysis with cyclic loading over a longer time period because of the unconditionally stable time increment $\Delta t$. One of the drawbacks of choosing implicit methods is the computational costs from updating the stiffness matrix for the time increments. The default time integration method in Abaqus is the generalized Newmark method: HHT-$\alpha$-method, described in Subsection 2.4.2 [51]. The default values of the Newmark and HHT-parameters are: $\alpha_H = -0.05$, $\beta = 0.276$ and $\gamma = 0.55$ such that the HHT $\alpha$-method is unconditionally stable. Reminder that the HHT $\alpha$-method is unconditionally stable when:

$$-\frac{1}{3} \leq \alpha_H \leq 0, \ \gamma = \frac{1}{2}(1 - 2\alpha_H) \ and \ \beta = \frac{1}{4}(1 - \alpha_H)^2$$

### 6.3.1 The Model

The FE-model of Bårdshaug Bridge is made with several simplifications. One of the main simplifications is that the model consists of three major components; two identical steel beams and one concrete slab. In this section the FE-model are described, and the simplifications included in the model are discussed. The detail in which the model is described below is sufficient enough for the reader to recreate the model in an FEA-software.
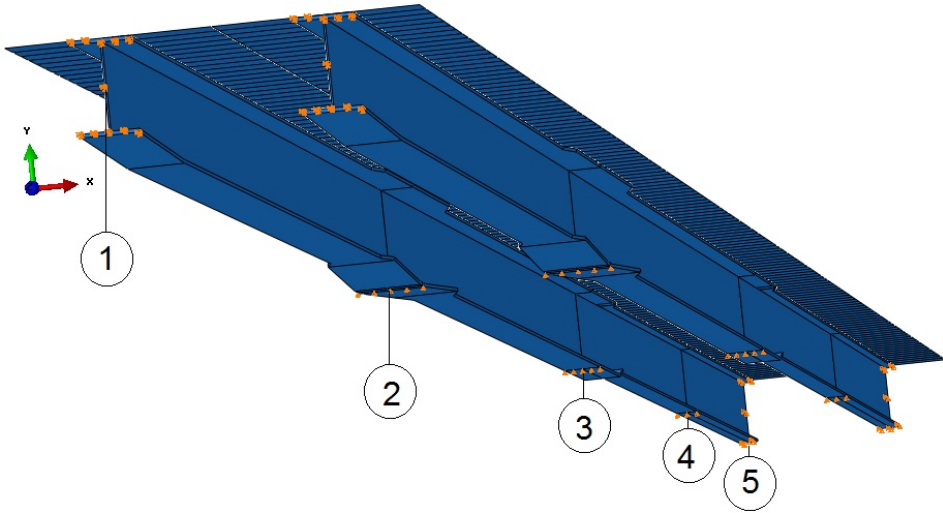


Figure 6.18: Abaqus model of Bårdshaug Bridge.

**Steel beams**

Bårdshaug Bridge has a varying cross section, due to the changing steel beam dimensions across its length, see Appendix B for details. To interpret this in the model, each part of the beam is created separately and later merged together. There are a total of four different constant cross sections over the entire bridge, and these are connected with connection beams, over approximately 2 meters, with linearly changing width and/or height. Solid elements are chosen for the steel beams in order to produce continuous beams along the length. The use of solid elements makes it possible to generate beam profiles in 3D, which is helpful for generating the part of the beams with varying dimensions. After generating each part of the cross section, the beams are put together using the "merge"-tool to form a single steel beam. Due to symmetry of the the bridge, the beam is duplicated and separated by 2.3 m, as seen in Figure 6.2 on page 78. The steel has a Young's modulus of 210 GPa and Poisson's ratio of 0.3.

**Concrete slab**

The concrete slab on top of the steel beams is steel reinforced with dimensions shown in Figure 6.2 on page 78, with a thickness on the walkway of 0.25 meters. The concrete slab is simplified to a rectangular cross section while excluding the steel reinforcement. The width and height of the concrete profile is set to 4.280 and 0.250 meters respectively. The value of Young's modulus for the concrete can be modified in order to account for creep and cracks in the concrete [52]. An average Young's modulus value can also be used when the concrete and steel reinforcement is modeled as one section, and to account for other simplifications of the model. The initial Young's modulus for the concrete used for Bårdshaug Bridge is 36 GPa after 28 days casting, with a Poisson's ratio at 0.15.

**Other Simplifications in The Model**

Other simplifications and adjustments are made such that the model is easy to reproduce for the reader and becomes more computationally cost effective, while still obtaining satisfying results in the modal analysis.

A significant simplification is the exclusion of the steel trusses and welding plates, shown in Figure 6.19, which are installed every sixth meter along the length of the bridge. The steel trusses are meant to distribute the load evenly between the steel beams, preventing local buckling, as well as stiffening and coupling the beams to increase rotational stiffness. Torsional modes are influenced the most by this rotational stiffness. Based on the modal analysis report of Bårdshaug Bridge (Table 6.3 page 80) the vertical and horizontal modes are more likely to influence the dynamic behavior of pedestrian loading than the torsional modes. The weight of all the trusses are small compared to the total weight of the bridge, $\approx 0.4$ % of the total mass. The steel trusses and welding plats have subsequently been removed from the FE-model.
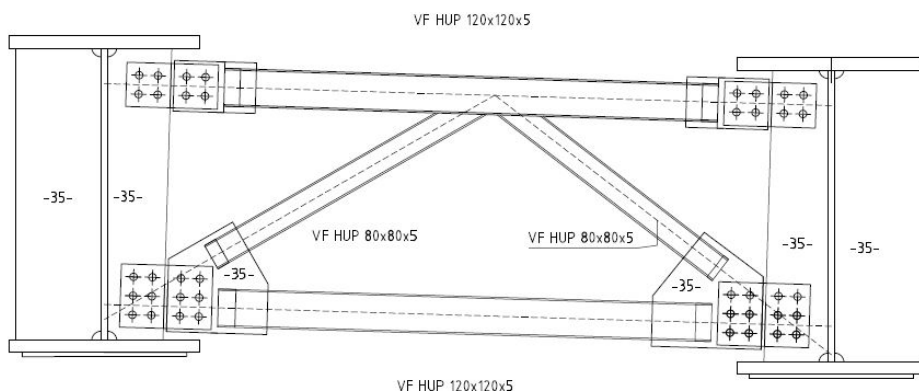


Figure 6.19: Cross section of the steel trusses and welding plates at column 2

Another simplification done, is that the three center columns are treated as springs in lateral direction, and locked in vertical direction using boundary conditions. A single spring is used under each steel beam at column 2, 3 and 4, see Figure 6.3 on page 78 for column numbering. Springs are not used under column 1 and column 5, as column 1 locks the steel beams in all three directions and column 5 locks the steel beams in lateral and vertical direction. Rotations are not locked in any of the columns.

**Interaction - Steel beams and concrete slab**

To better represent and understand the interaction between the steel and the concrete slab, two variations of Bårdshaug Bridge are modelled. The first model is created with full steel-concrete interaction. The second model is created with springs in longitudinal, lateral and vertical direction to simulate the steel-concrete interaction.

The first model contains only solid elements, and is used to run a simulation of complete interaction between the steel beams and the concrete slab. The full interaction is obtained by using tie-constraints on the steel and concrete surfaces. The tie-constraint locks contact surfaces between the steel beams and the concrete slab together, such that all displacements and rotations on both surfaces are equal.

In the second model the concrete slab is made with shell elements, while the steel beams remains in solid elements. The spring interactions are connecting the top surface of the steel to the bottom surface of the concrete slab. A single spring is placed every meter at the center of each steel beam surface, making the interaction between steel and concrete a total of 264 springs. Two different spring interaction models are made. One where the interaction in longitudinal direction is excluded, and one where the springs in longitudinal direction are stiffened to match the natural frequencies of the actual bridge.

## 6.3.2 Modal Analysis

To identify which of the simplified FE-models best represents the real bridge, a modal analysis is performed. The natural frequency and modal shapes are compared to the measurement data. The comparison is made with a percent-error for the natural frequencies, and a Modal Assurance Criterion (MAC)-values to account for the modal shapes. Modes shapes for the eight first modes are provided from the measurement data, and are assumed sufficient in describing the dynamic response of the bridge. Based on the accuracy of the natural frequencies and the MAC-values, a single FE-model is kept to which the load models presented in Chapter 5 are applied. For all FE-models the spring constants and/or the Young's modulus of the concrete are iterated to best match the first natural frequencies from the measurement data. A parameter study is performed and utilized to better understand and predict the behaviour when changing the parameters individually. The method and result of the parameter study is found in Appendix C.

**First model - Full interaction**

The iterated model with full steel-concrete interaction that yielded results closest to reality is based on the first natural frequencies in vertical and horizontal direction. The variables that are iterated are the E-modulus of the concrete and the springs between the steel beams and the columns, see Table 6.4. The MAC is shown in Figure 6.20 and the natural frequency with modal shape description is shown in Table 6.5.

Table 6.4: Properties iterated in full interaction model

| E-modulus concrete | Lateral spring constants [N/m] | | |
|---|---|---|---|
| [GPa] | Column 2 | Column 3 | Column 4 |
| 24 | $9.4 \ 10^6$ | $9.0 \ 10^6$ | $9.0 \ 10^6$ |

Table 6.5: Natural frequency and modal shapes, for the first model with full interaction

| Mode | Modal shape description | Frequency [Hz] |
|---|---|---|
| V1 | Span 1-2 and 2-3 in antiphase | 1.96 |
| V2 | Span 1-2 and 2-3 in phase | 2.92 |
| V3 | Span 3-4 dominant, all spans in phase | 4.02 |
| H1 | All columns in phase | 1.85 |
| H2 | Column 2 and 3 in anti-phase | 2.77 |
| T1 | Span 1-2 and 3-4 in phase, 2-3 in antiphase | 4.19 |
| T2 | Span 1-2 dominant, 2-3 in antiphase | 6.03 |
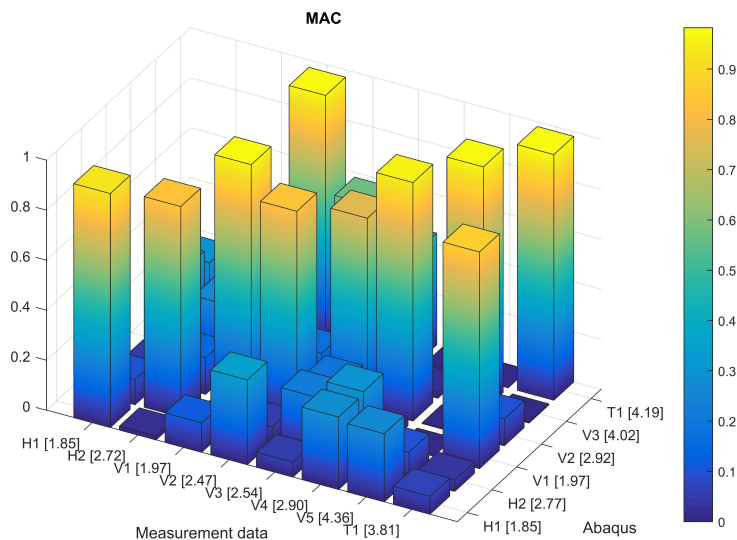


Figure 6.20: MAC for the first model

**Second model - Spring interaction, no longitudinal interaction**

In order to produce a different response the second model is treated as if there are no interaction between the concrete and the steel beams in the longitudinal direction ($\approx 0$ N/m). Springs in lateral and vertical direction in the interaction are set to minimize the interaction. Just like the first model, the springs between the steel beams and the columns, and the Young's modulus in the concrete are altered to match the natural frequency. Obtained properties and natural frequencies are given Table 6.6 and 6.7.

Table 6.6: Properties iterated for the second model

| E-modulus concrete [GPa] | Spring constants [N/m] | | | |
|---|---|---|---|---|
| | All columns to steel beams, lateral | Steel beams to concrete | | |
| | | Longitudinal | Vertical | Lateral |
| 36 | $1.6 \ 10^7$ | $10^{-5}$ | $10^{15}$ | $10^{15}$ |

Table 6.7: Natural frequencies and modal shape description for the second model

| Mode | Modal shape description | Frequency [Hz] |
|---|---|---|
| V1 | Span 1-2 and 2-3 in antiphase | 1.53 |
| V2 | Span 1-2 and 2-3 in phase. 1-2 dominant | 2.38 |
| V3 | Span 3-4 dominant, all spans in phase | 3.16 |
| H1 | All columns in phase | 1.86 |
| H2 | Column 2 and 3 in anti-phase | 2.78 |
| T1 | Span 1-2 and 3-4 in phase, 2-3 in antiphase | 3.46 |
| T2 | Span 1-2 dominant, 2-3 in antiphase | 4.05 |
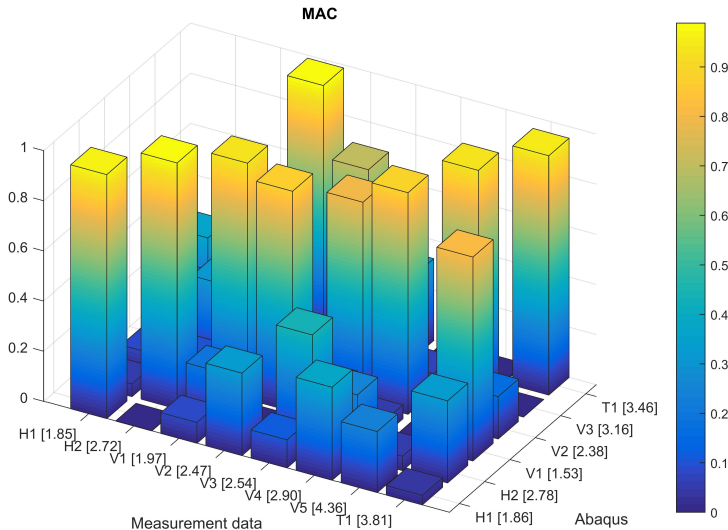


Figure 6.21: MAC for the second model

**Third model - Spring interaction, stiffer longitudinal interaction**

After observing the models with full and no interaction it is found that an iteration between the two model could better represent the actual bridge. A third model is made where the longitudinal springs are stiffened compared to the second model to approximate the interaction between the concrete slab and the steel beams. The horizontal springs in the columns are tuned to match the horizontal frequencies. Figure 6.23, 6.24 and 6.25 illustrates the first modes found in Abaqus from the new and improved model.

Table 6.8: Properties from the third model iterated to obtain a stiffer solution

| E-modulus concrete [GPa] | Spring constants [N/m] | | | |
|---|---|---|---|---|
| | All columns to steel beams, lateral | Steel beams to concrete slab | | |
| | | Longitudinal | Vertical | Lateral |
| 36 | $1.4 \ 10^7$ | $1.3 \ 10^8$ | $10^{15}$ | $10^{15}$ |

Table 6.9: Natrual frequency and modal shape description for the third model

| Mode | Modal shape description | Frequency [Hz] |
|---|---|---|
| V1 | Span 1-2 and 2-3 in antiphase | 1.99 |
| V2 | Span 1-2 and 2-3 in phase. 1-2 dominant | 2.89 |
| V3 | Span 3-4 dominant, all spans in phase | 3.97 |
| H1 | All columns in phase | 1.86 |
| H2 | Column 2 and 3 in antiphase | 2.96 |
| T1 | Span 1-2 and 3-4 in phase, 2-3 in antiphase | 3.54 |
| T2 | Span 1-2 dominant, 2-3 in antiphase | 4.32 |
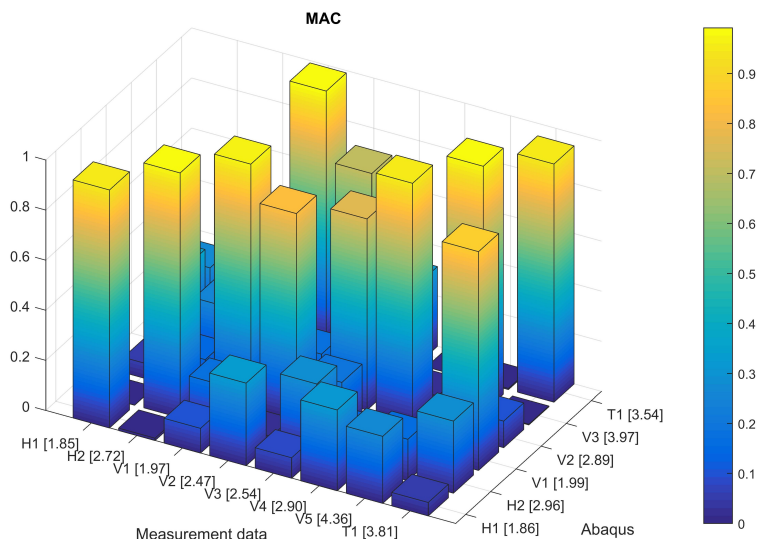


Figure 6.22: MAC for the third model

The third model is kept to perform the load model analysis, based on the precision of the MAC values and the accuracy of the natural frequencies. The accuracy of the natural frequencies for all three models are given in Table 6.10, and the numerical MAC values are given in Appendix D. It is worth noting from Table 6.10 that the first model yields the overall best accuracy of the first six natural frequencies, where the deviation for this model is greatest for the torsional modes. However, an uncertainty arises in this model from the lowered Young's Modulus. From the rule of mixtures, the Young's modulus of elasticity for steel reinforced concrete is expected to slightly increase with respect to the Young's modulus of the concrete [53]. The lowered Young's modulus from the first model is therefore considered unrealistic. If the first model is applied the same Young's modulus as the second and third model (36 GPa), the model would yield a very stiff solution. The second model yields a conservative solution with overall the lowest accuracy of the natural frequencies, where the values are generally too low compared to the actual bridge.

Table 6.10: The natural frequencies found from the three models compared against the actual modes of Bårdshaug Bridge

| Mode | Bårdshaug | First model | | Second model | | Third model | |
|---|---|---|---|---|---|---|---|
| | f [Hz] | $f_1$ [Hz] | $\Delta f_1$ [%] | $f_2$ [Hz] | $\Delta f_2$ [%] | $f_3$ [Hz] | $\Delta f_3$ [%] |
| H1 | 1.85 | 1.85 | 0 | 1.86 | 0.54 | 1.86 | 0.54 |
| H2 | 2.72 | 2.77 | 1.84 | 2.78 | 2.21 | 2.96 | 8.82 |
| V1 | 1.97 | 1.96 | 0.51 | 1.53 | 22.34 | 1.99 | 1.02 |
| V2 | 2.47 | - | - | - | - | - | - |
| V3 | 2.54 | - | - | - | - | - | - |
| V4 | 2.90 | 2.92 | 0.69 | 2.38 | 17.93 | 2,89 | 0.34 |
| V5 | 4.36 | 4.02 | 7.90 | 3.16 | 27.52 | 3.97 | 8.94 |
| T1 | 3.81 | 4.19 | 9.97 | 3.46 | 9.19 | 3.54 | 7.09 |
| T2 | 4.45 | 6.03 | 35.51 | 4.05 | 8.99 | 4.32 | 2.92 |
| T3 | 4.58 | - | - | - | - | - | - |
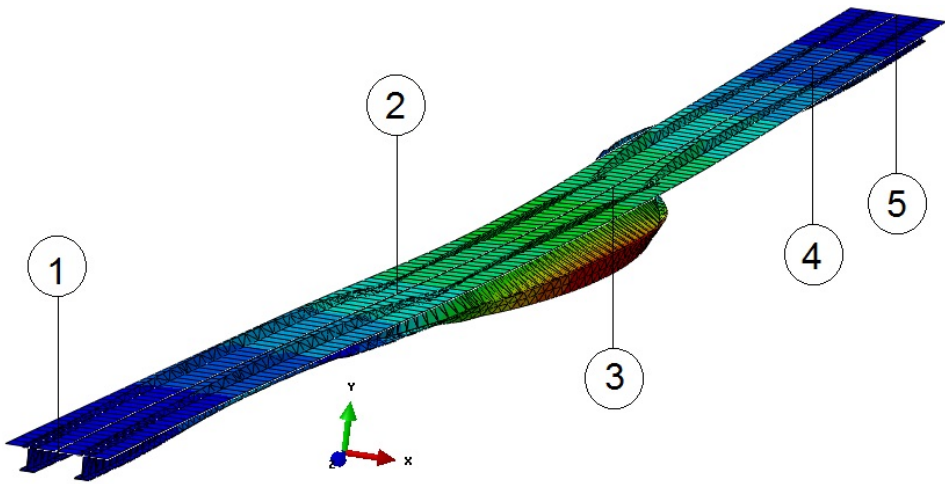
Figure 6.23: First horizontal mode from Abaqus. Natural frequency: 1.86 Hz.
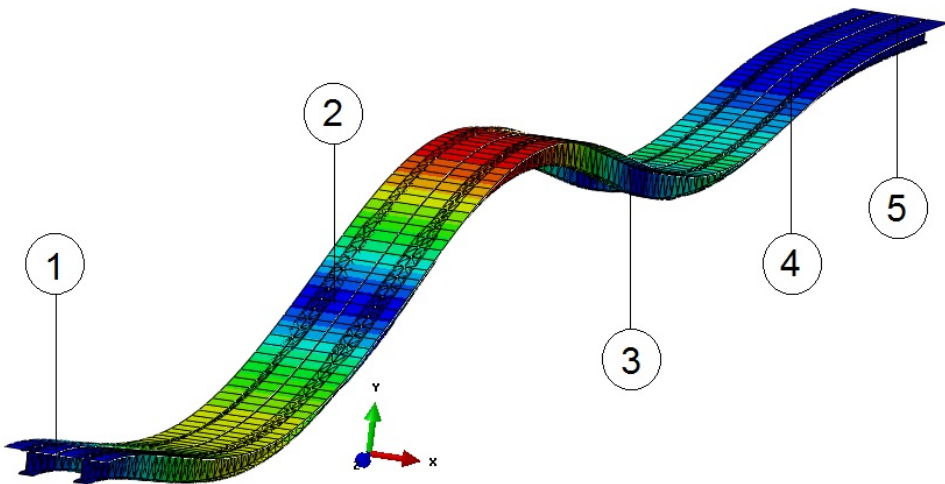


Figure 6.24: First vertical mode from Abaqus. Natural frequency: 1.99 Hz.
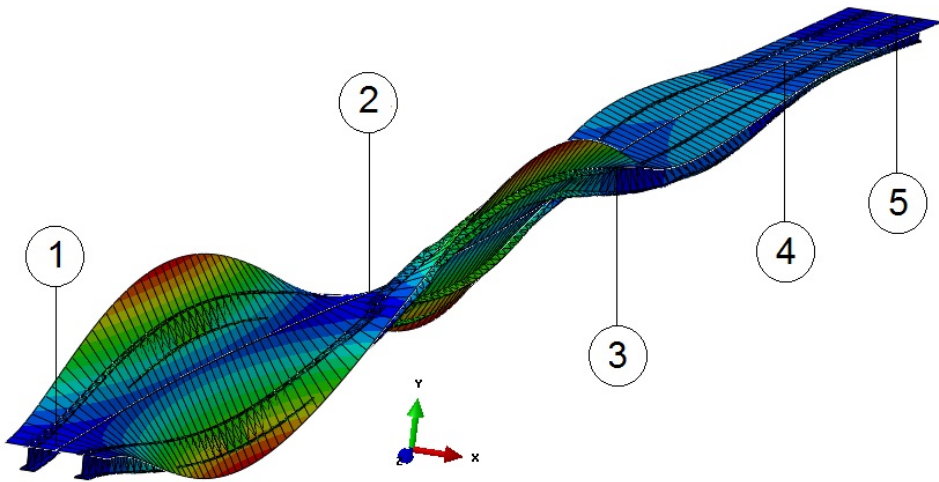
Figure 6.25: First torsional mode from Abaqus. Natural frequency: 3.54 Hz.

### 6.3.3 Damping

The material damping is applied in Abaqus using Rayliegh damping (see Section 3.4). The proportional damping coefficients $\alpha$ and $\beta$ are implemented directly. From the measurement data from Bårdshaug Bridge the modal damping was found to be around 1% for most modal shapes in the lower frequency domain [3]. The proportional damping coefficients are calculated from Equation (2.38) and (2.39) using the first two natural frequencies in vertical direction found in Abaqus (V1 and V4) and 1% damping for both modes.
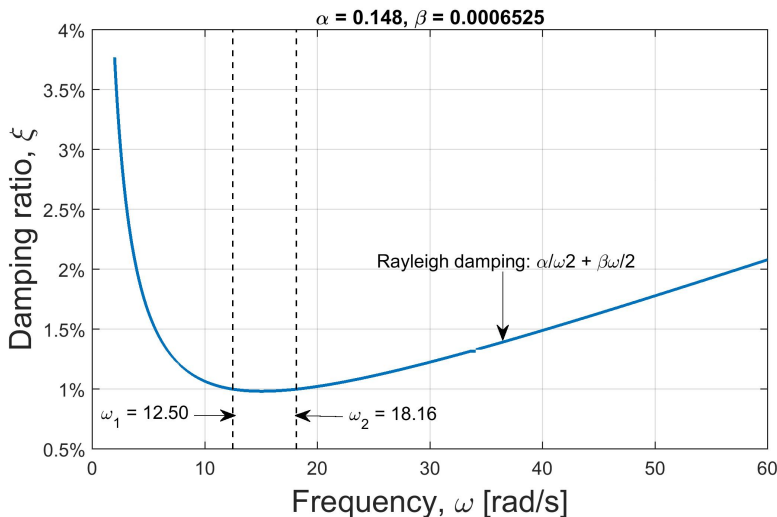


Figure 6.26: Rayleigh damping in Abaqus

Figure 6.26 shows the Rayleigh damping for the proportional damping coefficients given for Bårdshaug Bridge. The same proportional damping parameters are given to all materials in the model. The first two modes in vertical direction are chosen to compute the Rayleigh parameters in order to obtain greater damping of higher order modes and yield a response closer to the actual bridge as the noise is being damped. In addition it is the lower modes that will be excited by load models later in this thesis, and it is therefore desirable to have accurate values for the damping in these modes.

### 6.3.4 Abaqus Model Error Discussion

The models with spring interaction have modes where the steel beams are rotating independently of the concrete slab. The top of the steel beams are held in place while the bottom flanges are swaying in the lateral direction due rotation about the top of the steel beams. These rotations are also present during the horizontal modes, see Figure 6.23, and may affect the accuracy of the response of horizontal loading. This may be a consequence of the exclusion of the steel trusses and welding plates, which stiffens the steel beams. Another possible source of this error is that rotational springs are not applied between the steel beams and the concrete slab. These modes does not occur on the actual structure and resonance in these modes are assumed non-occurring when pedestrian induced forces are applied to the FE-model.

The torsional natural frequencies yield the least accurate results in all three models, where the full interaction model is too stiff, and the spring interaction models too conservative. Including the steel trusses and welding plates could help stiffen the spring interaction models such that more accurate results for the torsional modes are obtained.

It is also worth noting from Table 6.10 that V2, V3 and T3 are not obtained in the modal analysis from the FE-model. This may be another consequence of the structural changes, mainly a result of the exclusion of the steel trusses an welding plates. From the response spectrum in Figure 6.5 on page 81 it is observed that V2 and V3 are both part of the same broad banded peak with lower amplitude than V1 and V4, and may have a smaller impact on the dynamic behavior in vertical direction compared to V1 and V4.

The modeled bridge is generally lighter than the actual bridge structure. The steel trusses ($\approx$ 1600 kg), welding plates ($\approx$ 4500 kg), asphalt ($\approx$ 400 kg), handrails ($\approx$ 2000 kg) and steel reinforcement ($\approx$ 32600 kg) are excluded from the model and accounts for roughly 9 % of the total mass of the FE-model (455538 kg). For the next overhaul of the model, the steel trusses with welding plates and steel reinforcement are encouraged to be implemented, such that stiffness and mass matrices may better represent the actual bridge. The stiffness-values of the springs obtained from the iteration process are not useful in a FE-model where the steel trusses and welding plates are included, because the stiffness of the springs are affected by the overall stiffness of the bridge. However, the method

used for obtaining the interaction recommended. Very stiff lateral and vertical springs with lowered stiffness for longitudinal springs are considered critical for obtaining correct modes.

The chosen numerical model matches the lowest natural frequencies of the real bridge and the corresponding mode shapes, such that the eigenvalues, recall the Reyleigh quotient for an MDOF system, given in Equation (2.41):

$$\omega_i^2 = \frac{\{\overline{\mathbf{D}}\}_i [\mathbf{K}] \{\overline{\mathbf{D}}\}_i}{\{\overline{\mathbf{D}}\}_i [\mathbf{M}] \{\overline{\mathbf{D}}\}_i}$$

yields satisfying results. Since the mass of the model is lower than mass of the actual bridge, the equation above only yields the correct eigenvalues if the stiffness is also lowered, assuming the modal shapes are, to some extent, correct. As a result the model yields greater deflections and stresses than reality, such that a static analysis of the structure might yield critical values. The main objective of this model is to apply the different dynamic load models, compare their magnitude with their respective comfort criteria and validate the usage and simplicity of the models. The selected model is assumed to be sufficient for this dynamic analysis.

## 6.4 Applying Load to the Finite Element Model

Each load applied to the FE-model is defined by a unit magnitude deciding the load direction, and an associated amplitude describing the size and variation of the load. The amplitudes and the loads are contrived in a Python script in Notepad++, and applied as a whole to the model. The load step used for the pedestrian loading is a dynamic implicit step. Before applying the pedestrian loads from the scripts, the gravity load is applied to the model in a separate load step. The pedestrian loads are implemented to the FE-model with a fixed time increment equal to the sampling frequency of the load. Unconditionally stable implicit methods should be performed with time step $\Delta t$ in the range [9]:

$$T_{co}/30 \leq \Delta t \leq T_{co}/10 \tag{6.1}$$

Where $T_{co}$ is the smallest period to be integrated. The first vertical and horizontal modes are assumed to be sufficient in describing the behaviour as the guidelines describe loading with walking frequency that coincide with the first natural frequencies. The time period from the first mode: $T_{co} = 0.0503 \ s$ such that:

$$0.017 \ s \leq \Delta t \leq 0.05 \ s \tag{6.2}$$

A sampling frequency around 25 Hz ($\Delta t \approx 0.04 \ s$) is chosen. The exact sampling frequency varies with the direction of the load and the equation of the load model. The

sampling frequency of the load is crucial in obtaining satisfying results, as a greater sampling frequency yields more accurate results, but at the same time greatly increase the computational cost.

## 6.4.1 Modeling a Moving Load

For the concentrated loads simulating single pedestrians and groups moving across the bridge, each walking step is simulated as a concentrated load vector with varying amplitude, applied with the frequency given in the guidelines ($\approx 2$ Hz). Figure 6.27 on page 100 illustrates the principle of how the moving load is applied.

The steps are modelled 1 meter apart, as the the finite element model is already divided into sets every meter in order to create sets for the interaction springs. The step length of 1 meter contradicts several of the guidelines, as the walking step length is often set to be approximately 0.75 m. Having a step length of 0.75 m would require additional sets 0.75 m apart, which would be time consuming and unnecessary when the load frequency and force intensity are the relevant parameters to create the response from the steps. The vertical concentrated loads are defined as a point load in negative y-direction.

The load is applied to the FE-model as a moving load over either the mid span of the bridge, or all spans of the bridge, depending on the guideline. The analysis runs for 10 seconds longer than the load history time in order to observe damping.

Analysis for vertical and horizontal loads are executed separately. The separate execution is done to isolate the first modes in each direction such that noise is avoided, and the worst case scenario for loads in both directions can be obtained. The frequencies of the applied loads are also dependent on the direction of the load. Longitudinal loads are not applied to the FE-model of Bårdshaug Bridge, as there are no modes or risk of acceleration in this direction and only a few guidelines consider this scenario.

For the load models defined with a frequency equal the first natural frequency of the bridge, the first natural frequency of the FE-model is used in order to obtain the worst case scenario with resonance. For load models defined for the walking frequency 2 Hz is used for vertical loads, and 1 Hz is used for horizontal loads.
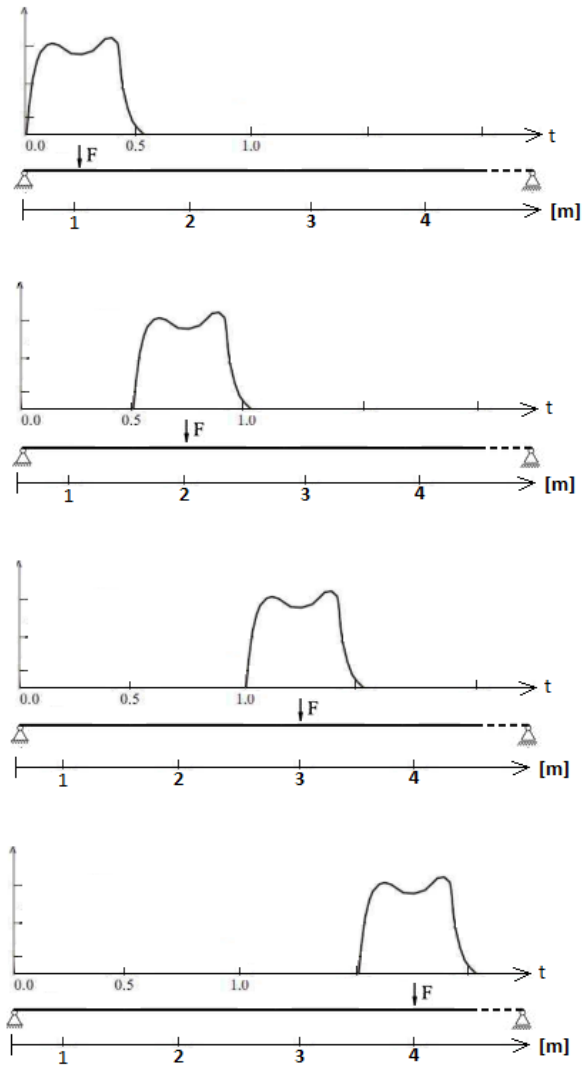
Figure 6.27: Illustration of how the moving load was applied to the model

## 6.4.2   Modeling a Distributed Load

There are two ways of modeling distributed loads in Abaqus; surface-based distributed loads and element based distributed loads. In this thesis, the distributed loads are modeled as surface pressure loads, which means that the load direction change as the bridge deck deflects.

The distributed loads simulate a crowd with a density of $\approx 0.5$ ped/m$^2$, passing the bridge at a constant speed. The load is applied to the FE-model as a equivalent number of pedestrians standing still on the bridge, exciting it with the same frequency and phase

as the first mode of the bridge structure, as shown for a general situation in Figure 6.28, and for Bårdshaug Bridge in Figure 6.29. Before applying the load, the first mode shape of the bridge and the inflection points of the mode is found, then the distributed loads are applied separately for sections divided by the inflection points. The distributed load is applied until steady state of acceleration is obtained.

For distributed loads the analysis run for 60 seconds, with the distributed load working for 40 seconds, in order to first obtain steady-state vibrations and then observe how the acceleration response decreases.

The equivalent number of pedestrians is determined analytically, by first obtaining the acceleration response of a pedestrian crowd with random walking frequencies passing a bridge, before finding the number of pedestrians exciting the bridge in the first mode needed to obtain the same acceleration response. The ratio between the found numbers is the factor used to account for the equivalent number of pedestrians, and the factor can be found from tables in the guidelines.SÉTRA, UK-NA, JRC and HIVOSS uses the equivalent number of pedestrians when applying the load to the bridge, while Eurocode is the only guideline considering crowd loads which does not account for this factor.
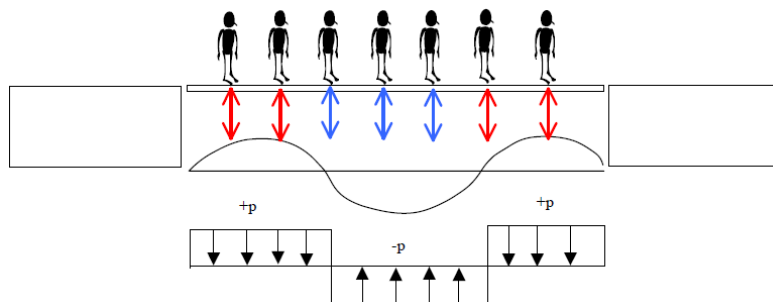


Figure 6.28: Distributed pedestrians, in phase with related to mode sign, SÉTRA
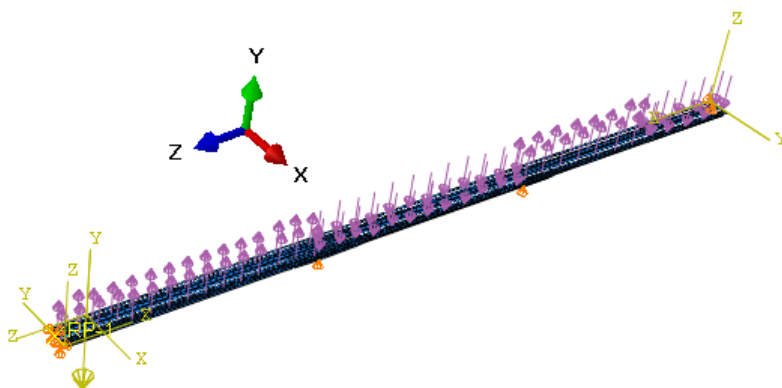


Figure 6.29: Distributed load applied to the finite element model.

None of the the load histories given for distributed loads includes the static force of the pedestrian crowd, leaving the loads to oscillate around zero. The exclusion of the static load does not affect the acceleration response, as the static force does not contribute to the acceleration values, however the static force should be applied to the model if the deflection is being considered, by adding the weight of the pedestrians to the total mass of the bridge. An increase of the total mass will change the natural frequency, and can therefore be important for the modelling. The crowd loads presented later has the density of approximately 0.5 pedestrian per square meter, which equal a weight of 16.000 kg, or 3.5 % of the total bridge mass. A simplified calculation of the change in natural frequencies are shown in Equation (6.3) and (6.4). The calculations are done for a SDOF system. The added mass from crowd loading is not applied to the FE-model as the guidelines does not specify this for a dynamic loading.

$$f_{original-mass} = \frac{1}{2\pi}\sqrt{\frac{k}{m}} = 1.97 \ Hz \tag{6.3}$$

$$f_{new-mass} = \frac{1}{2\pi}\sqrt{\frac{k}{1.03 * m}} = 1.94 \ Hz \tag{6.4}$$

# Chapter 7

# Results

In this chapter all the comfort criteria and load models are applied to Bårdshaug Bridge, and evaluated in regards to accuracy and usability. The value of each parameter used will be presented, but the descriptions of the parameters in each equation will not be repeated. The reader is advised to see Chapter 5 and 6 for information on how to determine the different parameter values.

## 7.1 Comfort Criteria Applied to Bårdshaug Bridge

In the following section the comfort criteria from the different guidelines from Chapter 5 will be evaluated for Bårdshaug Bridge.

### 7.1.1 Eurocode

Eurocode 0 provides a criteria for maximum acceleration on pedestrian bridges. The accelerations are given as a limit with no need for calculation. Recalling from Section 5.1:

Table 7.1: Reccomended maximum accelerations in Eurocode 0

| Load case | Acceleration limit $[\mathrm{m/s^2}]$ |
|---|---|
| Vertical vibration | 0.7 |
| Lateral vibration | 0.2 |
| Exceptional crowd conditions | 0.4 |

**Comments to the comfort criteria**

- A dynamic analysis must be performed if the natural frequency in vertical direction is less than 5 Hz or less than 2.5 Hz in horizontal direction.

- The exceptional crowd conditions are not assigned a specific direction. In this thesis the comfort criterion for this load scenario is assumed applicable in all directions.

### 7.1.2  BS 5400

The British Standard 5400, requires that vertical acceleration shall be considered for all natural frequencies less than or equal to 5 Hz. Recalling from Equation (5.7):

$$a \leq 0.5 f_0^{0.5}$$

Table 7.2: Comfort criteria of Bårdshaug Bridge from BS 5400 in vertical direction

| Frequency [Hz] | Comfort criteria [m/s$^2$] |
|---|---|
| 1.97 | 0.70 |
| 2.48 | 0.79 |
| 2.54 | 0.80 |
| 2.90 | 0.85 |
| 4.36 | 1.04 |

### 7.1.3  UK National Annex to Eurocode

The acceleration criteria for UK-NA, first given in Equation (5.13), is:

$$a_c = 1.0 k_1 k_2 k_3 k_4$$

Table 7.3: Comfort criteria and parameters of Bårdshaug Bridge from UK-NA in vertical direction

| Comfort criteria parameter | Value |
|---|---|
| $k_1$ | 1.3 |
| $k_2$ | 0.7 |
| $k_3$ | 1.0 |
| $k_4$ | 1.0 |

| Comfort criteria [m/s$^2$] |
|---|
| $a_c = 0.91$ |

**Comments to the comfort criteria**

- Bårdshaug Bridge is located in the center of Orkanger, where the population is 8,000 people. The footbridge is connecting the suburbs to an industrial area and a

camping site, making it a suburban crossing, and therefore $k_1 = 1.3$. The bridge works as the sole means of access from the camping site to the center of Orkanger, and on the base of this $k_2 = 0.7$. The height of the bridge is between 4 meters and 8 meters, making $k_3 = 1.0$. Finally $k_4 = 1.0$ as exposure factor is not determined for this project. The values of the response modifiers are picked from Table 5.5, 5.6 and 5.7.

### 7.1.4 Håndbok 185

In Håndbok 185 the comfort criteria is evaluated for vertical vibrations for all natural frequencies below 6 Hz. Recall Equation (5.21):

$$a_r \leq 0.25 f^{0.7782}$$

Table 7.4: Comfort criteria of Bårdshaug Bridge from Håndbok 185 in vertical direction

| Frequency [Hz] | Comfort criteria [m/s$^2$] |
|---|---|
| 1.97 | 0.42 |
| 2.48 | 0.51 |
| 2.54 | 0.52 |
| 2.90 | 0.57 |
| 4.36 | 0.79 |

**Comment on the comfort criteria**

- The guideline states that the acceleration criteria for horizontal acceleration should be found if the horizontal frequencies are within the critical range; 0.5-1.3 Hz. The first natural frequency in lateral direction for Bårdshaug Bridge is 1.85 Hz, and horizontal accelerations will not be considered

### 7.1.5 SÉTRA

SÉTRA gives comfort criteria for both vertical and horizontal acceleration. The criteria found from Table 5.14 and 5.15 are:

Table 7.5: Comfort criteria of Bårdshaug Bridge from SÉTRA

| Comfort criteria [m/s$^2$] |
| --- |
| **Vertical** |
| $a_c = 0.50$ |

| **Horizontal** |
| --- |
| $a_c = 0.10$ |

**Comment on the comfort criteria**

- The first natural frequency in vertical direction is in the frequency domain of maximum risk of resonance, while the first natural frequency in the horizontal direction is in the frequency domain of minimum risk of resonance. However, to avoid lock-in effect for horizontal vibrations the comfort level is also set to maximum.

### 7.1.6 ISO 10137

For ISO 10137 the comfort criteria is taken from the base curves, Figure 5.12 and 5.13 provided in Chapter 5.6.

Table 7.6: Comfort criteria on Bårdshaug Bridge from ISO 10137

| Direction | Frequency [Hz] | $a_c$ [m/s$^2$] | Multiplier | Comfort Criteria [m/s$^2$] |
| --- | --- | --- | --- | --- |
| Vertical | 1.97 | 0.0071 | 30 | 0.21 |
| | | | 60 | 0.43 |
| | 2.48 | 0.0063 | 30 | 0.19 |
| | | | 60 | 0.38 |
| | 2.54 | 0.0061 | 30 | 0.18 |
| | | | 60 | 0.37 |
| | 2.90 | 0.0058 | 30 | 0.17 |
| | | | 60 | 0.35 |
| | 4.34 | 0.005 | 30 | 0.15 |
| | | | 60 | 0.30 |
| Horizontal | 1.85 | 0.0036 | 60 | 0.22 |
| | 2.72 | 0.0046 | 60 | 0.28 |

**Comment on the comfort criteria**

- A reminder that the multiplier of 30 accounts for people that are standing still, while there is pedestrian traffic on the footbridge. Orkanger is not a sought after tourist town, nor is Bårdshaug Bridge an attraction for the local population and mainly used for transportation, such that the multiplier of the base curve is set to 60.

- The comfort criteria in vertical direction becomes increasingly conservative with increased natural frequency, where the critical frequency domain begins at 4 Hz and ends at 8 Hz from the base curve.

- The base curves are used for any building, and is not specific for pedestrian bridges such the normal walking frequency of 2 Hz is not weighted as heavily.

### 7.1.7 JRC and HIVOSS

The first natural frequency in lateral and vertical direction is in the critical range from Table 5.25, such that the comfort range that should be picked for Bårdshaug Bridge is the maximum. From Table 5.24 the comfort criteria yields:

Table 7.7: Comfort criteria of Bårdshaug Bridge from JRC

| Comfort criteria [m/s$^2$] |
| :---: |
| **Vertical** |
| $a_c = 0.50$ |

| Comfort criteria [m/s$^2$] |
| :---: |
| **Horizontal** |
| $a_c = 0.10$ |

Table 7.8: Critical number of pedestrians and parameters walking on Bårdshaug Bridge from JRC for horizontal direction

| Number of pedestrian parameter | Value |
| :--- | :--- |
| $\xi$ | 0.008 |
| $f$ | 1.85 Hz |
| $m^*$ | 42561 kg |
| $k$ | 300 Ns/m |

| Critical number of pedestrians |
| :---: |
| $N_L = 53$ |

To check the lateral vibration for lock-in effect, the critical number of pedestrians $N_L$ is calculated. Recall Equation (5.39):

$$N_L = \frac{8\pi\xi f m^*}{k}$$

**Comment on the comfort criteria**

- The value for critical number of pedestrians coincide with Statens Vegvesen's estimation of maximum pedestrians of 50 per hour. Noting however that $N_L$ is for 53 people acting on the bridge at the same time, and not walking across per hour

- The modal mass $m^*$ as found from the FE model for the first natural frequency in the horizontal direction

- In JRC and HIVOSS lateral vibrations are only checked if the first natural frequency is in the frequency domain 0.5 - 1.2 Hz. The first lateral natural frequency for Bårdshaug Bridge is 1.85 Hz, but the load model for horizontal vibrations and the critical number of pedestrians is kept for discussion purposes.

## 7.2 Load Models Applied to Bårdshaug Bridge

In this section, each of the load models presented in Chapter 5 are applied to the finite element model of Bårdshaug bridge presented in Chapter 6.3 following the procedure described in Chapter 6.4. While Chapter 5 describes each load model in detail, the following section illustrates the usage of the models. For each guideline the equations of the load models are first presented, before the calculated parameter values are shown, and the acceleration response on the bridge is found. All the acceleration histories for the different load models are found in Appendix E.

Few guidelines specify which value of the acceleration from the load models that shall be compared with the comfort criteria, and there are several ways to interpret the acceleration histories. For this thesis the maximum peak values, the 95th-percentile and the RMS of the acceleration peaks are considered for all load models applied to the finite element model of the bridge.

For the models calculated directly without modeling in the finite element program, only one value is obtained. The acceleration histories obtained from the load models on the FE model are recorded at the mid node of the second longest, where the maximum acceleration history occurs, see Figure 7.1. The peak values used to approximate the 95th-percentile and the RMS begins when the model starts oscillating at the natural frequency. For a concentrated load, simulating a moving pedestrian across the bridge, the

peak picking ends when the applied load history ends. For a pulsating distributed load, simulating a crowd on the bridge, the peak picking ends when the oscillation has stabilized. Figures 7.2 - 7.4 display the peak picking of accelerations for a single pedestrian walking across the bridge recorded at the maximum response point.

The horizontal load models for concentrated loads vary between being defined for the first horizontal natural frequency (1.86 Hz) and the horizontal walking frequency ($\approx$ 1 Hz). For the models defined for the horizontal walking frequency, both scenarios are applied to the FE-model and shown in Appendix E, in order to show readers what effect the horizontal loads has on a bridge with horizontal natural frequencies close to 1 Hz.
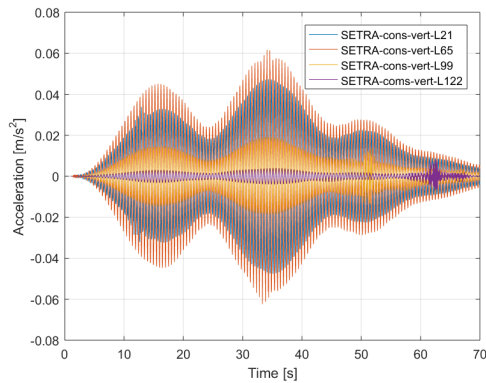


Figure 7.1: Acceleration histories for a single pedestrian crossing the bridge, recorded at the mid node of each span.
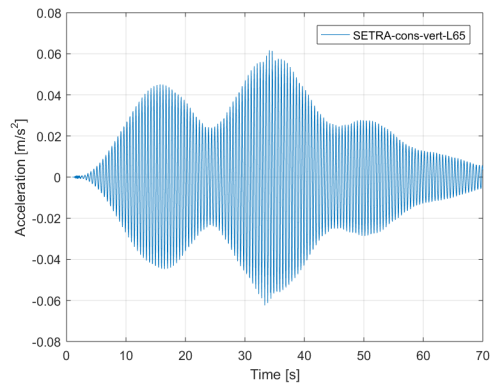


Figure 7.2: Acceleration history, recorded at the mid node of span 2.
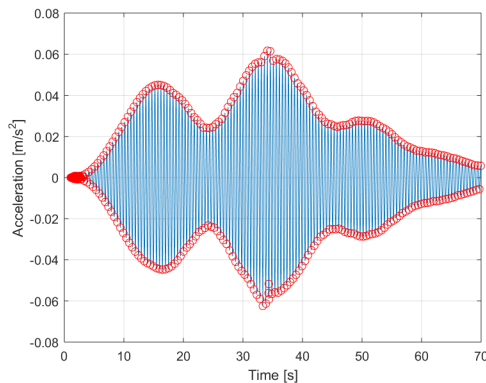


Figure 7.3: Peak picking of acceleration history graph.
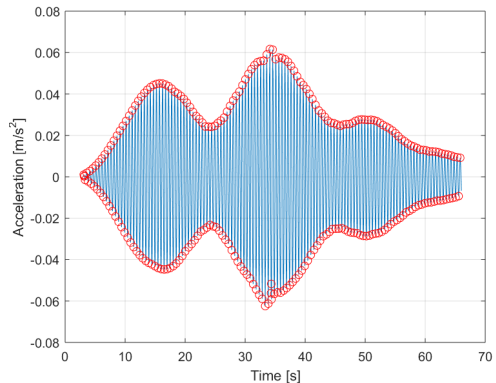


Figure 7.4: Peak values used to approximate 95th percentile and RMS

### 7.2.1 Euroocode

Recall from Section 5.1:

Single pedestrian:

$$a_{vert,1} = \frac{200}{M\xi} \qquad \text{for} \quad f_{ver} \leq 2.5 \text{ Hz}$$

$$a_{vert,1} = \frac{100}{M\xi} \qquad \text{for} \quad 2.5 < f_{ver} \leq 5.0 \text{ Hz}$$

$$a_{vert,jog} = \frac{600}{M\xi} \qquad \text{for} \quad 2.5 \leq f_{lat} \leq 3.5 \text{ Hz}$$

$$a_{hor,1} = \frac{50}{M\xi} \qquad \text{for} \quad 0.5 \leq f_{lat} \leq 2.5 \text{ Hz}$$

Groups of n pedestrians:

$$a_{vert,n} = 0.23 a_{vert,1} n k_{vert}$$

$$a_{hor,n} = 0.18 a_{hor,1} n k_{hor}$$

Table 7.9: Parameter values used for Eurocode load model

| Load model parameter | Value |
|---|---|
| **Single pedestrians** | |
| $M$ | 455538 kg |
| $\xi$ | 0.01 |
| $f_{vert}$ | 1.99 Hz |
| $f_{hor}$ | 1.86 Hz |
| **Groups of pedestrians** | |
| $A_{allspans}$ | 458.5 m$^2$ |
| $A_{midspan}$ | 51.6 m$^2$ |
| $n_{group}$ | 13 |
| $n_{cont.stream}$ | 86 and 275 |
| $k_{vert}(f_{vert})$ | 1 |
| $k_{hor}(f_{hor})$ | 0.52 |

Table 7.10: Acceleration of Bårdshaug Bridge obtained from Eurocode

| Acceleration[m/s$^2$] |
|---|
| **Single pedestrians** |
| $a_{vert,1} = 0.044$ |
| $a_{vert,jog} = 0.132$ |
| $a_{hor,1} = 0.011$ |
| **Group of pedestrians, n = 13** |
| $a_{vert,13} = 0.132$ |
| $a_{hor,13} = 0.013$ |
| **Cont. pedestrian stream, crowd - mid span** |
| $a_{vert,86} = 0.870$ |
| $a_{hor,86} = 0.089$ |
| **Cont. pedestrian stream, crowd - all spans** |
| $a_{vert,275} = 2.784$ |
| $a_{hor,275} = 0.283$ |

**Comments on the load models:**

- According to Živanović, Pavić and Ingólfsson [54] the load model presented in Eurocode 5 for timber structures can be utilized for any footbridge, as the load model is not timber specifić.

- For the calculations the total mass of the bridge are based on the finite element model, where the steel trusses, welding plates, asphalt, steel reinforcements and the handrails are excluded.

- For this load model the load is not applied to the finite element model, but calculated with basis in parameters from the bridge characteristics and the pedestrian load situation.

- The acceleration value for a continuous stream is dependent on the bridge deck area, however it is not specified in the guideline what area to use. The acceleration calculated for a crowd over all spans and over one span, is presented in the results, and it is worth noting that there is a very large difference between the two crowd accelerations values. How much the acceleration response vary with the bridge length will depend on the number of spans the bridge is divided into, which is not taken to account in Eurocode.

- It is not defined if the acceleration value is for loads applied with a frequency equal the natural frequency or the walking frequency. As the frequency of the load is not

a part of the equation, it is assumed that the acceleration obtained is associated with load applied in the first natural frequency.

## 7.2.2 BS 5400

Recalling from Section 5.2, and Equation (5.8) and (5.11).

Simplified method:

$$a = 4\pi^2 f_0^2 y_s K \psi \quad [\text{m/s}^2]$$

General method:

$$F = 180 \sin(2\pi f_0 T) \quad [\text{N}]$$

Table 7.11: Parameter values used for BS 5400 general load model

| Load model parameter | Value |
|---|---|
| $f_0$ [Hz] | 1.9863 |

Table 7.12: Acceleration values for BS 5400 general load model

| | Acceleration [m/s$^2$] | | |
|---|---|---|---|
| Load type | Max | 95%-percentile | RMS |
| Vertical Concentrated loads | 0.0367 | 0.0333 | 0.0211 |
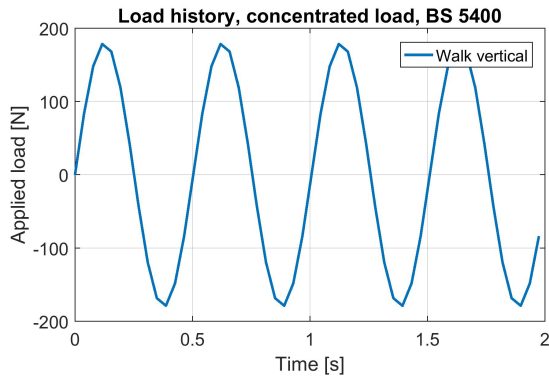


Figure 7.5: Load history, vertical concentrated general load model, BS 5400

**Comments on the load models:**

- The general load model is applied to all spans of the FE-model of the bridge.

- The simplified method presented in BS 5400 can not be used for Bårdshaug Bridge, as the simplified method is only defined for simply supported bridges with three spans or less. The general method is therefore used in the calculations for Bårdshaug Bridge.

### 7.2.3 UK National Annex to Eurocode

Recalling from Section 5.3, and Equation (5.15) and (5.17).

Single pedestrian and groups:

$$F(N) = F_0 k(f_v) \sqrt{1 + \gamma(N-1)} sin(2\pi f_v t) \qquad [\text{N}]$$

Crowds:

$$w(N,t) = 1.8 \frac{F_0}{A} k(f_v) \sqrt{\gamma \frac{N}{\lambda}} sin(2\pi f_v t) \qquad [\text{N/m}^2]$$

Table 7.13: Parameter values used for UK-NA load model

| Load model parameter | Value |
|---|---|
| **Single pedestrians and groups (Concentrated loads)** | |
| $N_{walk}$ | 4 (Class B) |
| $N_{jog}$ | 1 (Class B) |
| $F_{0,walk}$ | 280 N |
| $F_{0,jog}$ | 910 N |
| $f_v$ | 1.986 Hz |
| $k(f_v)$ | 1.0 |
| $\delta$ | 0.0628 |
| $\gamma$ | 1 |
| **Crowds (Distributed loads)** | |
| $N_{crowd}$ | 229 |
| $\rho$ | 0.5 (Class B) |
| A | 458.5 m$^2$ |
| $\xi$ | 0.5 % (Defined in Guideline) |
| $\delta$ | 0.0314 |
| $\gamma$ | 0.05 |
| $\lambda$ | 0.634 |
| S | 131 m |
| $S_e ff$ | 131 m (Conserative) |
| b | 3.5 m |
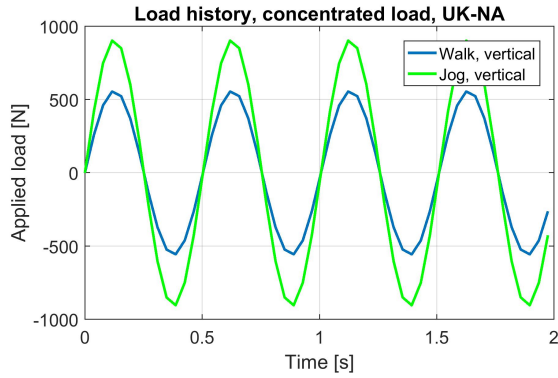
Figure 7.6: Load history, concentrated load model, UK-NA
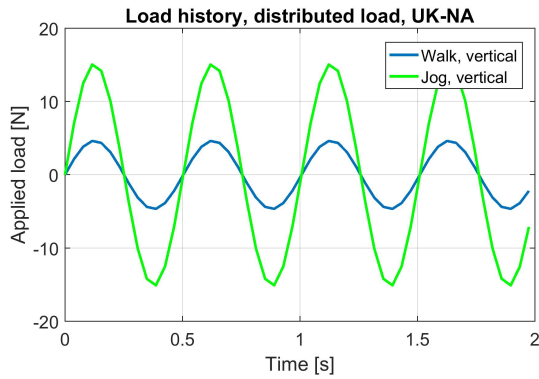


Figure 7.7: Load history, distributed load model, UK-NA

Table 7.14: Acceleration values for UK-NA load models

| | Acceleration [m/s$^2$] | | |
|---|---|---|---|
| Load type | Max | 95%-percentil | RMS |
| Vertical, walk Consentrated loads | 0.1142 | 0.1037 | 0.0657 |
| Vertical, jog Consentrated loads | 0.1856 | 0.1688 | 0.1071 |
| Vertical, walk Distributed loads | 0.1848 | 0.1805 | 0.1454 |
| Vertical, jog Distributed loads | 0.6007 | 0.5865 | 0.4826 |

**Comments on the load models:**

- The load models presented in UK-NA are applied to all spans of the FE-model of the bridge.

- The load history for jogging in UK-NA is simplified to be continuous, and is equal to the walking load history, except for greater load amplitudes. In real life jogging is characterized by a time interval between the running steps where there are no contact to the ground, see Chapter 4. In addition jogging loads usually occur at higher frequencies and speed than walking loads, which is not implemented in the jogging load model.

- The value which should be used for $\gamma$ for a single pedestrian is not defined, but as it is a reduction factor to accomplish for synchronization of pedestrians, it assumed to be 1.

- UK-NA and BS 5400 are the only guideline where the concentrated load models are oscillating around zero, causing the model to include negative values for the load. The negative values does not correspond to a real load scenario, making the load case look different from the others. However, the static load contribution does not affect the acceleration response.

### 7.2.4 Håndbok 185

Recalling from Section 5.4, and Equation (5.22).

Vertical reference acceleration:

$$a_r = 4\pi^2 f^2 W_s K \psi r \quad [\text{m/s}^2]$$

Table 7.15: Parameter values used for Håndbok 185 load model

| Load model parameter | Value |
|---|---|
| Vertical direction | |
| $f$ | 1.97, 2.48, 2.54, 2.90, 4.36 Hz |
| $W_s$ | 5.292e-5 m |
| $K$ | 0.92 |
| $L$ | 41 m |
| $\xi$ | 0.01 |
| $\psi$ | 10 |
| $r$ | 1.00 and 0.82 for $f = 4.36$ Hz |

Table 7.16: Reference acceleration for Bårdshaug Bridge from Statens Vegvesen håndbok 185

| Frequency [Hz] | Acceleration from load model [m/s$^2$] |
| --- | --- |
| 1.97 | 0.08 |
| 2.48 | 0.11 |
| 2.54 | 0.12 |
| 2.90 | 0.16 |
| 4.36 | 0.3 |

**Comments on the load model:**

- In Håndbok 185 the method of finding the reference acceleration is limited to bridges with equal to or less than three spans. This makes finding the reference acceleration for Bårdshaug Bridge difficult, as there are four spans with different lengths. This will directly affect the configuration factor $K$ and dynamic load factor $\phi$. Conservative values are chosen for the configuration factor $K$ and dynamic load factor $\phi$.

- The static deformation from the point load, $W_s$, is obtained from the FE-model.

## 7.2.5   SÉTRA

Recalling from Section 5.5, and Equation (5.27), (5.28) and (5.30).

For single pedestrians and groups:

$$F_{ver}(t) = G_0 + 0.4G_0 sin(2\pi f_m t) \quad [\text{N}]$$

$$F_{lat}(t) = 0.05G_0 sin(2\pi(\frac{f_m}{2})t) \qquad [\text{N}]$$

For crowds:

$$F_v(t) = dP cos(2\pi f_v t)N_{eq}\psi \qquad [\text{N/m}^2]$$

Table 7.17: Parameter values used for SÉTRA load model

| Load model parameter | Value |
|---|---|
| **Single pedestrians and groups** | |
| $G_0$ | 700 N |
| $f_{m,vertical}$ | 2 Hz |
| $f_{m,horizontal}$ | 1 Hz |
| **Crowds** | |
| Density class | III |
| $d$ | 0.5 ped/m$^2$ |
| $P_{vertical}$ | 280 N |
| $P_{longitudinal}$ | 140 N |
| $P_{lateral}$ | 35 N |
| $f_{v,vertical}$ | 1.99 Hz |
| $f_{v,horizontal}$ | 1.86 Hz |
| $\xi$ | 0.6 % (Defined in guideline) |
| $N_{eq}$ | 0.055 |
| $\psi$ | 1 |
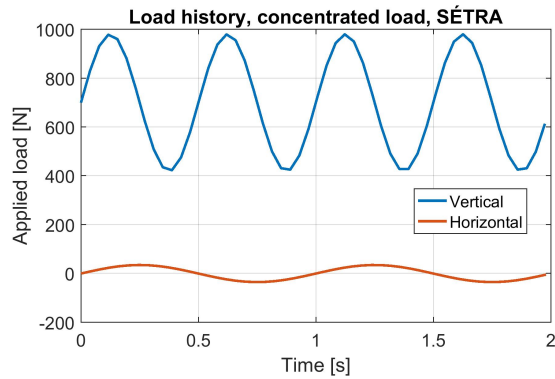


Figure 7.8: Load history, concentrated load model, SÉTRA
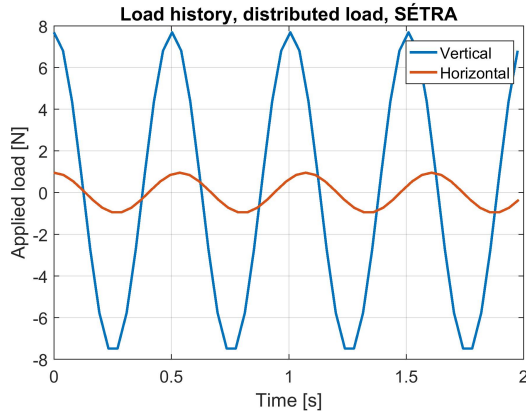
Figure 7.9: Load history, distributed load model, SÉTRA

Table 7.18: Acceleration values for SÉTRA load models

| | Acceleration [m/s$^2$] | | |
|---|---|---|---|
| Load type | Max | 95th-percentile | RMS |
| Vertical Concentrated loads | 0.0617 | 0.0534 | 0.0337 |
| Horizontal Concentrated loads | 0.0001 | 0.00008 | 0.00005 |
| Vertical Distributed loads | 0.2993 | 0.2955 | 0.2390 |
| Horizontal Distributed loads | 0.0363 | 0.0356 | 0.0283 |

**Comments on the load models:**

- The load models presented in SÉTRA are applied to all spans of the FE-model of the bridge.

- It is defined in the guideline that only one Fourier coefficient is necessary to get the required accuracy.

- For concentrated loads the parameter value $f_m$ is only defined as the walking frequency in the vertical direction despite that the parameter is used for load models in both vertical and horizontal direction. It is chosen to use the horizontal walking frequency (1 Hz) for the horizontal concentrated load model.

- It is chosen to use the damping given for steel-concrete composite bridges in the

guideline, and not the damping applied to the FE-model, in order to follow the guideline as it is written.

### 7.2.6 ISO 10137

Recalling from Section 5.6, and Equation (5.35) and (5.36):

$$F_{ver}(t) = Q(1 + \sum_{n=1}^{k} \alpha_{n,ver} sin(2\pi fnt + \phi_{n,ver})) \quad [\text{N}]$$

$$F_{lat}(t) = Q(1 + \sum_{n=1}^{k} \alpha_{n,lat} sin(2\pi fnt + \phi_{n,lat})) \quad [\text{N}]$$

Table 7.19: Parameter values used for ISO 10137 load model

| Load model parameter | Value |
|---|---|
| $Q$ | 700 N |
| $k$ | 1 |
| $\alpha_{n,vert}$ | 0.37 |
| $\alpha_{n,lat}$ | 0.1 |
| $f_{vert}$ | 1.99 Hz |
| $f_{lat}$ | 1 Hz |
| $\phi_{n,ver}$ | $\pi/2$ |
| $\phi_{n,lat}$ | $\pi/2$ |
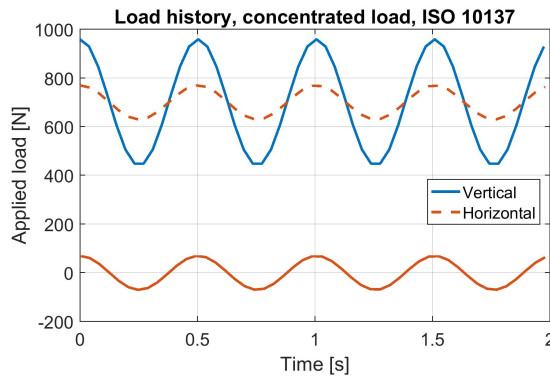


Figure 7.10: Load history, load model in ISO 10137

Table 7.20: Acceleration values for ISO 10137 load models

| | Acceleration [m/s$^2$] | | |
|---|---|---|---|
| Load type | Max | 95th-percentile | RMS |
| Vertical Concentrated loads | 0.0546 | 0.0500 | 0.0365 |
| Horizontal Concentrated loads | 0.0009 | 0.0002 | 0.0002 |

**Comments on the load models:**

- ISO 10137 does not give any specifications on where the pedestrian load should be applied, or what walking speed which should be used. The load is specified to be modeled as a worst case scenario, and previous research has interpreted this in different ways. In this thesis the load is chosen to be applied as a moving load over the span which has shown to give the biggest acceleration response; span 2, in order to maximize the acceleration response and minimize the computational cost. Walking speed is set to approximately 2 m/s.

- ISO 10137 presents the only load model for horizontal loading with a static load contribution, $Q$. In the guideline $Q$ is defined as "the static load of the participating person", and the load contribution for vertical and horizontal loading is not distinguished. A pedestrian will only have static load in vertical direction, and it is therefore unclear if $Q$ is meant to be the vertical static load (700 N) or the horizontal static load (0 N). However, if $Q$ is set to be the vertical static load, the horizontal load will not oscillate around 0 and therefore not concur with the horizontal load of a footstep, but if $Q$ is sat to the horizontal static load, 0 N, the whole expression equals zero. In order to make the the horizontal load model realistic, the first constant $Q$ in $F_{lat}$ is sat to be 0, and the following $Q$'s are given the value 700 N to maintain the given amplitude.

- It is not defined how many Fourier coefficients that is ideal to include in the model. For this thesis it is chosen to use 3 coefficients as the higher ones are not regarded as relevant for pedestrian induced loading (see Table 5.23).

- The Fourier coefficient $\alpha_{n,l}$ is only defined for structures with horizontal natural frequencies in the range of half the walking frequency, e.g. approximately 1 Hz. However, it is not mentioned what approach to use when the horizontal natural frequency is out of this range. For Bårdshaug Bridge, the first natural frequency in horizontal direction is 1.85, but the numerical coefficient for lateral direction given in the table in ISO 10137 is used.

### 7.2.7   JRC and HIVOSS

Recalling from Section 5.7 and 5.8, and Equation (5.41):

$$p(t) = Pcos(2\pi f_s t)n'\psi \qquad [\text{N/m}^2]$$

Table 7.21: Parameter values used for JRC/HIVOSS load model

| Load model parameter | Value |
|---|---|
| Traffic class | TC 3 |
| $P_{vert}$ | 260 N |
| $P_{lat}$ | 35 N |
| $f_{s,vert}$ | 1.99 Hz |
| $f_{s,hor}$ | 1.86 Hz |
| $n'$ | 0.03 |
| $\xi$ | 0.6 % (Defined in guideline) |
| $S$ | 458.5 m$^2$ |
| $\rho$ | 0.5 ped/m$^2$ |
| $\psi_v$ | 1 |
| $\psi_l$ | 1 |
| $\psi_{v,jog}$ | 0.2 |
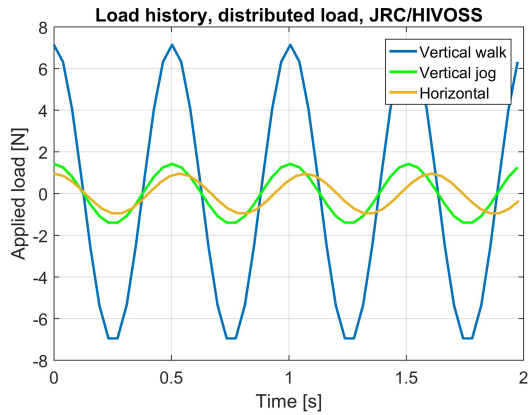


Figure 7.11: Load history, load model in JRC and HIVOSS

Table 7.22: Acceleration values for JRC/HIVOSS load models

| | Acceleration [m/s$^2$] | | |
|---|---|---|---|
| Load type | Max | 95%-percentile | RMS |
| Vertical, walk Distributed loads | 0.2832 | 0.2774 | 0.2238 |
| Vertical, jog Distributed loads | 0.0625 | 0.0612 | 0.0570 |
| Horizontal, walk Distributed loads | 0.0364 | 0.0357 | 0.0283 |

**Comments on the load models**

- The load models presented in JRC and HIVOSS are applied to all spans of the FE-model of the bridge.

- JRC and HIVOSS defines that the the 95th percentile of the acceleration histories shall be used to compare with the comfort criteria.

- It is chosen to use a pedestrian crowd with 0.5 ped/m$^2$ to match the other models best possible (which are given as 0.4, 0.5 and 0.6).

- Just like for SÉTRA, it is chosen to use the damping given for steel-concrete composite bridges in the guideline, and not the damping applied to the FE-model, in order to follow the guideline as it is written

- The jogging scenario in JRC/HIVOSS obtains a small value for Bårdshaug Bridge. This is a result of the reduction factor which becomes very small for the natural frequency 1.99 ( $\psi_{l,jog} = 0.2$), which the guideline encourages to use. The obtained acceleration value is in a smaller range than for the other vertical walking crowd load. Note that it is an advantage that the guideline includes a load scenario for higher frequencies, such that critical accelerations can still be evaluated for a structure with the fundamental natural frequency greater than the walking frequency.

### 7.2.8 Load History Summary
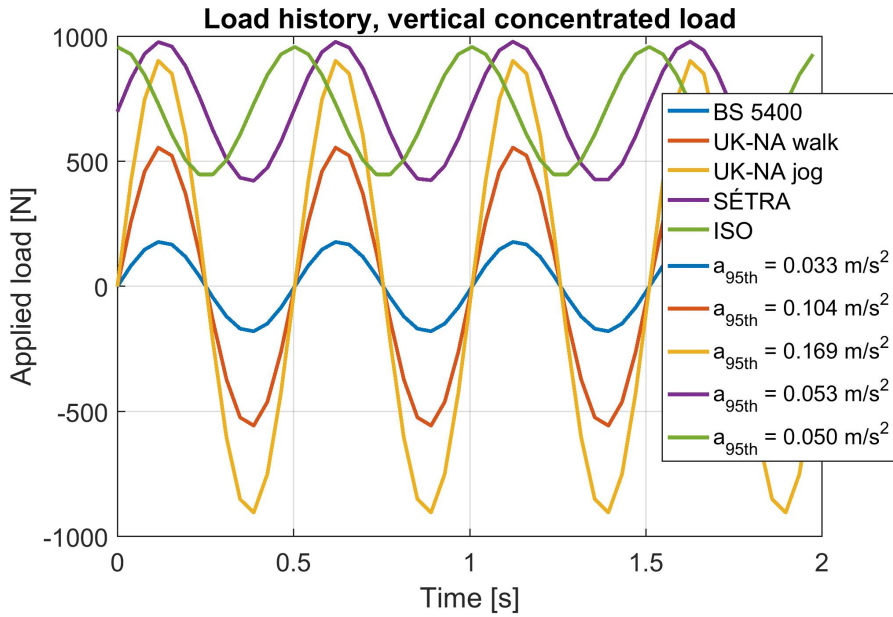


Figure 7.12: Vertical loading history of all concentrated load models in vertical direction
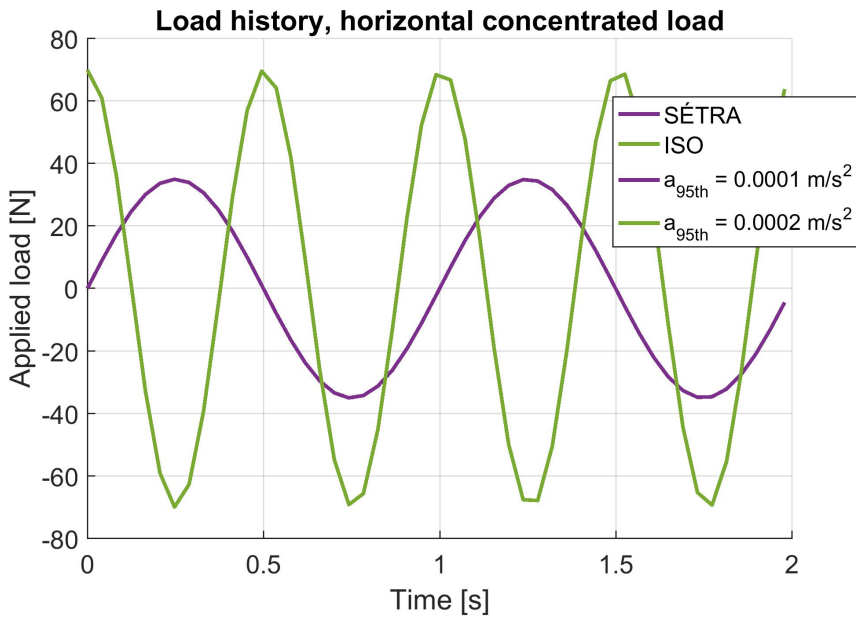


Figure 7.13: Vertical loading history of all concentrated load models in horizontal direction
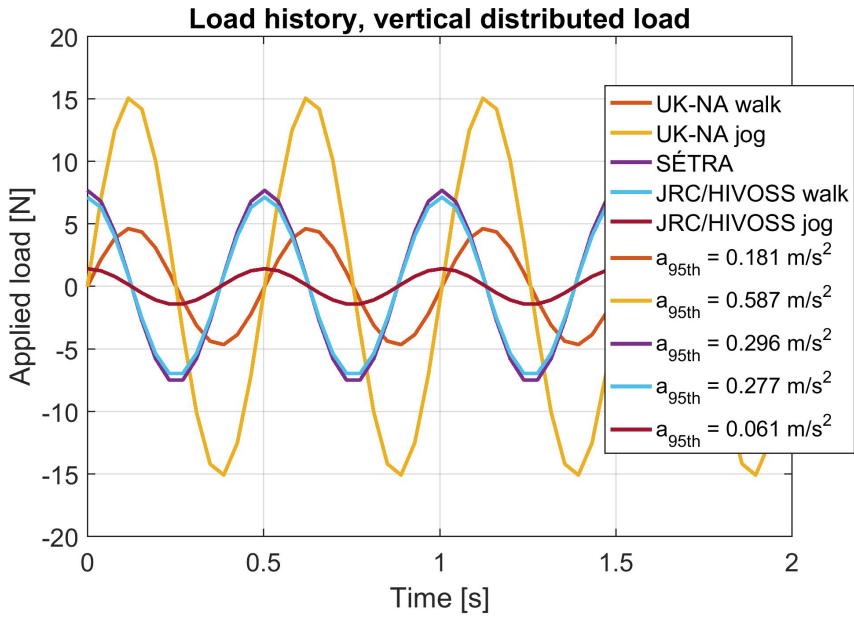
Figure 7.14: Vertical loading history of all distributed load models in vertical direction
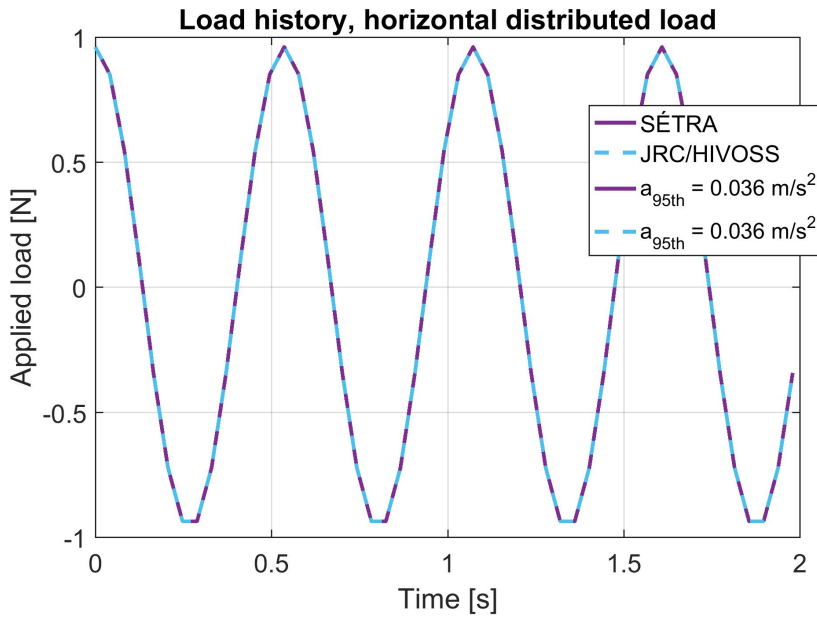


Figure 7.15: Vertical loading history of all distributed load models in horizontal direction

# Chapter 8

# Discussion

## 8.1 Comparing the Results of the Load Models

**Maximum-, RMS-, and 95th-percentile acceleration value**

The maximum peak value of the acceleration response has the benefit of being easy to read, as it can be picked directly from the graph without calculations. The disadvantage with the maximum peak value is that this is a single value, which might have a larger value than the trend, if an irregularity or error in the measurements occur. The uncertainty of the relevance of the maximum value makes it difficult to verify as a representative response.

The RMS value of the acceleration response pictures the acceleration intensity over the time interval, and decreases the importance of the peaks in a similar way as the mean value. Finding the RMS value requires calculations and is therefore more time consuming than finding the maximum peak value. The value of the RMS is dependent on the number of peaks, i.e. the length of time span, and how long the analysis are run for will have a major impact on the value. This makes it difficult to compare RMS-values obtained from models applied over time periods of different length, e.g. results from ISO 10137, modeled over one span compared with results from SÉTRA modeled over all spans.

The 95th-percentile acceleration value equals the acceleration peak values that the bridge is under 95% of the time. This value is less affected by irregular peaks appearing because of measurement mistakes or a sudden unexpected and unusual loading on the bridge. The 95th-percentile requires calculation, and is therefore more time consuming than the maximum peak value. The 95th-percentile is a more trustworthy value than the maximum value, as it is less prone to yield a value affected by irregularities and/or measurement errors.

The ratio between the maximum, 95th-percentile and RMS value of the acceleration is

similar for each guidelines. To avoid redundancy, only one acceleration value is chosen for the further discussion. Based on the previous discussion the 95th-percentile value is chosen to be used when comparing the acceleration response from the different load models, see Table 8.1. A summary of the RMS and maximum acceleration values are given in Appendix F. For acceleration response obtained by hand calculations (Eurocode and Håndbok 185), the obtained values are assumed to be comparable to the 95th-percentile values for the load models applied to the FE-model.

For load models describing both walking and jogging pedestrians it is chosen to use the value for walking pedestrians for the comparison, as this load scenario is presented in every guideline.

Table 8.1: Summary of 95th-percentile-values for acceleration response.

| Load type | 95th-percentile acceleration values [m/s$^2$] | | | | | | |
|---|---|---|---|---|---|---|---|
| | Euro-code | BS 5400 | UK-NA | Håndbok 185 | SÉTRA | ISO 10137 | JRC/ HIVOSS |
| Vert. conc. loads | 0.044 | 0.033 | 0.104 | 0.080 | 0.053 | 0.050 | - |
| Hor. conc. loads | 0.011 | - | - | - | 0.0001 | 0.0002 | - |
| Vert. dist. loads | 2.784 | - | 0.181 | - | 0.296 | - | 0.277 |
| Hor. dist. loads | 0.283 | - | - | - | 0.036 | - | 0.036 |

**Vertical concentrated loads**

The vertical concentrated loads simulating one pedestrian crossing the bridge are all modeled with a frequency of 1.99 Hz, equal both the vertical walking frequency and the first vertical natural frequency of the FE-model. None of the acceleration values from a single pedestrian crossing the bridge are in a critical range, which is expected as large accelerations does not occur on the actual Bårdshaug Bridge under normal use. UK-NA and Håndbok 185 are the guidelines which gives the greatest acceleration values for this load scenario. UK-NA includes a factor considering harmonic response, realistic pedestrian population and pedestrian sensitivity which is meant to reduce the load, but is given as 1 in the case for Bårdshaug Bridge as a result of the bridge having its first natural frequency similar to the walking frequency. UK-NA might be more sensitive to the fact that the load

is applied in the natural frequency and obtain larger values. The load model for Håndbok 185 is dependent on the static deformation on the middle span of the bridge, which is found from applying the static load to the FE-model. The FE-model used for Bårdshaug Bridge has reduced stiffness compared to the actual bridge, and therefore conservative results of this load model are obtained. A conservative acceleration value will normally be preferred rather than a less conservative one, in order to design a safe structure. At the same time a load model should not be too conservative, as this results in increased material usage, cost and environmental footprint.

The smallest acceleration value is obtained from BS 5400, which is only dependent on the natural frequencies and time. It is given a constant to decide the amplitude as 180 N, which is low compared to the constant deciding the amplitude for other guidelines, e.g. SÉTRA where the equivalent constant is given as 280 (=0.4*$G_0$).

**Horizontal concentrated loads**

The horizontal concentrated loads simulating one pedestrian crossing the bridge is the acceleration values with the biggest diversity in range of values, from 0.011 m/s$^2$ to 0.0001 m/s$^2$. The load model from Eurocode obtains the greatest acceleration value, and is only dependent on the mass and the damping of the structure; parameters which are easy to estimate but have big uncertainties attached. Factors such as length, number of spans, stiffness and natural frequencies are considered relevant factors for estimating the acceleration response, and are not included for a single pedestrian loading in Eurocode. In addition the acceleration values obtained from SÉTRA and ISO 10137 are both based on a load applied in the horizontal walking frequency (1 Hz), while the load model in Eurocode is assumed to be applied in the first horizontal natural frequency, giving it a much larger and not comparable acceleration value.

**Vertical distributed loads**

Five of the guidelines take distributed loads to consideration; Eurocode, UK-NA, SÉTRA, JRC and HIVOSS. All guidelines estimate the crowd load for a pedestrian crowd with a density of approximately 0.5 ped/m$^2$, or 229 pedestrians on the walkway. The density is dependent on the surrounding conditions, and defined in tables for UK-NA, SÉTRA and JRC/HIVOSS, and for Eurocode it is sat to the same value for the purpose of comparison. For Bårdshaug Bridge the estimated maximum traffic is 50 pedestrians and cyclists per hour, see Appendix G, and these crowd loads are therefore very unlikely to happen. Despite not being relevant for the discussed case, the discussion of the distributed load is included in order to also evaluate this part of the standards.

The first thing to note is that Eurocode obtains a much higher acceleration value than the other guidelines. The load model in Eurocode distinguish from the load models in

the other guidelines by obtaining the acceleration response by hand calculations, and not by applying the load to a FE-model. The crowd loads given in Eurocode is only dependent on the mass, damping, number of pedestrians and a reduction dependent on the natural frequency, and the equivalent number of pedestrians on the bridge is not taken to consideration. When this factor is excluded, it is assumed that the acceleration value reflects that the whole crowd is exciting the bridge in the eigen mode, which is very unlikely to happen and leads to large acceleration values.

UK-NA is the guideline which obtains the lowest acceleration value due to vertical distributed loads. This is a result of that UK-NA, in addition to take to account for the equivalent number of pedestrians, includes a reduction factor for desynchronized pedestrians which further reduces the load.

For both vertical and horizontal loads SÉTRA and JRC gives similar acceleration values, as a result of similar load models. The equations are written in different ways, but after multiplying load parameters it is shown that the load models are only separated by the defined value for the amplitude of loading. For vertical forces the value given in SÉTRA is 280 while it is 260 for JRC/HIVOSS, however, for horizontal loads the force amplitude for both load models equals 35, and the results are therefore exactly the same.

**Horizontal distributed loads**

The acceleration values for the horizontal distributed loads have the same characteristics as the vertical distributed loads; the overall values are larger than the concentrated loads, Eurocode obtains the largest acceleration values, and UK-NA obtains the lowest acceleration values. All the guidelines the which consider the horizontal distributed loads are dependent on the same parameters as for the vertical distributed loads and the arguments outlined in the previous paragraph is valid for the horizontal distributed loads too.

## 8.2 Comfort Criteria Compared to Associated Load Models

In this chapter the comfort criteria obtained form the guidelines will be compared to the acceleration values from the respective load models. For comfort criteria which distinguish between different natural frequencies, the criteria for the first natural frequency will be used, as this is the frequency the load is given when applied to the FE-model and because for most of the guidelines the first natural frequency yields the critical comfort criteria.

When comparing the acceleration values with the comfort criteria it is important to be aware that the vertical loads are applied in the first vertical natural frequency of the bridge, which for Bårdshaug Bridge corresponds to the normal walking frequency. Some models (UK-NA and SÉTRA for crowds) specify that the first natural frequency is the required frequency because it gives the worst case scenario, while other models (SÉTRA for single pedestrians, ISO 10137 and JRC/HIVOSS) specify that the load is to be applied in the walking frequency. In order to also make the discussion valid for bridges with natural frequencies outside the vertical walking frequency domain, selected vertical load models are applied to the FE-model using a frequency diverting from the first natural frequency in vertical direction, shown and discussed in Section 8.4. Note that the natural frequency is only similar to the walking frequency for vertical loads. Horizontal loads are applied at the horizontal walking frequency (1 Hz), away from the first horizontal natural frequency (1.85 Hz).

For this section the acceleration values are obtained by strictly following the guidelines, and the acceleration results together with their respective comfort criteria are shown in Table 8.2 on the next page.

Table 8.2: Summary of all comfort criteria and acceleration values

| Guideline | Type | Direction | Comfort Criteria $a_c$ [m/s²] | Modeled Acceleration $a$ [m/s²] | Difference $\Delta a = a_c - a$ [m/s²] | Deviation $a/a_c$ [%] |
|---|---|---|---|---|---|---|
| Eurocode | Single | Vertical Walk | 0.7 | 0.044 | 0.260 | 6.3 |
| | | Vertical Jog | | 0.132 | 0.568 | 18.9 |
| | | Horizontal | 0.2 | 0.011 | 0.189 | 5.5 |
| | Crowd span 2 | Vertical | 0.4 | 0.870 | -0.470 | 217.5 |
| | | Horizontal | | 0.089 | 0.311 | 22.3 |
| | Crowd all spans | Vertical | | 2.784 | 2.384 | 696 |
| | | Horizontal | | 0.283 | 0.117 | 70.6 |
| BS 5400 | Single | Vertical | 0.7 | 0.033 | 0.667 | 4.8 |
| UK-NA | Single | Vertical Walk | 0.91 | 0.104 | 0.806 | 11.3 |
| | | Vertical Jog | | 0.169 | 0.741 | 18.6 |
| | Crowd | Vertical Walk | | 0.181 | 0.729 | 19.9 |
| | | Vertical Jog | | 0.587 | 0.323 | 64.5 |
| Håndbok 185 | Single | Vertical | 0.42 | 0.08 | 0.340 | 19.0 |
| SÉTRA | Single | Vertical | 0.5 | 0.052 | 0.448 | 10.4 |
| | | Horizontal | 0.1 | 0.00008 | 0.099 | 0.1 |
| | Crowd | Vertical | 0.5 | 0.296 | 0.239 | 53.8 |
| | | Horizontal | 0.1 | 0.036 | 0.064 | 36.0 |
| ISO 10137 | Single | Vertical | 0.43 | 0.050 | 0.380 | 11.6 |
| | | Horizontal | 0.22 | 0.0002 | 0.21 | 0.1 |
| JRC/ HIVOSS | Crowd | Vertical Walk | 0.5 | 0.277 | 0.223 | 55.4 |
| | | Vertical Jog | 0.5 | 0.061 | 0.439 | 12.2 |
| | | Horzontal Walk | 0.1 | 0.036 | 0.064 | 36.0 |

For all guidelines where the comfort criteria are dependent on the natural frequency of the structure, the first natural frequency yield the critical acceleration, with the exception of ISO 10137 in vertical direction. Eurocode and UK-NA are the only guidelines where the comfort criteria are independent of the natural frequencies of the structure. UK-NA is also the only guideline where the comfort criterion is based on the surrounding conditions, which makes the critical acceleration obtained from UK-NA for Bårdshaug Bridge the least conservative.

The comfort criteria ranges widely for a single pedestrian in vertical direction, from 0.91 m/s$^2$ for UK-NA to 0.43 m/s$^2$ for ISO 10137. The horizontal comfort criteria are more consistent, ranging from 0.22 m/s$^2$ for ISO 10137 to 0.1 m/s$^2$ for SÉTRA and JRC/HIVOSS. The consistency and generally conservative values of the comfort criteria in horizontal direction might be a result of pedestrian interaction and lock-in. Horizontal vibrations due to the lock-in effect garnered a lot of attention after the opening of the Millennium Bridge. Where it was shown that a slight increase in excitation caused lock-in, which again caused the pedestrians to widen their steps to maintain balance and led to a further excitement of the structure. As a result of this, together with the pedestrian sensibility to horizontal movements, the comfort criteria in horizontal direction are in a smaller range than the vertical.

From Table 8.2 it is noted that BS 5400, UK-NA and Håndbok 185 are the only guidelines that does not provide criteria for lateral vibrations. The reason being that these guidelines are supplementing the Eurocode, such that the horizontal comfort criteria and load model in Eurocode is used.

Another observation from the comparison is that the criteria for all accelerations for a single pedestrian is satisfied. This is as expected, as normal walking does not cause problematic excitation for the real structure of Bårdshaug Bridge.

Eurocode provides a high degree of versatility, with several comfort criterion, loading scenarios and activities. The acceleration obtained from the load model for a single pedestrian is well below the critical acceleration, while the crowd loadings are very conservative in the vertical direction and does not satisfy the comfort criterion. The reason for the conservative values obtained in Eurcode is, as closer discussed in the previous section, that the crowd load simulates an entire whole crowd exciting the bridge in the first mode. For situations where the comfort criteria is not met in the Eurocode, the analyst is encouraged to add damping mechanisms to the structure.

UK-NA only provides one comfort criterion, while it provides four loading scenarios; single- and crowd loading for walking and jogging. It is not specified if the comfort criterion is applicable for all scenarios, or if it is specific for one. The comfort criterion in UK-NA gives the greatest accepted acceleration out of all the guidelines. The high comfort criterion is followed by significant acceleration responses from the load models, and the

scenario of a jogging crowd in UK-NA gives the greatest acceleration response among all the load models applied to the numerical model. All loads scenarios presented in UK-NA satisfy the the comfort criteria, and as discussed in the previous section, the crowd loading has an added reduction factor to take to account for desynchronized pedestrians, and is therefore expected to be lower than the comfort criteria for Bårdshaug Bridge.

In addition to the load scenario in vertical and horizontal direction, JRC and HIVOSS also provides a criterion which is not acceleration, but a critical number of pedestrians, $N_L = 53$. This describes the number of people distributed over the whole span that will cause a lock-in effect due to pedestrian lateral loading, and was derived after lock-in occurred at the opening of the Millenium bridge [29]. Implementing a similar criterion for vertical loading such as for Eurocode could be beneficial to better predict the stream of people.

Table 8.2 ultimately illustrates that a pedestrian bridge may satisfy the SLS depending on the guideline, e.g. satisfied for ISO 10137, but not for Eurocode for Bårdshaug Bridge. A dilemma arises if an arbitrary pedestrian bridge is designed, and it is found that conservative guidelines, e.g Eurocode or UK-NA, does not satisfy SLS, while less conservative guidelines, e.g. ISO 10137 or JRC, satisfies SLS. In this situation the analyst has to decide whether to reinforce the structure in order to satisfy the conservative guidelines, or to follow a less conservative guideline and conclude that the bridge is safe. The latter can have serious consequences when regarding vibrations because of the unpredictable nature of pedestrian loading.

## 8.3    Computational Time in Guidelines

The load models from the guidelines estimates the acceleration through hand calculations (Eurocode and Håndbok 185), pulsating loads applied to numerical models (UK-NA, SÉTRA, ISO and JRC/HIVOSS) or both (BS 5400).

The hand calculations of single pedestrian loads from Eurocode are very time efficient and only requires a good approximation of mass, damping ratio and number of pedestrians present to estimate the response. The hand calculation methods in Håndbok 185 and the simplified method presented in BS 5400 are identical, and slightly more comprehensive than the Eurocode, as more parameters need to be defined. These parameters are easily obtained through tables and figures if the stiffness, first vertical natural frequencies, damping ratio and span widths are estimated. The main challenge in using this method is to correctly predict the natural frequencies, as the acceleration from the load model is a function of the natural frequencies squared. In the critical frequency domain between 1 and 4 Hz the reference acceleration varies with a factor of 16, such that the modal analysis required for the calculations can be time consuming for accurate results. The natural frequencies must also be defined in Eurocode to obtain reduction factors for crowd loading,

but can easily be set to unity to maintain conservative values.

Running the pulsating load models on the numerical model yield the same computational cost for all models, because the dynamic analysis is run with equal time steps and period. Note that the computational cost is reduced if the output data is requested to record few nodal points or elements, such as the mid and quarter points on all spans. How easy each of the pulsating loads are to interpret varies. The simplified method in BS 5400 is, as mentioned, one of the more comprehensive hand calculations. However, according to BS 5400 this method is only valid for bridges with maximum three spans, and the generalized method in BS 5400 is therefore used. The general method is only dependent on the natural frequency of the bridge as a parameter, and is therefore the most time efficient load modal to preform out of the pulsating load model applied to the FE-model. All the pulsating load models have many parameters, but for most guidelines the parameter values are all found in tables and the load is therefore easy to apply. The exception is the crowd load for UK-NA and JRC which require calculations in order to obtain the equivalent number of pedestrians, and are therefore more time consuming.

## 8.4 Applying Load Outside The Natural Frequency

As mentioned, the first vertical natural frequency for Bårdshaug Bridge coincide with the vertical walking frequency ($\approx$ 2 Hz). To increase the relevance of the discussion for bridges with different natural frequencies, the effect of applying a load with a frequency different from the natural frequency is evaluated in the following section. Figure 8.1 - 8.4 illustrates the effect of changing the load frequency from 1.99 Hz to 2.2 Hz for the acceleration histories obtained from the load models given in SÉTRA.
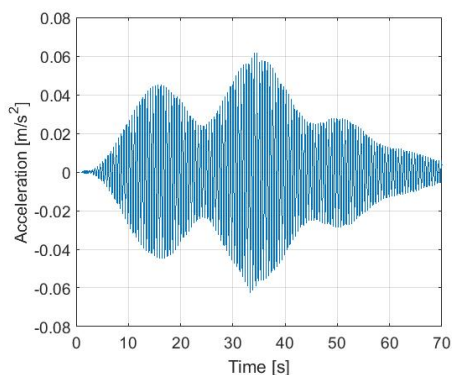


Figure 8.1: Acceleration history, concentrated load, frequency = 1.99 Hz
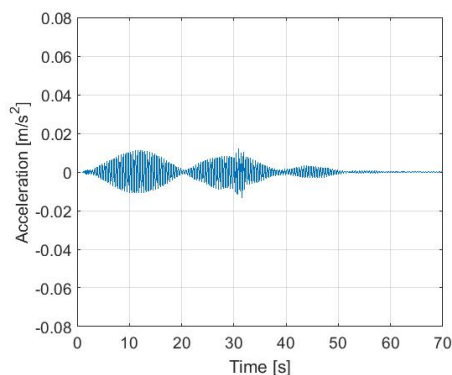


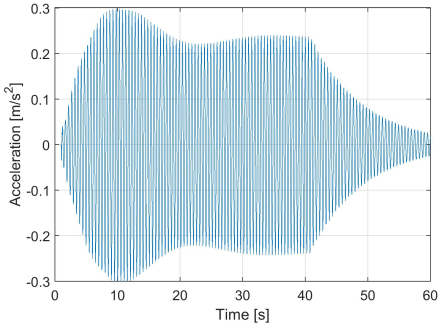Figure 8.2: Acceleration history, concentrated load, frequency = 2.2 Hz

Figure 8.3: Acceleration history, distributed load, frequency = 1.99 Hz
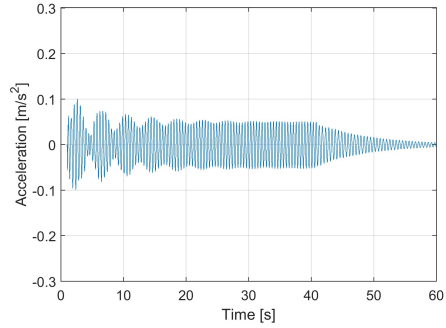


Figure 8.4: Acceleration history, distributed load, frequency = 2.2 Hz

Table 8.3: Acceleration values for load applied with 2.2 Hz versus 1.9 Hz

| Load type | Acceleration [m/s²] | | |
|---|---|---|---|
| | Max | 95%-percentile | RMS |
| Vertical Concentrated loads Freq. = 2.2 Hz | 0.0118 | 0.0088 | 0.0047 |
| Vertical Concentrated loads Freq. = 1.99 Hz | 0.0617 | 0.0534 | 0.0337 |
| Vertiacal Distributed loads Freq. = 2.2 Hz | 0.1000 | 0.0682 | 0.0550 |
| Vertical Distributed loads Freq. = 1.99 Hz | 0.2993 | 0.2955 | 0.2390 |

As Figure 8.1 - 8.4 and Table 8.3 shows that the acceleration value decreases drastically when the frequency of the load is applied outside the natural frequency. This states the importance of designing pedestrian bridges with natural frequencies outside the walking frequencies. The decrease in acceleration value is 84 % for concentrated loads and 78 % for distributed loads. The frequency of the load will have a greater impact on the distributed loads because these are applied simultaneously over the whole bridge and the concentrated load is moving across one span at the time. Note that for some load models, e.g. the load model in vertical direction for jogging crowds in JRC/HIVOSS, the load increases for

certain frequencies outside the walking frequency, as the reduction factor multiplied with the load obtains a greater value.

An observation from the acceleration history from distributed loads applied at the natural frequency on the numerical model is that the acceleration response yields a peak before stabilizing. As an example see Figure 8.3 from the distributed load of SÉTRA. This peak shows a transient part of the acceleration which is greater than the stationary solution for the resonating loading. The peak occurs because the crowd loading is suddenly applied all along the bridge such that the initial velocity is greater than the stationary response, and the response falls to the stationary response due to damping.

## 8.5    Acceleration From Measurement Data

The acceleration values for Bårdshaug Bridge are obtained from peak picking of the measured acceleration data on Bårdshaug Bridge using MATLAB, and are given in the Table 8.4 and 8.5. Note that the load models for single pedestrian load in vertical direction given in the guidelines are applied to the FE-model so that resonance occurs, while resonance was not reported during the the measurements on the real structure, and the tables are therefore not directly comparable.

Table 8.4: Accelerations in vertical direction from measurement data

| Acceleration [m/s$^2$] | | |
|---|---|---|
| Max | 95th-percentile | RMS |
| 0.3982 | 0.0248 | 0.0165 |

Table 8.5: Accelerations in horizontal direction from measurement data

| Acceleration [m/s$^2$] | | |
|---|---|---|
| Max | 95th-percentile | RMS |
| 0.1947 | 0.0153 | 0.0122 |

Based on the maximum measurement data from Bårdshaug Bridge, the 95th-percentile from the guidelines seems reasonable. It is worth noting that the source of the maximum acceleration was due to an impulse load from a car driving over a 2x8 inch timber beam. This maximum acceleration is a unique peak in the time series and yields a magnitude which is not reoccurring, see Figure 8.5. The second largest peak is $\approx 0.165$ m/s$^2$ and the third largest peak is $\approx 0.139$ m/s$^2$, neither of these peaks are common over the time series, and are most likely not a result of pedestrian loading.
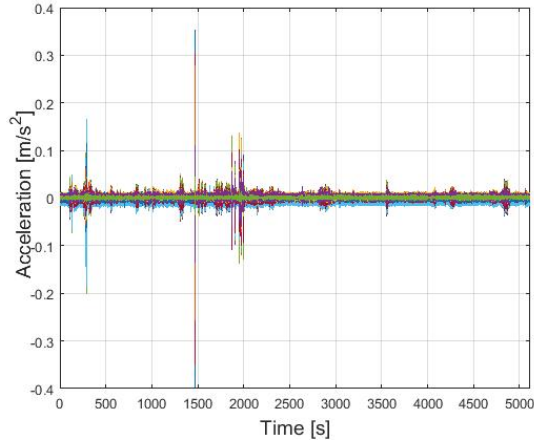
Figure 8.5: Acceleration data of all 18 nodes in vertical direction on Bårdshaug Bridge

Unfortunately, the modal analysis report of Bårdshaug Bridge does not provide data for what type of pedestrian loading were present during the measurements. Such that, in addition to resonance not occurring during the measurements, a realistic load scenario comparison between the response from the two hour long time series from the bridge and the response from the numerical model can not be sufficiently described. Note that the accelerations values on the real structure never falls completely to rest, and the obtained acceleration values are dependent on a lot of noise. The noise greatly affects the RMS-value, and makes the value challenging to use for comparison with load model results.

The 95th-percentile of the acceleration value in vertical direction from the measurement data is less than every acceleration value for the vertical concentrated load models as expected. However, it is worth noting that measurement data yields a 95th-percentile vertical acceleration value in the same order of magnitude as for the vertical concentrated load models.

The RMS and 95th-percentile of the acceleration from the measurement data are greater than the values obtained from the concentrated horizontal load models. The vertical and horizontal accelerations from the measurement data are in the same order of magnitude, which is not the case for any of the load models under the same loading. This may suggest that the 95th-percentile and RMS acceleration values from Tables 8.4 and 8.5 are based on noise or ambient loading. Another suggestion is that the horizontal load models poorly predict the acceleration responses on the structure.

# Chapter 9

# Conclusion and Further Work

## 9.1 Summary and Conclusion

The main objective of this thesis has been to evaluate and compare different load models and comfort criteria given in guidelines for pedestrian loading, with respect to accuracy and usability. The guidelines taken into consideration are Eurocode, BS 5400, UK National Annex to Eurocode, Håndbok 185, SÉTRA, ISO 10137, JRC - Design of Footbridges for Human Induced Vibrations and HIVOSS. In addition, a desired outcome has been to obtain an approach to the modelling of a pedestrian bridge in order to achieve accurate dynamic behaviour for the model, and obtain realistic acceleration output when pedestrian loads are applied. A case study was done for Bårdshaug Bridge, a pedestrian bridge located in Orkanger, Norway.

The different guidelines taken into consideration have vast variations in the approach to the simplification of the pedestrian load and how to obtain a comfort criterion; from including only mass and damping, like Eurocode, to also including length, number of pedestrians and natural frequencies, like UK-NA and SÉTRA. The load parameters are weighted differently depending on the guideline, such that a more comprehensive load model not necessarily yields the most accurate result. The different approaches and simplifications causes large variation in the results, making it challenging to recommend a single guideline for obtaining the most realistic responses. It is shown that a guideline can obtain a good approximation for the acceleration values for one case, but poor approximations for other cases. For example Eurocode, which would yield the exact same acceleration values for Bårdshaug Bridge, as it would for a longer and more slender bridge if the mass and damping ratio were the same. This is not desired as a long and more slender bridge may be more prone to resonance than Bårdshaug Bridge.

**Guideline Accuracy and Usability**

For all the guidelines the criteria for single pedestrian loading were met, which is expected as Bårdshaug Bridge does not have any reported problems regarding vibrations. The only scenario where the acceleration value exceeded the comfort criteria was for the load model for crowd loads in Eurocode. The load model in Eurocode does not include a factor to account for desynchronized pedestrians, and therefore the only guideline which assume that the an entire crowd is exciting the bridge in an eigen mode. This scenario is very unlikely to happen and leads to large acceleration values. It is found that it is desirable that a load model is applied to the FE-model, and that it includes not only single and crowd loading, but also group loads, in order to obtain the acceleration value under normal use.

A good load model should include factors such as number of pedestrians, length, number of spans, stiffness, damping and natural frequencies in order to be usable in a general case. At the same time a good load model needs to be easy to utilize in a numerical model and/or hand calculation, and not be dependent on factors which are hard to predict in the design phase. A load model should include both vertical and horizontal loads, and more than one load scenario so the analyst has the opportunity to calculate for different scenarios and make their own assumptions and iterations if necessary. A good comfort criteria has to reveal when a bridge will obtain large accelerations, but also classify a bridge as safe if uncomfortable accelerations do not occur. On the basis of this, and the accelerations obtained from Bårdshaug Bridge, SÉTRA is chosen as the desirable guideline to use for vibrations on a pedestrian bridge. SÉTRA obtains realistic acceleration values, is relatively easy to apply to a FE-model, has load models for single pedestrians, groups and crowd is both vertical and horizontal direction, and if desired it is possible to obtain an even more exact load model by including more Fourier coefficients. In this thesis the comfort criterion is set to maximum comfort, and the criterion is still met. SÉTRA also accounts for lock-in by limiting the comfort criterion in the horizontal direction.

**Finite Element Model**

The simplified FE-model yields a good approximation for 7 out of 10 modes in the frequency domain 1.85 - 4.45 Hz. Existing modes with higher natural frequencies can not be denied, but these modes will have very low responses under ordinary usage, such that the dynamic loading for normal use on the model of Bårdshaug Bridge is considered sufficiently described. The simplifications regarding the exclusion of the steel trusses and welding plates in the numerical model is not recommended, as the numerical model is lighter and less stiff than the actual bridge. As a consequence this simplification the second and third vertical modes and third torsional mode is not found in the FE-model.

Through the iteration process of the FE-model of Bårdshaug Bridge it is found that the

steel-concrete interaction is best treated using linear springs in all directions. Compared to the numerical model with full interaction which yields a solution that is too stiff.

The FE-model of Bårdshaug Bridge is designed in order to obtain a realistic dynamic behaviour through structural simplifications, and the emphasized features of the model can either be used to make a model with a similar approach, or in combination with other modelling strategies to create an overall realistic model.

## 9.2 Recommendations for Further Work

- The work presented in this thesis shows that further research is necessary in order to create a new model for both vertical and horizontal pedestrian load. The model should be applicable for all pedestrian bridges, taking to account structural features like length, number of spans, slenderness and damping. The model should also take to account the characteristics of the human step as the overlap between footsteps, that each step has two peaks and synchronization. A new model should use MC-simulations finding the coefficients, as this is shown to be good in order to predict the value of random variables. Newer pedestrian load models such as Butz's and Nakamuras can for example be used as a basis.

- It would be interesting to see a continuation of the work done in this thesis, where the load models are applied to several FE-models of existing pedestrian bridges, and acceleration measurements with controlled loading are applied to the same bridges. It would be preferable to apply the same loads several times to accurately describe a single pedestrian loading.

- I would also be interesting to see a further development of comfort criteria for pedestrian bridges. An interesting area of research would be to investigate if acceleration criteria are enough to limit the vibrations in a footbridge, and if it could be advantageous to have criteria for other parameters, e.g. critical natural frequency domain or minimum damping in the structure.

- Regarding the FE-model, the simplifications has made the assembly simple and computationally more cost effective. For further work however, the numerical model is recommended to apply the steel trusses and welding plates to account for the added stiffness and mass to reduce the source of errors. Another recommendation is to account for the steel reinforcement in the concrete, asphalt, handrails and pedestrian crowds with an added mass tool.

# Bibliography

[1] Mathisen KM. TKT4201 Structural Dynamics, Lecture 2 - Free undamped and damped vibration, 2015.

[2] Nilsson M, Mårtenson A. Dynamic Analysis of Pedestrian Load Models for Footbridges, 2014.

[3] Petersen ØW, Frøseth GT. Vibrasjonsmålinger - Gangbro over Orkla ved Bårdshaug. Technical report, Department of Structural Engineering, Norwegian University of Science and Technology, November 2016.

[4] Brunet T, Leng J, Mondain-Monval O. Soft acoustic metamaterials. *Science*, 342(6156):323–324, 2013.

[5] Gil-Martín LM, Carbonell-Márquez JF, Hernández-Montes E, Aschheim M, Pasadas-Fernández M. Dynamic magnification factors of sdof oscillators under harmonic loading. *Applied Mathematics Letters*, 25(1):38–42, 2012.

[6] Cook RD, Malkus DD, Plesha ME, Witt RJ. *Concepts and applications of finite element analysis, fourth edidtion*. John Wiley & Sons, 2002.

[7] Chowdhury I, Dasgupt SP. Computation of rayleigh damping coefficients for large systems. *The Electronic Journal of Geotechnical Engineering*, 8(0):1–11, 2003.

[8] Mathisen KM. TKT4201 Structural Dynamics, Lecture 7 - Solution of the dynamic equilibrium equations by explicit direction, 2016.

[9] Mathisen KM. TKT4197 Nonlinear Finite Element Analysis, Lecture 8 - Solution of the dynamic equilibrium equations by implicit integration (2), 2016.

[10] Henri G. Numerical integration for structural dynamics. *CEE 541. Structural Dynamics*, 2016.

[11] Wood WL, Bossak M, Zienkiewicz OC. An alpha modification of newmark's method. *International Journal for Numerical Methods in Engineering*, 15(10):1562–1566, 1980.

[12] Weisstein EW. Fourier series. *Wolfram Research, Inc.*, 2002.

[13] Newland DE. *An Introduction to Random Vibrations, Spectral and Wavelet Analysis Longman Scientific & Technical*. England, 1993.

[14] Solheim AS. Instrumentering av hardangerbrua. Master thesis, NTNU, June 2013.

[15] Hassani S. Dirac delta function. In *Mathematical Methods*, pages 289–319. Springer, 2000.

[16] Sheehy P, Martz E. Doing monte carlo simulation in minitab statistical software. In *ASQ Lean Six Sigma Conference*, 2012.

[17] Brownjohn JMW, Živanović S, Pavić A. Crowd dynamic loading on footbridges. *CRC Press*, 2009.

[18] Kobayashi M. Prediction and control of pedestrian induced vibration on an interior footbridge. Master's thesis, Technical University of Denmark, Department of Civil Enigneering, Denmark, 2011.

[19] Heinzel G, Rüdiger A, Schilling R. Spectrum and spectral density estimation by the Discrete Fourier Transform (DFT), including a comprehensive list of window functions and some new at-top windows. *Teilinstitut Hannover*, 2002.

[20] Gaupta HR, Mehra R, Batan S. Power Spectrum Estimation using Welch Method for various Window Techniques. *International Journal of of Scientific Research Engineering and Technology (IJSRET)*, 2:389–392, 2013.

[21] Xiaoming Y, Yujian J, Yonghong L. Matlab simulation and analysis of the welch method in the classical power spectrum estimation. *Electronic Test*, 7:029, 2011.

[22] Welch PD. The use of fast fourier transform for the estimation of power spectra: A method based on time averaging over short, modified periodograms. *IEEE Transactions on audio and electroacoustics*, 15(2):70–73, 1967.

[23] Peeters B, Ventura CE. Comparative study of modal analysis techniques for bridge dynamic characteristics. *Mechanical Systems and Signal Processing*, 17(5):965–988, 2003.

[24] Peeters B, De Roeck G. Stochastic system identification for operational modal analysis: a review. *Journal of Dynamic Systems, Measurement, and Control*, 123(4):659–667, 2001.

[25] Grandić IS. Serviceability verification of pedestrian bridges under pedestrian loading. *Tehnički vjesnik*, 22(2):527–537, 2015.

[26] Chopra AK. *Dynamics of Structures: Theory and Applications to Earthquake Engineering*, volume 5. Pearson Education Inc., 2016.

[27] Pastor M, Binda M, Harčarik T. Modal assurance criterion. *Procedia Engineering*, 48:543–548, 2012.

[28] Allemang RJ. The modal assurance criterion–twenty years of use and abuse. *Sound and vibration*, 37(8):14–23, 2003.

[29] Dallard P, Fitzpatrick T, Flint A, Low A, Smith RR, Willford M, Roche M. London millennium bridge: pedestrian-induced lateral vibration. *Journal of Bridge Engineering*, 6(6):412–417, 2001.

[30] Bachmann H, Ammann W. *Vibrations in structures: induced by man and machines*, volume 3. Iabse, 1987.

[31] Zoltowski K. Pedestrian bridge, load and response. In *Proceedings of the Second International Conference Footbridges*, pages 247–248, 2005.

[32] Fanning P, Archbold P, Pavic A. A novel interactive pedestrian load model for flexible footbridges. In *Proceeding of the 2005 Society for Experimental Mechanics Annual Conference on Experimental and Applied Mechanics, Portland, Oregon, June*, pages 7–9, 2005.

[33] Pavić ET Ingólfsson S., Živanović A. Modeling spatially unrestricted pedestrian traffic on footbridges. *Journal of Structural Engineering*, 136(10):1296–1308, 2010.

[34] Ezeonwu-Emmanuel C, Oji UC. Simulation of Solutions to Excessive Vibration Problems of Pedestrian Footbridges. Master's thesis, Blekinge Institute of Techology, Karlskorna, Sweeden, 2008.

[35] Nakamura S. Model for lateral excitation of footbridges by synchronous walking. *Journal of Structural Engineering*, 130(1):32–37, 2004.

[36] Ingólfsson E. *Pedestrian-induced lateral vibrations of footbridges*. PhD thesis, DTU Civil Engineering, 2011.

[37] Gimsing NJ, Georgakis CT. *Cable supported bridges: concept and design*. John Wiley & Sons, 2011.

[38] European Committee for Standardization (CEN). Eurocode 0 - Basis for structural design. Standard, European Commission (EC), Europe, 2016.

[39] European Committee for Standardization (CEN). Eurocode 4 - Design of composite steel and concrete structures - Part 2: General rules and rules for bridges. Standard, European Commission (EC), Europe, 2009.

[40] European Committee for Standardization (CEN). Eurocode 2 - Design of concrete structures - Part 1-1: General rules for buildings. Standard, European Commission (EC), Europe, 2010.

[41] European Committee for Standardization (CEN). Eurocode 3 - Design of steel structures - Part 2: Steel bridges. Standard, European Commission (EC), Europe, 2009.

[42] BS 5400 The Steel and Concrete Bridges Standards Committee. British Standard 5400 - Steel, concrete and composite bridges - Part 2: Specification for loads. Standard, British Standard Institution (BSI), Great Britain, 2005.

[43] British Standard Institution (CEN) UK-NA. UK National Annex to Eurocode 1: Actions on structures - Part2: Trafficload on bridges. Standard, British Standard Institution (BSI), Great Britain, 2008.

[44] The Norwegian Public Roads Administration. Statens Vegvesen Håndbok N400 - Bruporsjektering. Standard, The Norwegian Public Roads Administration, Statens Vegvesen (SVV), Norway, 2015.

[45] The Norwegian Public Roads Administration. Statens Vegvesen Håndbok N400 - Bruporsjektering. Standard, The Norwegian Public Roads Administration, Statens Vegvesen (SVV), Norway, 2009.

[46] SÉTRA French Ministry of Transport and Infrastructure. Service d'Études Techniques des Routes et autoroutes. Technical guide, French Ministry of Transport and Infrastructure., Paris, October 2006.

[47] ISO 10137 International Organization for Standardization. Bases for design of structures-Serviceability of buildings and walkways against vibration. Standard, International Organization for Standardization, Geneva, CH, 2007.

[48] JRC Scentific and Technical Reports. Design of Lightweight Footbridges for Human Induced Vibrations. Standard, European Commission, Norway, May 2009.

[49] Butz C, Feldmann M, Heinemeyer Ch, Sedlacek G, Chabrolin B, Lemaire A, and Lukic M, Martin PO, Caetano E, Cunha A,. Advanced load models for synchronous pedestrian excitation and optimised design guidelines for steel foot bridges (synpex). *RFCS-Research Project RFS-CR-03019*, 2007.

[50] Research Fund for Coal HIVOSS and Steel (RFCS). Design of footbridge guideline. Standard, British Standard Institution (BSI), April 2008.

[51] Abaqus Documentation 6.12 analysis user's manual. `https://things.maths.cam.ac.uk/computing/software/abaqus_docs/docs/v6.12/books/usb/default.htm?startat=pt03ch06s03at07.html`. Accessed: 2017-05-18.

[52] European Committee for Standardization (CEN). Eurocode 2 - Actions on structures - Part 2: Traffic loads on bridges. Standard, European Commission (EC), Europe, 2008.

[53] Liu GR. A step-by-step method of rule-of-mixture of fiber-and particle-reinforced composite materials. *Composite structures*, 40(3-4):313–322, 1997.

[54] Reynolds P, Živanović S, Pavic A. Vibration serviceability of footbridges under human-induced excitation: a literature review. *Journal of sound and vibration*, 279(1):1–74, 2005.

# Appendices

# Appendix A

# Eurocode: Natural Frequencies in Design Process

The first natural frequency $n_0$ can be obtained form Eurocode 1 part 2 for a "simply supported bridge subject to bending only" by:

$$n_0 = \frac{17.75}{\sqrt{\delta_0}} \qquad \text{[Hz]} \quad \text{(A.1)}$$

Where $\delta_0$ is the deflection, in mm, at the mid span due to permanent actions, calculated using a short term modulus for concrete bridges, in accordance with a loading period appropriate to the natural frequency of the bridge.

The upper limit of the first natural frequency, $n_0$, is governed by dynamic enhancements due to track irregularities and is given in equation (A.2).

$$n_0 = 94.76 L^{-0.748} \qquad \text{[Hz]} \quad \text{(A.2)}$$

For bridges where the first natural frequency, $n_0$, exceeds the upper limit, a dynamic analysis is required. The lower limit of $n_0$ is governed by dynamic impact criteria and is given by:

$$n_0 = 80 L^{-1} \qquad \text{for} \quad 4m \leq \text{L} \leq 20m \qquad \text{(A.3)}$$

$$n_0 = 23.58 L^{-0.592} \qquad \text{for} \quad 20m < \text{L} \leq 100m \qquad \text{(A.4)}$$

where $L$ is the span length for simply supported bridges or the determinant length $L_\Phi$ for other bridge types. $L_\Phi$ is found from table 6.2 in Eurocode 1 part 2, see figures A.1-A.3 below.

**Table 6.2 - Determinant lengths $L_\Phi$**

| Case | Structural element | Determinant length $L_\Phi$ |
|---|---|---|
| **Steel deck plate:** closed deck with ballast bed (orthotropic deck plate) (for local and transverse stresses) | | |
| | Deck with cross girders and continuous longitudinal ribs: | |
| 1.1 | Deck plate (for both directions) | 3 times cross girder spacing |
| 1.2 | Continuous longitudinal ribs (including small cantilevers up to 0,50 m)[a] | 3 times cross girder spacing |
| 1.3 | Cross girders | Twice the length of the cross girder |
| 1.4 | End cross girders | 3,6m [b] |
| | Deck plate with cross girders only: | |
| 2.1 | Deck plate (for both directions) | Twice cross girder spacing + 3 m |
| 2.2 | Cross girders | Twice cross girder spacing + 3 m |
| 2.3 | End cross girders | 3,6m [b] |
| **Steel grillage:** open deck without ballast bed [b] (for local and transverse stresses) | | |
| 3.1 | Rail bearers:<br>- as an element of a continuous grillage<br>- simply supported | 3 times cross girder spacing<br><br>Cross girder spacing + 3 m |
| 3.2 | Cantilever of rail bearer [a] | 3,6m |
| 3.3 | Cross girders (as part of cross girder/ continuous rail bearer grillage) | Twice the length of the cross girder |
| 3.4 | End cross girders | 3,6m [b] |

[a] In general all cantilevers greater than 0,50 m supporting rail traffic actions need a special study in accordance with 6.4.6 and with the loading agreed with the relevant authority specified in the National Annex.
[b] It is recommended to apply $\Phi_3$

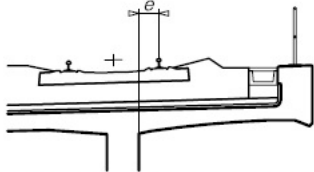Figure A.1: Determinant length $L_\Phi$, from Eurocode 1

Table 6.2 (continued)

| Case | Structural element | Determinant length $L_\Phi$ |
|---|---|---|
| **Concrete deck slab with ballast bed** (for local and transverse stresses) | | |
| 4.1 | Deck slab as part of box girder or upper flange of main beam | |
| | - spanning transversely to the main girders | 3 times span of deck plate |
| | - spanning in the longitudinal direction | 3 times span of deck plate |
| | - cross girders | Twice the length of the cross girder |
| | - transverse cantilevers supporting railway loading | <br><br>- $e \le 0{,}5$ m: 3 times the distance between the webs<br>- $e > 0{,}5$ m: [a]<br>**Figure 6.11 - Transverse cantilever supporting railway loading** |
| 4.2 | Deck slab continuous (in main girder direction) over cross girders | Twice the cross girder spacing |
| 4.3 | Deck slab for half through and trough bridges: | |
| | - spanning perpendicular to the main girders | Twice span of deck slab + 3m |
| | - spanning in the longitudinal direction | Twice span of deck slab |
| 4.4 | Deck slabs spanning transversely between longitudinal steel beams in filler beam decks | Twice the determinant length in the longitudinal direction |
| 4.5 | Longitudinal cantilevers of deck slab | - $e \le 0{,}5$ m: 3,6m [b]<br>- $e > 0{,}5$ m: [a] |
| 4.6 | End cross girders or trimmer beams | 3,6m [b] |

[a] In general all cantilevers greater than 0,50 m supporting rail traffic actions need a special study in accordance with 6.4.6 and with the loading agreed with the relevant authority specified in the National Annex.
[b] It is recommended to apply $\Phi_3$

NOTE For Cases 1.1 to 4.6 inclusive $L_\Phi$ is subject to a maximum of the determinant length of the main girders.

Figure A.2: Determinant length $L_\Phi$, from Eurocode 1, continued

**Table 6.2 (continued)**

| Case | Structural element | Determinant length $L_\Phi$ |
|---|---|---|
| **Main girders** | | |
| 5.1 | Simply supported girders and slabs (including steel beams embedded in concrete) | Span in main girder direction |
| 5.2 | Girders and slabs continuous over $n$ spans with $$L_m = 1/n \, (L_1 + L_2 + .. + L_n) \qquad (6.6)$$ | $L_\Phi = k \times L_m, \qquad (6.7)$ but not less than max $L_i$ $(i = 1,...., n)$ <br><br> $n = 2 \quad 3 \quad 4 \quad \geq 5$ <br><br> $k = 1{,}2 \quad 1{,}3 \quad 1{,}4 \quad 1{,}5$ |
| 5.3 | Portal frames and closed frames or boxes: <br><br> - single-span <br><br><br><br> - multi-span | <br><br> Consider as three-span continuous beam (use 5.2, with vertical and horizontal lengths of members of the frame or box) <br><br> Consider as multi-span continuous beam (use 5.2, with lengths of end vertical members and horizontal members) |
| 5.4 | Single arch, archrib, stiffened girders of bowstrings | Half span |
| 5.5 | Series of arches with solid spandrels retaining fill | Twice the clear opening |
| 5.6 | Suspension bars (in conjunction with stiffening girders) | 4 times the longitudinal spacing of the suspension bars |
| **Structural supports** | | |
| 6 | Columns, trestles, bearings, uplift bearings, tension anchors and for the calculation of contact pressures under bearings. | Determinant length of the supported members |

Figure A.3: Determinant length $L_\Phi$, from Eurocode 1, continued

# Appendix B

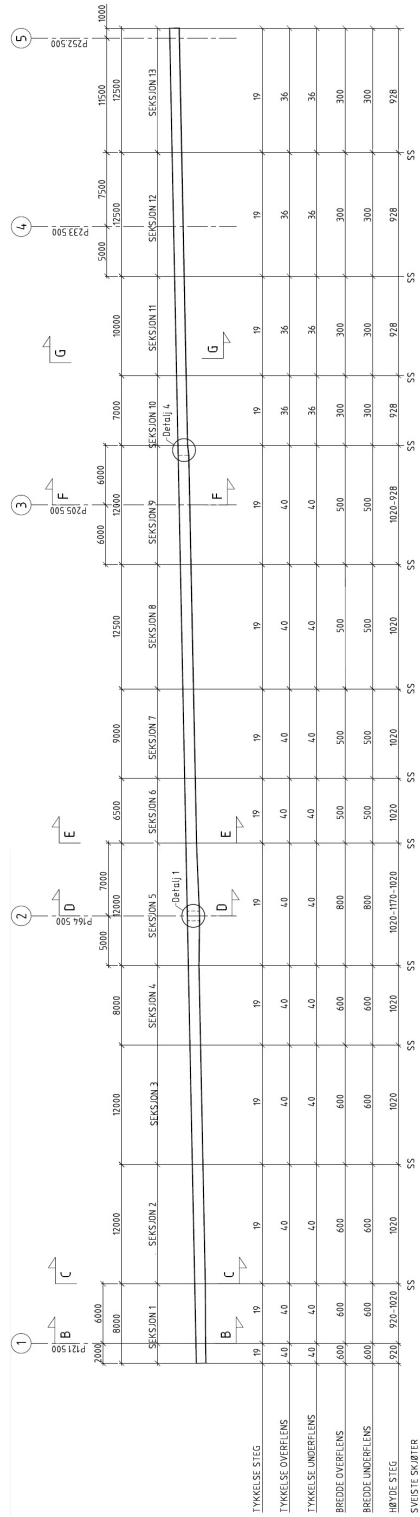# Steel beam variations along Bårdshaug Bridge

Figure B.1: General descriptions of the varying steel beams along Bårdshaug Bridge
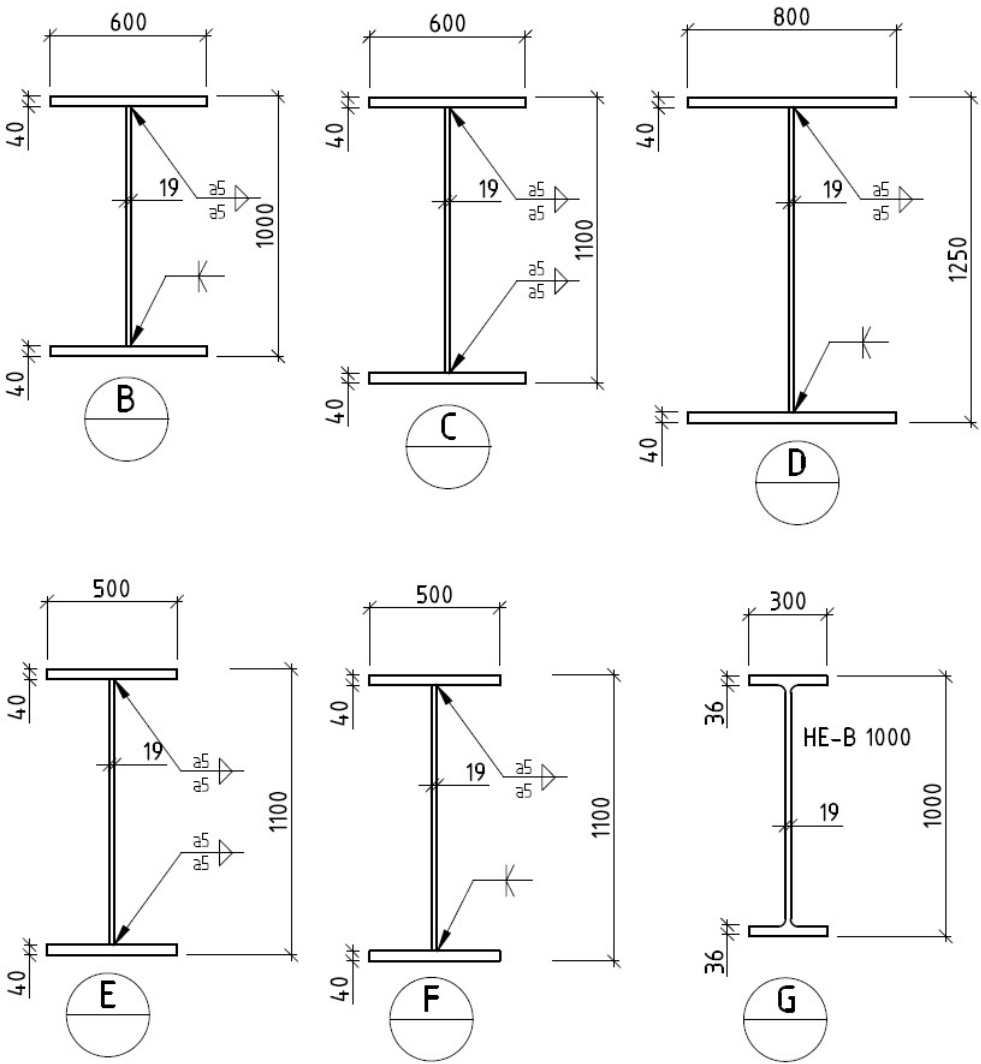
Figure B.2: Cross section of the steel beams along Bårdshaug Bridge at

# Appendix C

# Modeling Bårdshaug Bridge; Parameter Study

The general procedure in the parameter study was changing the values of the spring constants and Young's modulus of the concrete to obtain the natural frequencies and verified with modal assurance criterion. The iteration process is shown in Table C.1, C.2 and C.3. The three main variables that were iterated were the concrete Young's modulus, longitudinal springs between steel beams and concrete slab and horizontal springs between steel beams and columns. The result that yielded closest natural frequencies and modal shapes to the actual bridge is shown in Table 6.8. The following tables show the influence of each variable for the three different modal shapes.

Table C.1: Parametric study of Young's modulus influence on the natural frequencies. Springs between steel beams and columns and springs between steel beams and concrete slab are held constant.

| E-mod. concrete [GPa] | Natural frequencies for the first modes [Hz] | | | | | | | |
| | Horizontal | | Vertical | | | Torsional | | |
| | 1 | 2 | 1 | 2 | 3 | 1 | 2 | 3 |
|---|---|---|---|---|---|---|---|---|
| 20 | 1.816 | 3.061 | 1.910 | 2.921 | 4.032 | 2.912 | 3.769 | 5.365 |
| 25 | 1.836 | 3.108 | 1.955 | 2.986 | 4.126 | 3.197 | 4.011 | 5.720 |
| 30 | 1.853 | 3.179 | 1.991 | 3.040 | 4.200 | 3.419 | 4.232 | 6.087 |
| 36 | 1.870 | 3.261 | 2.026 | 3.092 | 4.273 | 3.668 | 4.476 | 6.453 |

| Average change per GPa | 0.003 | 0.012 | 0.007 | 0.011 | 0.015 | 0.048 | 0.044 | 0.069 |
|---|---|---|---|---|---|---|---|---|

Table C.2: Parametric study of longitudinal spring constants between the steel beams and concrete slab. Concrete Young's modulus and spring constant between steel beams and columns held constant.

| Longit. springs [N/m] | Natural frequencies for the first modes [Hz] | | | | | | | |
| | Horizontal | | Vertical | | | Torsional | | |
| | 1 | 2 | 1 | 2 | 3 | 1 | 2 | 3 |
|---|---|---|---|---|---|---|---|---|
| 1 | 1.767 | 2.721 | 1.529 | 2.381 | 3.161 | 3.502 | 4.072 | 5.847 |
| $10^5$ | 1.767 | 2.722 | 1.530 | 2.382 | 3.162 | 3.502 | 4.072 | 5.847 |
| $10^9$ | 1.860 | 3.173 | 1.978 | 2.982 | 4.128 | 3.636 | 4.405 | 6.356 |
| $10^{10}$ | 1.868 | 3.247 | 2.019 | 3.075 | 4.255 | 3.661 | 4.454 | 6.441 |
| $10^{12}$ | 1.870 | 3.260 | 2.026 | 3.090 | 4.271 | 3.667 | 4.474 | 6.452 |
| $10^{15}$ | 1.870 | 3.261 | 2.026 | 3.092 | 4.273 | 3.668 | 4.476 | 6.453 |

| Average change per order of magnitude of N/m | 0.006 | 0.039 | 0.031 | 0.050 | 0.075 | 0.012 | 0.029 | 0.044 |

Table C.3: Parametric study of spring constants between steel beams and column. Concrete Young's modulus and spring constant between steel beams and concrete slab held constant

| Horizontal springs [N/m] | Natural frequencies for the first modes [Hz] | | | | | | | |
| | Horizontal | | Vertical | | | Torsional | | |
| | 1 | 2 | 1 | 2 | 3 | 1 | 2 | 3 |
|---|---|---|---|---|---|---|---|---|
| $10^5$ | 0.728 | 2.074 | | | | 3.654 | 4.462 | 6.453 |
| $10^7$ | 1.757 | 3.154 | | Unaffected | | 3.665 | 4.473 | 6.452 |
| $1.3 \; 10^7$ | 1.870 | 3.261 | | | | 3.668 | 4.476 | 6.453 |
| $10^{10}$ | 3.102 | 5.978 | | | | 3.684 | 4.344 | 6.452 |

| Average change per order of magintude of N/m | | | | | | | | |
|---|---|---|---|---|---|---|---|---|
| | 0.449 | 0.635 | | | | 0.007 | 0.022 | 0.002 |

For each of the iteration processes the other two variables were chosen to be in the approximate domain such that the first natural frequencies could be obtained. These two variables were held constant throughout the iteration process.

# Appendix D

# Model Assurance Criterion - Numerical Tables

Table D.1: MAC value in % of the first model - full interaction

| Full interaction | | Abaqus | | | | | |
|---|---|---|---|---|---|---|---|
| | | H1 [1.85] | H2 [2.77] | V1 [1.97] | V2 [2.92] | V3 [4.02] | T1 [4.19] |
| Measurement data | H1 [1.85] | 94 | 10 | 6 | 36 | 29 | 0 |
| | H2 [2.72] | 2 | 84 | 15 | 26 | 9 | 28 |
| | V1 [1.97] | 12 | 0 | 97 | 2 | 0 | 97 |
| | V2 [2.47] | 34 | 6 | 83 | 17 | 2 | 58 |
| | V3 [2.54] | 6 | 23 | 19 | 76 | 2 | 45 |
| | V4 [2.90] | 29 | 30 | 3 | 95 | 3 | 1 |
| | V5 [4.36] | 27 | 11 | 0 | 0 | 97 | 0 |
| | T1 [3.81] | 7 | 5 | 87 | 11 | 0 | 98 |

Table D.2: MAC value in % of the second model - spring interaction, no longitudinal interaction

| No longitudinal interaction | | Abaqus | | | | | |
|---|---|---|---|---|---|---|---|
| | | H1 [1.86] | H2 [2.78] | V1 [1.53] | V2 [2.38] | V3 [3.16] | T1 [3.46] |
| Measurement data | H1 [1.85] | 97 | 5 | 8 | 27 | 37 | 3 |
| | H2 [2.72] | 0 | 98 | 11 | 32 | 5 | 22 |
| | V1 [1.97] | 8 | 19 | 94 | 5 | 0 | 99 |
| | V2 [2.47] | 33 | 1 | 88 | 10 | 3 | 70 |
| | V3 [2.54] | 11 | 44 | 14 | 80 | 5 | 33 |
| | V4 [2.90] | 37 | 25 | 6 | 88 | 7 | 0 |
| | V5 [4.36] | 24 | 6 | 0 | 3 | 93 | 1 |
| | T1 [3.81] | 4 | 33 | 81 | 17 | 0 | 95 |

Table D.3: MAC value in % of the third model - Spring interaction, stiffer longitudinal springs

| Longitudinal spring interaction | | Abaqus | | | | | |
|---|---|---|---|---|---|---|---|
| | | H1 [1.86] | H2 [2.96] | V1 [1.99] | V2 [2.89] | V3 [3.97] | T1 [3.54] |
| Measurement data | H1 [1.85] | 95 | 0 | 6 | 37 | 28 | 3 |
| | H2 [2.72] | 1 | 98 | 14 | 26 | 9 | 21 |
| | V1 [1.97] | 10 | 18 | 97 | 2 | 0 | 99 |
| | V2 [2.47] | 33 | 3 | 82 | 17 | 1 | 71 |
| | V3 [2.54] | 8 | 29 | 20 | 76 | 1 | 32 |
| | V4 [2.90] | 32 | 13 | 2 | 96 | 2 | 0 |
| | V5 [4.36] | 27 | 17 | 0 | 0 | 98 | 0 |
| | T1 [3.81] | 5 | 29 | 87 | 11 | 0 | 95 |

# Appendix E

# Acceleration History of Load Models Applied to FE-model

**British Standard 5400**
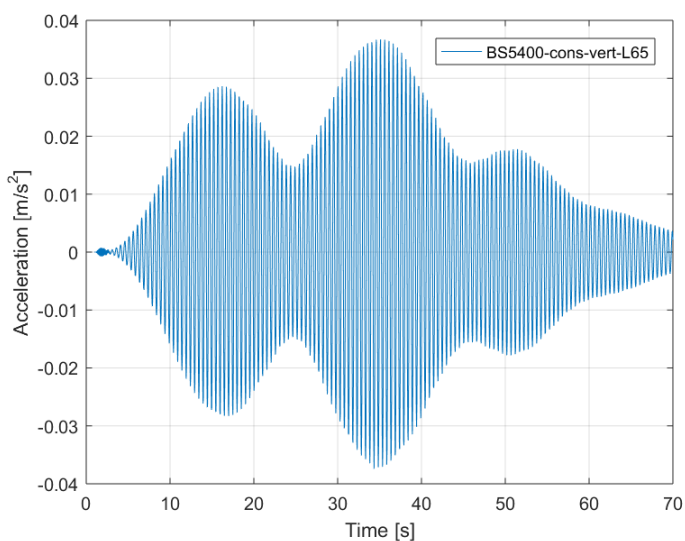


Figure E.1: Acceleration history, load model from BS 5400, moving concentrated load in vertical direction, walking, applied to the FE-model of Bårdshaug Bridge.
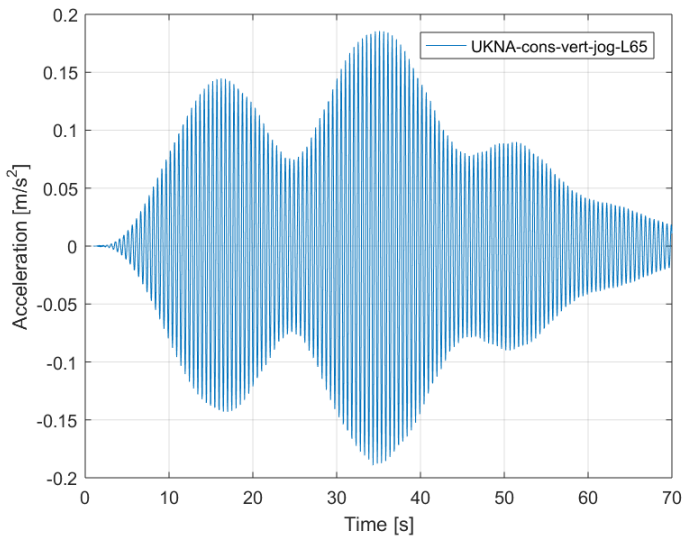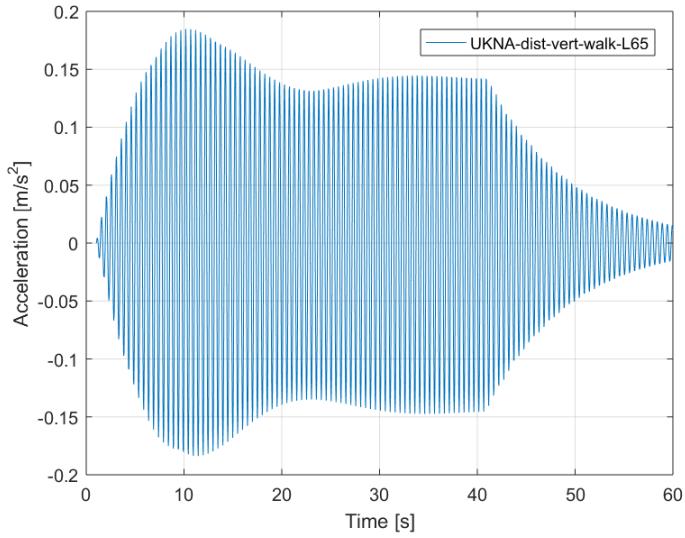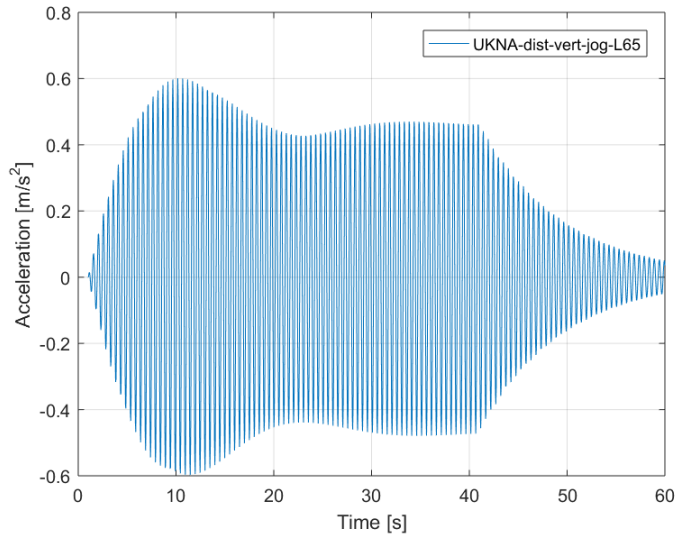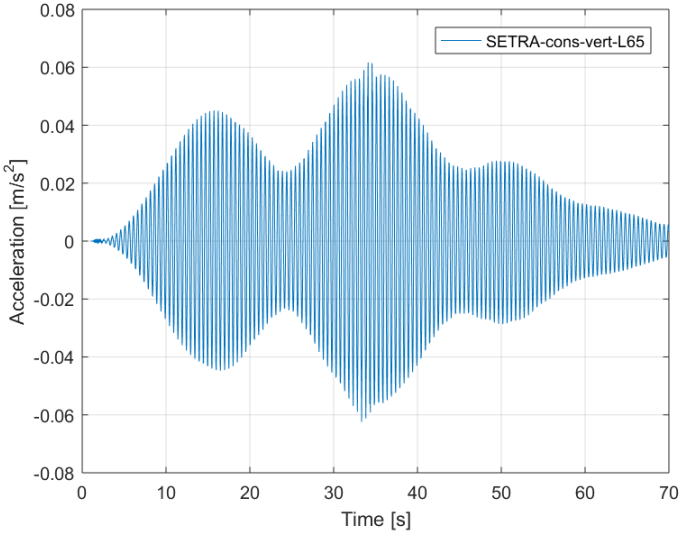
**UK national annex to Eurocode**
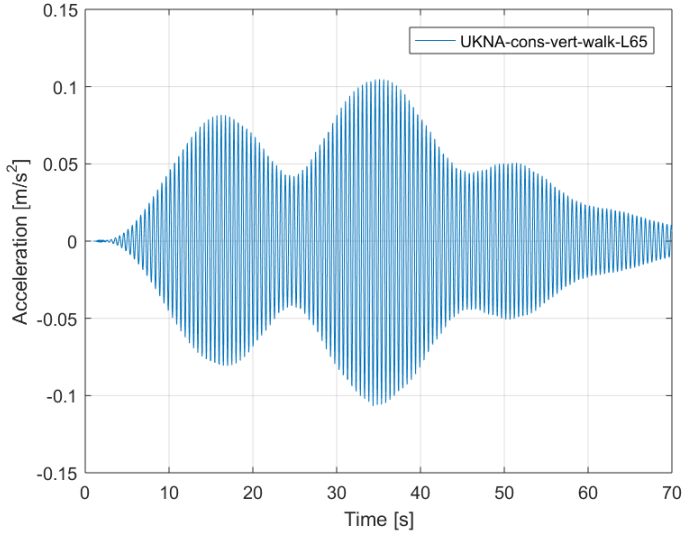


Figure E.2: Acceleration history, load model from UK-NA, moving concentrated load in vertical direction, walking, applied to the FE-model of Bårdshaug Bridge.
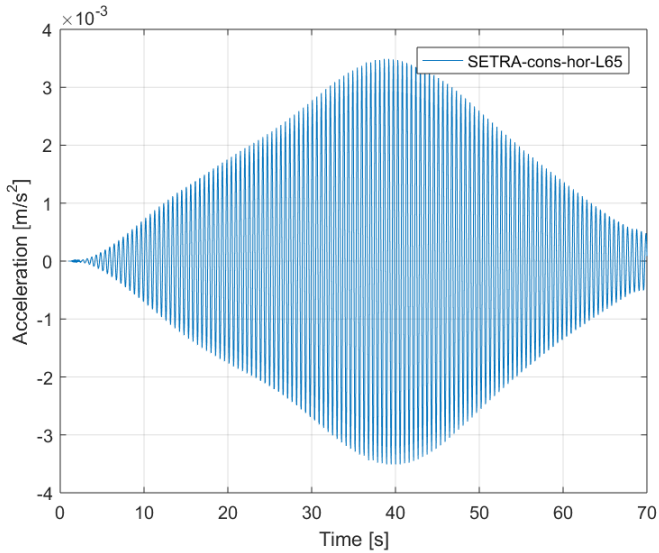


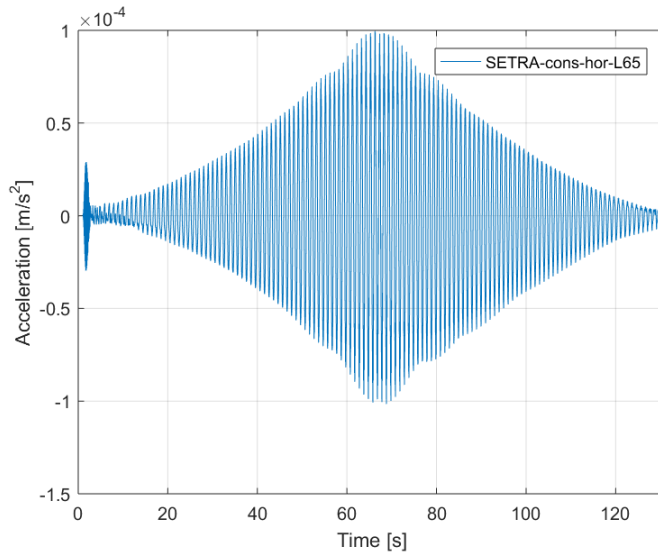Figure E.3: Acceleration history, load model from UK-NA, moving concentrated load in vertical direction, jogging, applied to the FE-model of Bårdshaug Bridge.

Figure E.4: Acceleration history, load model from UK-NA, distributed load in vertical direction, walking, applied to the FE-model of Bårdshaug Bridge.



Figure E.5: Acceleration history, load model from UK-NA, distributed load in vertical direction, jogging, applied to the FE-model of Bårdshaug Bridge.

**SÉTRA**



Figure E.6: Acceleration history, load model from SÉTRA, moving concentrated load in vertical direction, applied to the FE-model of Bårdshaug Bridge.



Figure E.7: Acceleration history, load model from SÉTRA, moving concentrated load in horizontal direction, applied to the FE-model of Bårdshaug Bridge. Load applied in the frequency of the first lateral mode.
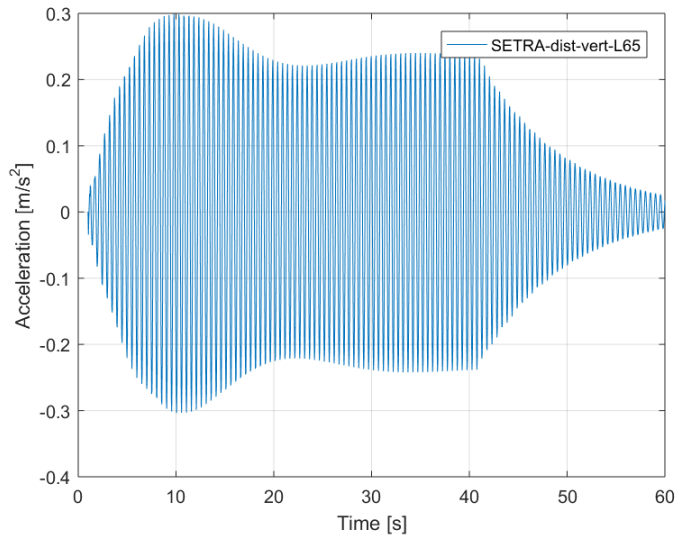
Figure E.8: Acceleration history, load model from SÉTRA, moving concentrated load in horizontal direction, applied to the FE-model of Bårdshaug Bridge. Load applied in the horizontal step frequency.



Figure E.9: Acceleration history, load model from SÉTRA, distributed load load in vertical direction, applied to the FE-model of Bårdshaug Bridge.
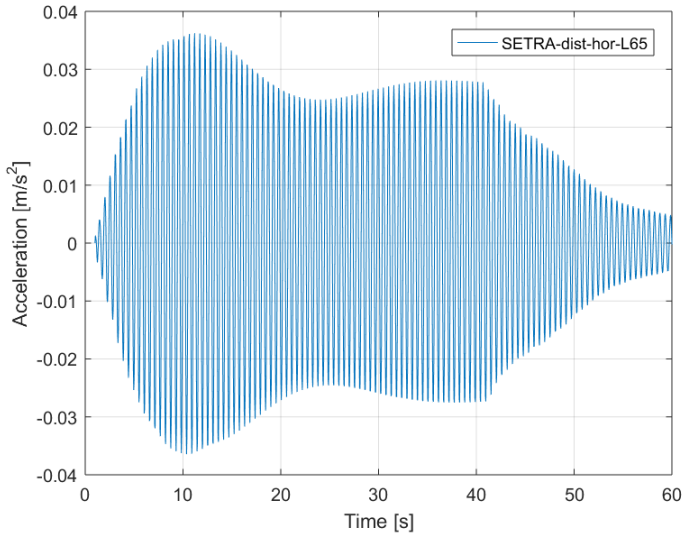
Figure E.10: Acceleration history, load model from SÉTRA, distributed load load in horizontal direction, applied to the FE-model of Bårdshaug Bridge.
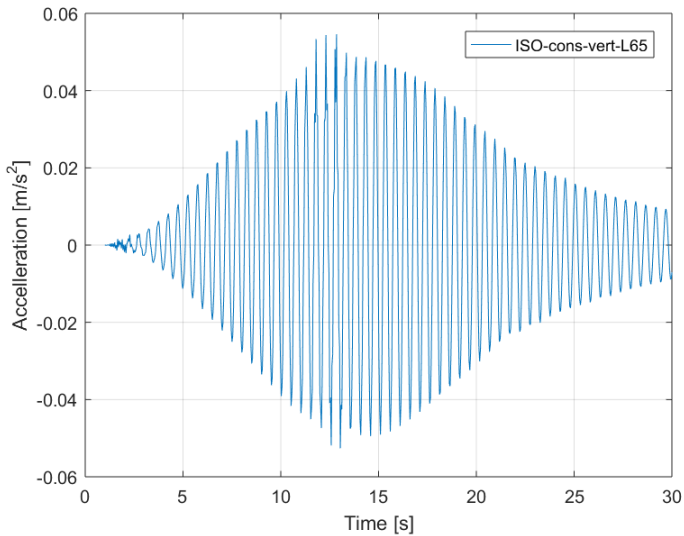
**ISO 10137**



Figure E.11: Acceleration history, load model from ISO 10137, moving concentrated load in vertical direction, applied to the FE-model of Bårdshaug Bridge.
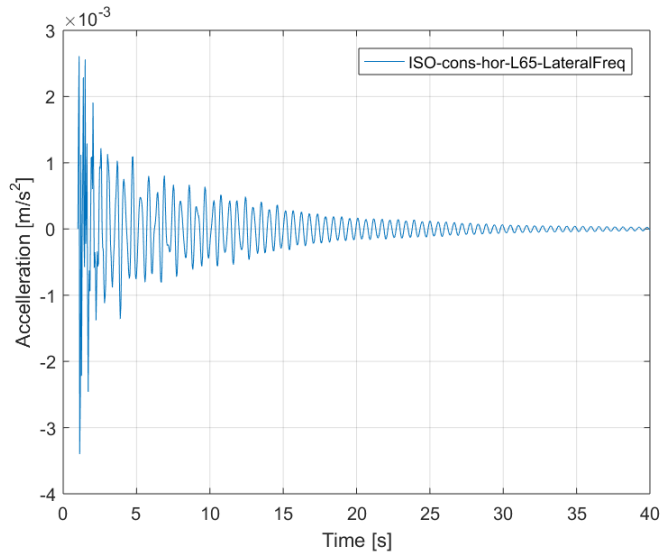
Figure E.12: Acceleration history, load model from ISO 10137, moving concentrated load in horizontal direction, applied to the FE-model of Bårdshaug Bridge. Load applied in the frequency of the first lateral mode.
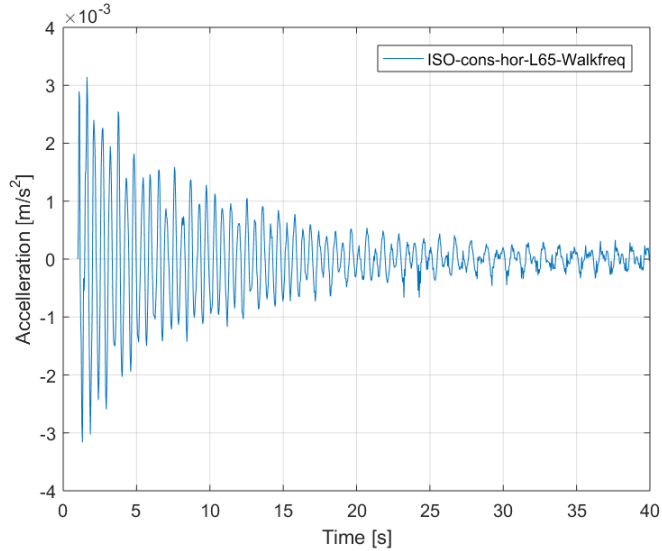


Figure E.13: Acceleration history, load model from ISO 10137, moving concentrated load in horizontal direction, applied to the FE-model of Bårdshaug Bridge. Load applied in the horizontal step frequency.
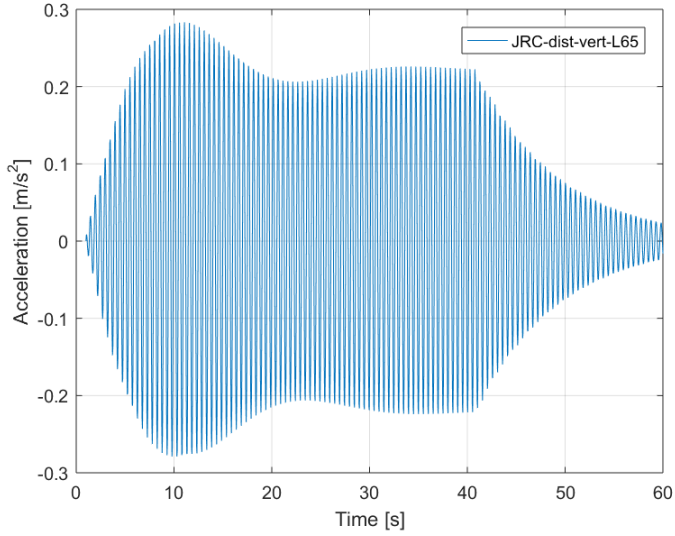
**JRC and HIVOSS**



Figure E.14: Acceleration history, load model from JRC and HIVOSS, distributed load load in vertical direction, applied to the FE-model of Bårdshaug Bridge.
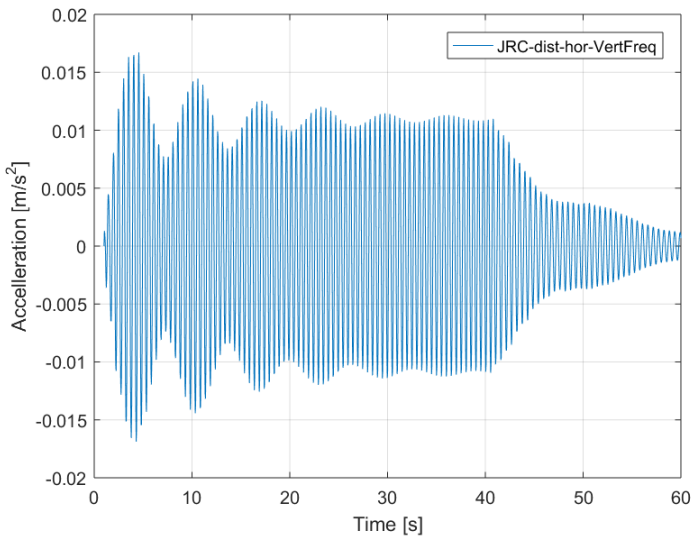


Figure E.15: Acceleration history, load model from JRC and HIVOSS, distributed load load in horizontal direction, applied to the FE-model of Bårdshaug Bridge. Vertica natural frequency.
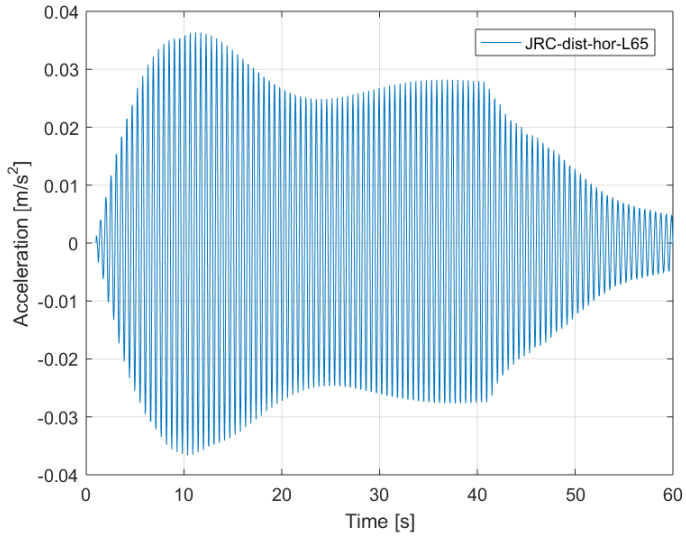
Figure E.16: Acceleration history, load model from JRC and HIVOSS, distributed load load in horizontal direction, applied to the FE-model of Bårdshaug Bridge.
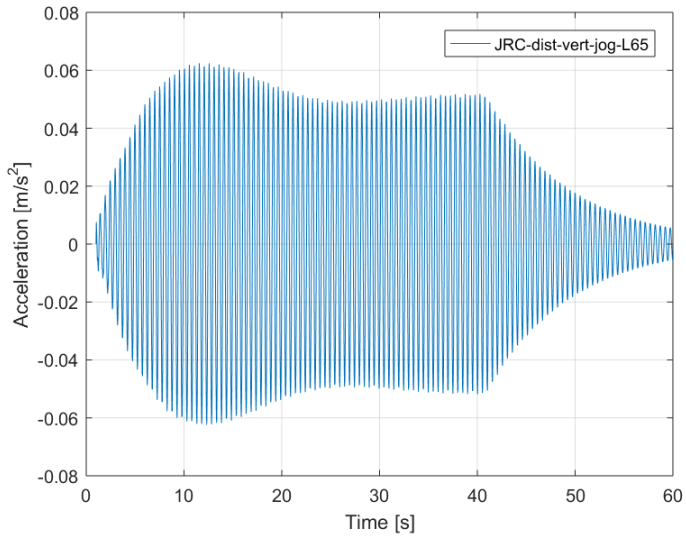


Figure E.17: Acceleration history, load model from JRC and HIVOSS, distributed jogging load load in vertical direction, applied to the FE-model of Bårdshaug Bridge.

# Appendix F

# Summary of Acceleration Response Values

Table F.1: Summary of maximum values for acceleration response.

| Load type | Max acceleration $[m/s^2]$ | | | | | | |
|---|---|---|---|---|---|---|---|
| | Euro-code | BS 5400 | UK-NA | Håndbok 185 | SÉTRA | ISO 10137 | JRC/ HIVOSS |
| Vert. conc. loads | 0.044 | 0.0367 | 0.1142 | 0.08 | 0.0617 | 0.0546 | - |
| Hor. conc. loads | 0.011 | - | - | - | 0.0001 | 0.0009 | - |
| Vert. dist. loads | 0.87 | - | 0.1848 | - | 0.2993 | - | 0.2832 |
| Hor. dist. loads | 0.089 | - | - | - | 0.0363 | - | 0.0364 |

Table F.2: Summary of RMS-values for acceleration response.

| Load type | RMS acceleration values $[m/s^2]$ | | | | | | |
|---|---|---|---|---|---|---|---|
| | Euro-code | BS 5400 | UK-NA | Håndbok 185 | SÉTRA | ISO 10137 | JRC/ HIVOSS |
| Vert. cons. loads | - | 0.0211 | 0.0657 | - | 0.0337 | 0.0365 | - |
| Hor. cons. loads | - | - | - | - | 0.00005 | 0.0002 | - |
| Vert. dist. loads | - | - | 0.1454 | - | 0.2390 | - | 0.2238 |
| Hor. dist. loads | - | - | - | - | 0.0308 | - | 0.0308 |

# Appendix G

# General Description, Bårdshaug Bridge

**MERKNADER:**
G/s-bru med bredde 3.5m. Stålbjelkebru med betongdekke uten samvirke.
Ferdigstilles år 2016 dato ....
Antatt maks 50 gående og syklende i timen.

Prosjekteringsgrunnlag:
| | |
|---|---|
| SVV håndbok 185: | Bruprosjektering, 2011. |
| SVV håndbok 026: | Prosesskode 2, 2007. |

Pålitelighet, kontroll og utførelse
| | |
|---|---|
| Pålitelighetsklasse | 3 iht. NS-EN 1990 |
| Kontrollklasse | Utvidet kontroll iht. NS-EN-1990 |
| Betong | Utførelsesklasse 3 iht. NS-EN 13670 |
| | Nøyaktighetsklasse B iht: R762, Tabell 84-2 |
| Stål | Utførelse iht. HB R762 Prosesskode 2 og NS-EN 1090 |
| Lager | Toleranse plassering +/- 5 mm høyde og side |

Materialer:
| | |
|---|---|
| Plasstøpt betong: | B45 SV-30. (B55 i akse 2) |
| Armering: | B500NC iht. NS 3576-3 |
| Bestandighetsklasse: | MF40. |
| Luftinnhold: | 5±1.5%. |
| Overdekning: | 75 mm |
| Tilslagsstørrelse: | D100=22mm |
| Stålkvalitet: | S355 ML |
| Boltekvalitet: | Bolter, skruer og dybler skal være i syrefast kvalitet A4-80 iht.NS-EN ISO 3506. Muttere og skiver skal være i samme rustfrie dokumenterbare kvalitet. Skruer skal være av kvalitet 8.8. |

Overflatebehandling:
Beleggsystem 1, metallisering pluss epoxy/polyretan iht. HB 026. Farge: RAL 7024.

Forskaling:
| | |
|---|---|
| Synlige flater: | Bordforskaling og lemmer, se teknisk beskrivelse. Hjørner avfases med 20 mm trekantlist, var. avfasing riegel. |
| Fundamentering Akse 1-5: | Borede betongpeler, med omfattende og gjentatt injeksjon under bunn av pel etter at den er utstøpt og avbundet (Peleveiledningen 2012, kapitel 4.2.5). Entreprenøren må dokumentere at effekten er oppnådd. Det må ikke føre til noen skader på eksisterende bru under installering av pelene. Landkarløs. |
| Belegningstype: | A3-4. |
| Max vekt: | 1.5 kN/m2. |

Lager/fuger:
Brua utføres med fugekonstruksjon i akse 5. Fugeåpning avklares med byggherre
Fastlager akse 1, Glidelager akse 2 – 5,
Lager faststøpes etter stålmontasje. Se egen lagertegning.

Rekkverk: G/s-sprosserekkverk. Farge: RAL 7024.

Flomvannstand: +5.3 200-års flom

Figure G.1: General description of Bårdshaug Bridge